

Advanced Data Analytics for Additive Manufacturing Energy Consumption Modelling, Prediction, and Management under Industry 4.0



Jian Qin

School of Engineering
Cardiff University

A thesis submitted to Cardiff University
for the degree of Doctor of Philosophy

September 2019

Acknowledgements

First, I would like to express my heartfelt thanks to my supervisor Dr. Ying Liu. His knowledge, experience, patience, support, and encouragement have been constant throughout these four years, and without him, I would not be where I find myself today. His approach to research and his concern for the development of his students have been inspirational, and I am incredibly grateful for having had the privilege of working with such outstanding professional.

I would also like to thank my co-supervisor, Dr. Roger Grosvenor sincerely. His knowledge and his willingness to share it with me have had a profound impact on my work. Many thanks to my colleagues, Chong Chen, Paul O'Regan, and Jacob Hill, for their help and encouragement.

I am thankful to my family, who has been at my side every step of the journey, enduring my grumbling and celebrating the victories. I owe them everything that I am and everything that I ever will be.

ABSTRACT

The topic of 'Industry 4.0' has become increasingly important in both industry and academia since it was first published. Under this trending topic, many related capabilities required by current manufacturing systems have been pointed out in both academia and industry, such as automation, sustainability, and intelligence. Additive manufacturing (AM) is one of the most popular manufacturing systems in the era of Industry 4.0. Although the AM system tends to become increasingly automated and flexible, the issue of energy consumption still attracts attention. It is related to many attributes in different components of an AM system, which are represented as multiple source data, such as process operation data, working environment data, design-relevant data, and material condition data. How to integrate and analyse the multi-source data for AM energy modelling, prediction, and management has become a crucial research question.

This research was structured according to four themes. Firstly, a categorical classification is proposed based on the research gaps between current manufacturing systems and Industry 4.0 requirement. Nine varied applications are generated relying on their classification to provide a roadmap to raise the intelligence level of manufacturing systems to achieve Industry 4.0 requirement. Inspired by this classification, a framework was designed for leading the research of AM energy consumption modelling, prediction, and management. The framework includes four layers, data sensing and collection layer, data pre-process and integration layer, data analytics layer, and knowledge and application layer. This four-layered framework covers the entire knowledge discovery process from data generation to performance presentation.

Secondly, due to multi-source data of the AM systems usually involving nested hierarchies, a hybrid approach is proposed to tackle the issue. This hybrid approach incorporates clustering and deep learning technologies to integrate the multi-source data which is collected by the Internet of Things (IoT), to model energy consumption

for AM systems. Multi-source data is analysed and collected. The data collection methods are introduced within the validation of a selective laser sintering (SLS) system. Results derived using this hybrid approach reveal that it outperforms pre-existing approaches.

Thirdly, while existing studies reveal that AM energy consumption modelling largely depends on the design-relevant features in practice, it has not been given sufficient attention. Therefore, in this research, design-relevant features are examined with respect to energy consumption prediction based on the study of AM energy modelling. By reviewing the literature of Design for AM and analysing some representative design models, AM design patterns are obtained and listed. Two types of design-relevant features are found, part-design features and process-planning features. The AM energy consumption knowledge, hidden in the design-relevant features, is exploited for prediction through a design-relevant data analytics approach.

Finally, methods enabling energy consumption management are provided in this research, which includes framework, modelling, prediction and the optimisation. The energy consumption optimisation method is based on particle swarm optimisation (PSO), and driven by deep learning technology, named as deep learning driven particle swarm optimisation (DLD-PSO). The proposed optimisation method aims to reduce the energy utility by optimising the design-relevant features. Deep learning was introduced to address several issues, in terms of increasing the search speed and enhancing the global best of PSO. The approaches proposed in this research were validated with the data collected from the target AM system, and the results reveal their merits.

The expected main achievement of this research is to pave the way for AM energy consumption modelling, prediction, and management through the advanced data analytics, which provides a feasibility study for achieving Industry 4.0. As such, it offers great potential as a route to achieve a more practical and generalised implementation of digital and intelligent manufacturing.

Table of Contents

Acknowledgements	ii
ABSTRACT	iii
Table of Contents	v
List of Tables	xi
List of Figures	xiii
List of Symbols	xvii
List of Abbreviations	xix
Research Achievements	xxi
Chapter 1 Introduction	1
1.1 Background	1
1.2 Motivations.....	3
1.3 Research Objectives	4
1.4 Thesis Outline	5
1.5 Contributions	7
Chapter 2 Related Works	9
2.1 Introduction	9
2.2 AM Technologies	9
2.2.1 Popular AM Technologies.....	10
• Electron beam melting (EBM)	11
• Selective laser melting (SLM).....	11

•	Selective laser sintering (SLS)	12
•	Fused deposition modelling (FDM)	13
•	Stereolithographic (SLA)	13
2.2.2	Data Generation of the AM Process	14
2.2.3	Design for Additive Manufacturing (DfAM)	16
2.2.4	Short Summary	19
2.3	AM Energy Consumption Analysis and Impacts	20
2.3.1	Energy Consumption Comparison of Different AM Technologies..	20
2.3.2	AM Energy Consumption Impact Factors	21
2.3.3	Design-relevant Impacts on AM Energy Consumption	23
2.3.4	Short Summary	25
2.4	Advanced Data Analytics	25
2.4.1	Process Optimisation by Advanced Data Analytics	26
2.4.2	Advanced Data Analytics for AM	28
2.4.3	Short Summary	32
2.5	A Critical View.....	32
Chapter 3	A Framework for AM Energy Consumption Analytics under Industry 4.0	34
3.1	Introduction	34
3.2	A Framework of AM Energy Consumption Modelling Prediction, and Management under Industry 4.0.....	35

3.2.1	Data Sensing and Collection Section	37
3.2.2	Data Pre-process and Integration Section	37
3.2.3	Data Analytics Section	38
3.2.4	Knowledge and Application Section.....	39
3.3	Feasibility Study Setup.....	40
3.3.1	Introduction of the Experimental SLS Machine.....	40
3.3.2	Unit Energy Consumption of the AM Process	42
3.3.3	Evaluation Metrics	44
3.4	Summary	45
Chapter 4	Multi-source Data Analytics for AM Energy Consumption	
Modelling	46
4.1	Introduction	46
4.2	Multi-source Data Sensing and Collection.....	47
4.2.1	Multi-source Data Sensing and Collection for an AM Process.....	47
4.2.2	Hardware Setup of Data Sensing and Collection for the Target System	49
	• System monitoring file	49
	• IoT data collecting system.....	51
	• Product design CAD models	55
4.3	AM Energy Consumption Modelling using Multi-source Data.....	56
4.3.1	Multi-source Data Integration	56
4.3.2	Merge Neural Network for Multi-source Data Modelling	59

4.4	Evaluation of AM Energy Modelling using Multi-source data.....	60
4.4.1	Results of Conventional Machine Learning (ML) Approaches	61
4.4.2	Results of the Multi-source Data Modelling	64
4.4.3	Discussion.....	66
4.5	Summary.....	67
Chapter 5	Design-relevant Data Analytics for AM Energy Consumption Prediction	68
5.1	Introduction	68
5.2	AM Energy Consumption Prediction	69
5.2.1	AM Energy Consumption Impact Feature Comparison	69
5.2.2	Pattern Analysis of Design-relevant Data	72
5.2.3	Energy Consumption Prediction based on Design-relevant Data	74
5.3	Evaluation of AM Energy Consumption Prediction using Design-relevant Data	76
5.3.1	Design-relevant Data Description	77
5.3.2	Results of Energy Consumption Prediction based on Design-relevant Data	82
5.3.3	Discussion.....	83
5.4	Summary.....	85
Chapter 6	Data-driven AM Energy Consumption Management.....	86
6.1	Introduction	86
6.2	Data-driven AM Energy Consumption Management.....	86

6.2.1	Process of Data-driven AM Energy Consumption Management.....	87
6.2.2	Deep Learning Driven Particle Swarm Optimisation (DLD-PSO) ..	88
	• Objectives of DLD-PSO.....	89
	• Process of DLD-PSO.....	89
6.3	Evaluation of DLD-PSO	92
6.3.1	Introduction of AM Built Examples for Energy Consumption Management.....	92
6.3.2	Feature Restriction	95
6.3.3	Optimisation Results of DLD-PSO	96
6.3.4	Optimised Design-relevant Features	105
6.3.5	Discussion	110
6.4	Summary	111
Chapter 7	Achievements and Conclusions	112
7.1	Achievements	112
7.2	Discussion and Reflection.....	115
7.3	Conclusions	117
	References	118
	Appendix A Advanced Data Analytics Technologies.....	129
A.1	Data mining	129
A.2	Conventional machine learning algorithms.....	130
A.3	Deep learning	133
	Appendix B Additional Results and Datasets.....	137

B.1 More Results of Different Clustering Quantity	137
B.2 Design-relevant Dataset.....	139
B.3 Design-relevant Feature Optimisation Process	144
Appendix C Core Programming Coding	156
C.1 IoT Platform Data Sensing and Collecting.....	156
C.2 Ad-hoc Wireless Network Data Receiving	157
C.3 Benchmark Algorithms	158
C.4 Merged Neural Network.....	159
C.5 Design-relevant Dataset Generation.....	160

List of Tables

Table 2.1 Energy consumption comparison between different AM technologies	20
Table 2.2 Energy consumption related attributes of AM systems in literature.....	21
Table 3.1 Material data collected from the support company material sheet	42
Table 3.2 Basic information of the unit energy consumption of experimental machine	44
Table 4.1 Data description of Job file	50
Table 4.2 Data description of Report file.....	50
Table 5.1 Weights of process operation features	70
Table 5.2 Weights of design-relevant features.....	70
Table 5.3Weights of material condition features	71
Table 5.4 Weights of working environment features.....	71
Table 5.5 Design-relevant feature description.	79
Table 5.6 The basic statistic information of the design-relevant data.....	81
Table 5.7 The prediction results of the three models	82
Table 5.8 The weights of the design-relevant features extracted from the merged neural networks.	83
Table 6.1 Examples used for energy consumption management in the different ranges of energy consumption.....	94
Table 6.2 The restriction of the design-relevant features in the four optimised build examples.....	95
Table 6.3 The comparison between the predictive and the actual energy consumption	96
Table 6.4 Comparison between the conventional PSO and DLD-PSO	104
Table 6.5 The optimised results of Build No.1	106

Table 6.6 The optimised results of Build No.2	107
Table 6.7 The optimised results of Build No.3	108
Table 6.8 The optimised results of Build No.4	109
Table B.1 Conventional ML results using layer-levelled dataset in 1 to 20 clusters.	137
Table B.2 Convectional ML results using merged dataset in 1 to 20 clusters.	138
Table B.3 The entire design-relevant dataset	139

List of Figures

Figure 2.1 Schematic of EBM adapted from Węglowski et al. (2016).....	11
Figure 2.2 Schematic of SLM adapted from Gross et al. (2014).....	12
Figure 2.3 Schematic of SLS adapted from Sing et al. (2017)	12
Figure 2.4 Schematic of FDM adapted from Tanikella et al. (2017).....	13
Figure 2.5 Schematic of SLA adapted from Wang et al. (2015).....	14
Figure 2.6 AM system data generation process	16
Figure 4.1 Multi-source data sensing and collection using IoT for an AM process ..	48
Figure 4.2 Parameter setting features viewed by EOS-Formats software	49
Figure 4.3 DHT11 sensor located in the material cylinder	51
Figure 5.1 Two examples of products made by target SLS system.....	72
Figure 5.2 CAD models of another SLS production.....	73
Figure 5.3 AM energy consumption modelling based on the design-relevant data...	75
Figure 5.4 Autodesk Netfabb interface for collecting design-relevant data, which example build was on 15 th September 2017.....	77
Figure 5.5 Information shown by Autodesk Netfabb	78
Figure 6.1 The process of the DLD-PSO	90
Figure 6.2 The CAD models of the optimised examples.....	93
Figure 6.3 Part-designer-oriented optimisation result comparison between the conventional and the DLD-PSO for Build No.1	97
Figure 6.4 Process-operator-oriented optimisation result comparison between the conventional and the DLD-PSO for Build No.1	97
Figure 6.5 Designer-and-operator-oriented optimisation result comparison between the conventional and the DLD-PSO for Build No.1	98

Figure 6.6 Part-designer-oriented optimisation result comparison between the conventional and the DLD-PSO for Build No.2	98
Figure 6.7 Process-operator-oriented optimisation result comparison between the conventional and the DLD-PSO for Build No.2	99
Figure 6.8 Designer-and-operator-oriented optimisation result comparison between the conventional and the DLD-PSO for Build No.2	99
Figure 6.9 Part-designer-oriented optimisation result comparison between the conventional and the DLD-PSO for Build No.3	100
Figure 6.10 Process-operator-oriented optimisation result comparison between the conventional and the DLD-PSO for Build No.3	100
Figure 6.11 Designer-and-operator-oriented optimisation result comparison between the conventional and the DLD-PSO for Build No.3	101
Figure 6.12 Part-designer-oriented optimisation result comparison between the conventional and the DLD-PSO for Build No.4	101
Figure 6.13 Process-operator-oriented optimisation result comparison between the conventional and the DLD-PSO for Build No.4	102
Figure 6.14 Designer-and-operator-oriented optimisation result comparison between the conventional and the DLD-PSO for Build No.4	102
Figure B.1 Bottom area and part quantity optimisation (designer-and-operator-oriented) process for Build No.1	144
Figure B.2 Filling degree of part and total optimisation (designer-and-operator-oriented) process for Build No.1	144
Figure B.3 Height of part and total optimisation (designer-and-operator-oriented) process for Build No.1	145
Figure B.4 Rate between height and length of part and total build optimisation (designer-and-operator-oriented) process for Build No.1	145
Figure B.5 Rate between width and height of part and total build optimisation (designer-and-operator-oriented) process for Build No.1	146

Figure B.6 Rate between width and length of part and total build optimisation (designer-and-operator-oriented) process for Build No.1	146
Figure B.7 Bottom area and part quantity optimisation (designer-and-operator-oriented) process for Build No.2	147
Figure B.8 Filling degree of part and total optimisation (designer-and-operator-oriented) process for Build No.2.....	147
Figure B.9 Height of part and total optimisation (designer-and-operator-oriented) process for Build No.2	148
Figure B.10 Rate between height and length of part and total build optimisation (designer-and-operator-oriented) process for Build No.2.....	148
Figure B.11 Rate between width and height of part and total build optimisation (designer-and-operator-oriented) process for Build No.2.....	149
Figure B.12 Rate between width and length of part and total build optimisation (designer-and-operator-oriented) process for Build No.2.....	149
Figure B.13 Bottom area and part quantity optimisation (designer-and-operator-oriented) process for Build No.3.....	150
Figure B.14 Filling degree of part and total optimisation (designer-and-operator-oriented) process for Build No.3.....	150
Figure B.15 Height of part and total optimisation (designer-and-operator-oriented) process for Build No.3	151
Figure B.16 Rate between height and length of part and total build optimisation (designer-and-operator-oriented) process for Build No.3.....	151
Figure B.17 Rate between width and height of part and total build optimisation (designer-and-operator-oriented) process for Build No.3.....	152
Figure B.18 Rate between width and length of part and total build optimisation (designer-and-operator-oriented) process for Build No.3.....	152
Figure B.19 Bottom area and part quantity optimisation (designer-and-operator-oriented) process for Build No.4.....	153

Figure B.20 Filling degree of part and total optimisation (designer-and-operator-oriented) process for Build No.4	153
Figure B.21 Height of part and total optimisation (designer-and-operator-oriented) process for Build No.4	154
Figure B.22 Rate between height and length of part and total build optimisation (designer-and-operator-oriented) process for Build No.4	154
Figure B.23 Rate between width and height of part and total build optimisation (designer-and-operator-oriented) process for Build No.4	155
Figure B.24 Rate between width and length of part and total build optimisation (designer-and-operator-oriented) process for Build No.4	155

List of Symbols

a_i : Actual values

b_{dk} : Bias in artificial neural network

Δb_b : Bias of build-level neural network section

Δb_f : Bias of full connection neural network section

Δb_l : Bias of layer-level neural network section

C_1 : Cognitive factor 1 for PSO

C_2 : Cognitive factor 2 for PSO

CL_{ci}^j : Centre point of each clustering for layer-level data

d_{knn} : Euclidean distance for k -NN

D_i : Design-relevant data

E_{dk} : Squared error in artificial neural network

E_e : Energy consumption of each energy consumer

e_{RMSE} : Root mean square error

E_T : Total energy consumption

E_U : Unit energy consumption

$f_b(\cdot)$: Activation function of build -level neural network section

$f_c(\cdot)$: Clustering function

$f_d(\cdot)$: Activation function in artificial neural network

$f_f(\cdot)$: Activation function of full connection neural network section

$f_l(\cdot)$: Activation function of layer-layer-level neural network section

$f_m(\cdot)$: Function of merged neural network

$f_{sig}(\cdot)$: Sigmoid function

$g_{best}(t)$: Global best particle

L_{ni}^j : Layer-level raw dataset

MCC : Model correlation coefficient

M_T : Total mass of producing parts

O_{dk} : Desired output of each layer in artificial neural network

PD_g : Part-design data

$p_{best}(t)$: Personal best particle

p_i : Predicted values

PP_h : Process-planning data

t : Number of Iteration of PSO

v_i : Iteration velocity of PSO

W : Matrix of weights, extracted from prediction model

w_0 : Inertia weight for PSO

w_B : Weight of each neuron on each build-level neural network section

w_{dki} : Weight in artificial neural network

w_{fi} : Weight of each neuron on each full connection neural network section

w_{LR} : Weights for each input in Linear regression

w_{Lic} : Weight of each neuron on each layer-level neural network section

y_B : Output of each neuron on build-level neural network section

y_{dk} : Output values in artificial neural network

y_f : Output of each neuron on full connection neural network section

y_L : Output of each neuron on layer-level neural network section

\hat{y}_{LR} : Linear regression predicted attribute

List of Abbreviations

AM: Additive manufacturing

ANN: Artificial neural network

BFO: Bacterial foraging optimisation

CAD: Computer added design

CNC: Computer numerical control

CPS: Cyber-physical system

DAR: Digital array radar

DfAM: Design for additive manufacturing

DT: Decision tree

DL: Deep learning

EAS: Evolutionary and swarm algorithm

EBM: Electron beam melting

ETL: Extract transform and load

FDM: Fused deposition modelling

GA: Genetic algorithm

GMAW: Gas metal arc welding

IoT: Internet of Things

KDD: Knowledge discovery in database

LCA: Life cycle analysis

LR: Linear regression

MCC: Model correlation coefficient

MNN: Merged neural network

ML: Machine learning

PSO: Particle swarm optimisation

RMSE: Root mean square error

RP: rapid prototyping

SVM: Support vector machine

SLS: Selective laser sintering

SLM: Selective laser melting

SLA: Stereolithographic

k-NN: *k*-nearest neighbors

Research Achievements

Journal papers:

Qin J, Liu Y., Grosvenor R., Lacan F. and Jiang Z., 2019. *Deep learning-driven particle swarm optimisation for additive manufacturing energy optimisation*. Journal of Cleaner Production, p.118702. **(Impact factor: 6.395)**

Chen C, Liu Y, Kumar M., **Qin J**, and Ren Y., 2019. *Energy Consumption Modelling Using Deep Learning Embedded Semi-supervised Learning*. Computers & Industrial Engineering. 2019, 135: 757-765. **(Impact factor: 3.518)**

Qin J, Liu Y, and Grosvenor R., *Multi-source data analytics for AM energy consumption prediction*. Advanced Engineering Informatics. 2018, 38:840-850. **(Impact factor: 3.772)**

Qin J, and Liu Y., 2019 *Industrial Internet of Learning (IIoL): Advanced Data Analytics based Knowledge Chains between Edges, Fogs and the Cloud*. **(Working paper)**

Conference papers:

Chen C, Liu Y, Kumar M, and **Qin J.**, *Energy Consumption Modelling Using Deep Learning Technique—A Case Study of EAF*. Procedia CIRP. 2018, 1;72(1):1063-8.

Qin J, Liu Y, and Grosvenor R., *Data analytics for energy consumption of digital manufacturing systems using Internet of Things method*. Conference on Automation Science and Engineering (CASE), IEEE, 2017, 482-487.

Qin J, Liu Y, and Grosvenor R., *A Framework of Energy Consumption Modelling for Additive Manufacturing Using Internet of Things*.Procedia CIRP. 2017, 63:307-312.

Qin J, Liu Y, and Grosvenor R., *A categorical framework of manufacturing for industry 4.0 and beyond*. Procedia CIRP. 2016, 52:173-178. **(Google scholar citations: 352, 08th Nov 2019)**

Other research achievements:

Liu Y, and **Qin J.**, *IoT-enabled Facility Monitoring System for Smart University Living Experience*. Digital Catapult and Jisc funded proposal. **(£1,700, July 2019 – July 2020)**

Chapter 1 Introduction

1.1 Background

Since the first industrial revolution, subsequent revolutions have resulted in radical changes in manufacturing, from water and steam powered machines to electrical and digital automated production. Manufacturing processes have become increasingly complicated, automatic, and sustainable, which provide people to operate machines, efficiently and persistently (Wahlster, 2012). Nowadays, manufacturing has played a more essential role in the world, especially in European countries. About 17% of the GDP in European countries is accounted for by manufacturing, which also creates approximately 32 million job positions with many supplementary occupations (Commission, 2015). In this background, Industry 4.0 has been proposed which has greatly promoted the development of manufacturing, especially for intelligent manufacturing.

Industry 4.0 requires manufacturing to be not only integrated, automated, predictive, and intelligent, but also sustainable and renewable (Stock and Seliger, 2016). More details about Industry 4.0 will be introduced in chapter 2. At present, industrial production activities use about 35% of the entire global electricity supply, which produces approximately 20% of total carbon emissions. In the last 20 years, there has been an increase of more than 50% in greenhouse gas emission which is released by the top five manufacturing countries. The manufacturing sustainability has never escaped the academia's and industry's attention. It is also an indispensable research topic in the age of Industry 4.0. The energy consumption is considered as one of the

most crucial fields of sustainability. It is known that the energy efficiency of production processing is normally below 30%. For some specific process, the losses of energy are unexpectedly high, for example, the energy loss of rough milling process is about 60%, and the finishing is about 95% (Dietmair and Verl, 2009). Therefore, increasingly researches have been paying close attention to energy consumption and its environmental and financial impact. In most manufacturing systems, energy consumption is part of essential standards to measure the benefits. Highly efficient energy usage can not only reduce production costs, and expand profit margins, but also solve associated environmental and social problems (Park et al., 2009).

As one of the most popular manufacturing systems in the age of Industry 4.0, AM has become increasingly employed, due to digitalisation, automation, flexibility, and customisation. According to the ISO/ASTM 52900 international standard, AM is defined as ‘process of joining material to make parts from 3D model data, usually layer upon layer, as opposed to subtractive manufacturing and formative manufacturing methodologies’ (ISO/ASTM, 2015). It is also called 3D printing or rapid prototyping (RP). The first AM system emerged in 1987, which used the laser to solidify the light-sensitive liquid polymer. With the over 20 years of development, current AM systems can even produce multiple material products which is now a popular topic of AM research (Wohlers and Gornet, 2014). In 2015, the AM industry, including commercial products and services is worth USD 5.165 billion which grew 25% compared to 2014. Specifically, there were 808 metal AM machines and 278,385 desktop 3D printers sold in 2015, which are produced by 62 manufacturers from worldwide (Wohlers, 2016).

Comparing with the traditional manufacturing processing, the AM processing is a low energy efficiency system within the high-yield production, in terms of over hundreds mega joule per kilogram (Baumers et al., 2011). Many factors impact the energy consumption of AM process, and according to the Life Cycle Analysis (LCA), the AM energy consumption is one of the most critical elements affecting environmental impact (Kellens et al., 2011). Reducing AM energy consumption is one of the principal research targets for manufacturing sustainability in the age of Industry 4.0.

1.2 Motivations

The AM process is widely known as a complex system including various technologies, such as electron beam melting (EBM), selective laser melting (SLM), and selective laser sintering (SLS) (Ford and Despeisse, 2016). Different processing technologies show different energy consumption rates due to various impact factors (Qin et al., 2017). These factors are identified in the entire AM process. Generally, a typical AM process includes six stages (Convert, Locate and orient, Adding support structure, Slice, Build, and Post-process). In this standard process, related attributes, including evident and hidden energy consumption relevant factors, can be digitalised and connected in a virtual world using IoT techniques as different types of data (Gubbi et al., 2013).

Because the data is collected from various sources, this data is defined as the multi-source data (Yager, 2004), which are often used to build data analytics models for ascertaining the AM system relevant information and knowledge (Boyes et al., 2018). The multi-source data is generally collected by different methods (Chan et al., 2018). This data involves various features and dimensions, which tends to be nested as a multiple hierarchical structure. The features of this data structure are rarely independent (Rajeswaran and Blackstone, 2018). This data is difficult to integrate using typical data integration methods, such as the extract, transform, and load (ETL) technique (Yin and Kaynak, 2015). Under this complicated data environment, it is very challenging to integrate the multi-source data which includes the multiple hierarchical structure for building the prediction model (Cavalheiro and Carreira, 2016).

Besides, due to AM's high design freedom for producing end-use parts, AM processes provide part designers with a valuable opportunity to produce a wide range of parts (Thompson et al., 2016). However, the high design freedom of production also results in the AM process being more complicated, in terms of complex mechanical structures and unique design features. Furthermore, in some multiple-part production processes, such as selective laser sintering (SLS) and selective laser melting (SLM) (Gibson et al., 2010), a single AM production process can build several different parts at the same time. In these processes, the orientations and locations of the parts are determined by

process operators, which is noted as an AM process planning issue (Zhang et al., 2014). Due to the high design freedom in part production and the various processing plans in each AM process, AM systems are able to create countless possibilities for multiple part production, offering part designers and process operators a variety of options in part and process design (Peng et al., 2018).

In order to help part designers and process operators to understand AM process design, design for additive manufacturing (DfAM) was proposed. The term DfAM is derived from design for manufacturing and assembly (DfMA) (Thompson et al., 2016). Similar to DfMA, DfAM includes numerous design-relevant aspects, such as material design, part geometry design, and process planning, each of which involves many design-relevant features (Gibson et al., 2010). These features also play into factors that impact AM energy consumption, which are decided before starting the producing process by part designers and process operators (Qin et al., 2018). Modelling the design-relevant data of AM systems to predict energy consumption, and then reducing it by optimising the designs and decisions of part designers and process operators have become a crucial research topic for improving AM systems.

1.3 Research Objectives

Following the background and motivations, this research aims to pave the way for AM energy consumption modelling, prediction, and management, which provides a feasibility study for Industry 4.0. To achieve the aim of this research, the following research questions have been formulated:

- 1. What is the implementation plan for AM energy consumption analytics based on the understanding of Industry 4.0?*
- 2. What is the impact data information of AM energy consumption, and how to sense, collect, and integrate the data of these impact features from multiple resources to build the energy consumption model?*

3. *Out of these impact features, what is the most essential features for AM energy consumption modelling, and how to predict energy consumption by using these features?*
4. *How to deliver AM energy consumption management including framework, modelling, prediction, and optimisation, and what are the suggestions for the decision-makers to manage AM energy consumption?*

The origin and relevance of these research questions will be made clear in chapter 2 through a thorough literature review. The answers of these research will be detailed in chapters 3, 4, 5 and 6. The outline of this thesis will be introduced in the next section.

1.4 Thesis Outline

Chapter 1 aims to provide broader contexts and background as to the motivation and significance of the research provided in this thesis.

Chapter 2, Literature Review, provides a thorough review of the existing body of literature. It is divided into three main parts: (1) the details of different AM technologies, including the working principles, standard data, design for AM (DfAM) and research of AM process optimisation. (2) the AM energy consumption analysis and its impact features, including energy consumption comparison of various AM technologies, impact features of AM energy consumption, design-relevant impact feature of AM energy consumption. (3) the advanced data analytics, including current popular data analytics for AM, the introduction of machine learning and deep learning, and advanced data analytics for the AM.

In **Chapter 3**, a framework is proposed for modelling, predicting, and managing the energy consumption on the AM process in the second half of this chapter. The framework consists of four layers, the data sensing and collection layer, the data preprocess, and integration layer, the data analytics layer and knowledge and application layer. The approaches proposed in chapter 4, 5 and 6 are based on this framework.

Chapter 4 focuses on multi-source data analytics on the AM process. The chapter firstly introduces a detailed data sensing and collection approach for an AM process. This data sensing and collection approach can collect four primary datasets from an AM process, design-relevant dataset, working environment dataset, material condition dataset, and operation dataset. By using the multi-source data, a data integrating, and modelling approach is then proposed for AM energy consumption modelling in this chapter. In addition, the approach proposed in the chapter is validated by the case study. The results are compared to the benchmarks and show the merits.

In **Chapter 5**, the energy consumption impact features are compared firstly. Due to the literature review and finding of feature comparison, AM design-relevant features are examined and targeted as the main inputs of AM energy consumption prediction. Based on the CAD models collected from the target SLS system, the characteristics of design for the AM process are determined, including part design and process planning. These two types of design-relevant features are decided by two groups of people, part designers, and process operators. With the understanding of the design-relevant features, an AM energy consumption prediction method is proposed. Relying on the previous work, design-relevant data is used as the input dataset. Moreover, the method is validated on a real AM system. Results are compared to the one from multi-source data modelling and benchmarks.

Chapter 6 aims to create the management of AM energy consumption in terms of framework, modelling, prediction, and optimisation. Based on the modelling and prediction approach, this chapter proposes a deep learning-based particle swarm optimisation (DL-PSO) algorithm to increasing AM energy efficiency for energy consumption management. Compared to the conventional PSO, the proposed algorithm can increase the search speed and enhance the global best. The optimisation results are validated by four examples which cost different energy consumption and included various designs. The results have shown that the optimisation can reduce energy consumption significantly. In addition, with the optimised design-relevant data, part designers and process operators can be guided to modify their design and decision for saving energy.

Chapter 7 concludes this thesis by re-visiting and answering the research questions provided in this chapter. In the conclusions chapter, the entire research is discussed and reflected. The restrictions and future works are examined. In addition, the main contributions to the body of knowledge resulting from this research are summarised.

1.5 Contributions

This thesis makes several contributions to the wider body of knowledge.

1. A contribution is made within the field of AM with the framework of achieving Industry 4.0. The framework focuses on AM energy consumption modelling, prediction, and management. It outlines technical stages to achieve Industry 4.0 levelled manufacturing system in terms of AM energy consumption topic.
2. In order to model AM energy consumption, a comprehensive multi-source data integrating and modelling approach is proposed. This approach shows the way from sensing and collecting data from target AM system to integrate and model AM energy consumption.
3. Based on the multi-source data analytics of AM energy consumption, an energy consumption prediction method is provided using the design-relevant data, which AM energy consumption can be predicted before the production. Two types of design-relevant features are included, which are determined by part designers and process operators. In the case study, 12 design-relevant features, decided by part designers and process operators, are examined and were used to build the energy consumption model.
4. To manage the energy consumption by optimising the design-relevant feature, a deep learning-based particle swarm optimisation (DL-PSO) method is proposed. The DL-PSO can obtain better results with lower time cost comparing to the conventional PSO. In the feasibility study, reducing energy consumption is the main purpose of energy management. The proposed method was tested on four productions, and energy consumption has been reduced significantly.

Consequently, this PhD research has achieved the aim of improving the AM system to Industry 4.0 level, in terms of modelling, predicting, and managing the energy consumption by using advanced data analytics technologies.

Chapter 2 Related Works

2.1 Introduction

This chapter reviews the related works and previous relevant research concerning the three main sections, AM technologies, impacts on AM energy consumption and advanced data analytics. In section 2.2, five popular AM technologies are reviewed at the beginning. With the knowledge of AM processing, the data generation process of the AM process is presented for determining the data that is generated during the AM production process. Especially, the design for additive manufacturing (DfMA) is then examined. Several previous AM process optimisation studies are reviewed at the end of this section. The information and research of AM energy consumption is reviewed in Section 2.3. The energy consumption of five popular AM technologies is compared. Following it, the impacts of AM energy consumption is studied based on the relevant literature, which are divided into three classes, processing attributes, design-relevant attributes, and material attributes. The design-relevant impacts are highlighted, which is considered as the essential impacts. The advanced data analytics is reviewed in section 2.4, including popular conventional machine learning algorithms, basic deep learning knowledge and algorithm, and the previous research of advanced data analytics for AM.

2.2 AM Technologies

The AM process is widely known as a complex and popular digital system in Industry 4.0. The AM is also called 3D printing, Additive fabrication, Rapid prototyping, and

Freeform fabrication (Gardan, 2016). The first AM systems was built in the 1980s as a solution for producing prototyping quickly. The AM systems began with the initial commercialisation of the plastic process, which was known as Stereolithography (SL) in 1987. With rapid development, the AM has become a wide ranging fabrication system in Industry 4.0. AM can produce single and multiple material, various size, and even the end-used parts (Wohlers and Gornet, 2014).

AM includes various technologies, such as electron beam melting (EBM) (Węglowski et al., 2016), selective laser melting (SLM) (Gross et al., 2014), and selective laser sintering (SLS) (Gross et al., 2014), fused deposition modelling (FDM) (Tanikella et al., 2017) and STereoLithography (SLA) (Wang et al., 2015). Due to the various working principles, these AM technologies are very different regarding the main components, material supply, and the producing parts. These five AM technologies will be introduced in this section firstly. However, a typical AM process generally includes six stages (Convert, Locate and orient, Support structure, Slice, Build, and Post-process). In this standard process, various data is generated including many features, such as process features, working environment features, design-relevant features and material condition features. The data generation process of AM process will be examined in section 2.3.2. In these features, the design-relevant features are recently focused by many researchers due to the complex structure and high degree of freedom of AM produced parts, which is claimed as the term, design for additive manufacturing (DfAM). The DfAM will be explained following the AM data generation. At the end of this section, the previous works about AM process optimisation will be reviewed and discussed.

2.2.1 Popular AM Technologies

Five popular AM technologies are introduced in this section with detailed schematics, EBM, SLM, SLS, FDM, and SLA. The working principles and main material supply are different.

- **Electron beam melting (EBM)**

The EBM technology uses a concentrated beam of electrons to melt metal powder or filament (wire) material to build products. Figure 2.2 shows the schematic metal wire-based EBM system. The electron beam gun releases the electron beam to melt the metal material that is supplied by a material feeder on build bed. On the build bed, the melting alloy pool fuses with the prior deposit to build the re-solidified alloy which combines the producing part. The main supply materials of this AM technology is either beam or power type, such as Ti-6Al-4V, 316L, and stainless steel. It is highlighted that the EBM process is approximately 95% energy efficient. This is 5 to 10 times better than the laser-based AM process (Huang et al., 2016, Xu et al., 2018).

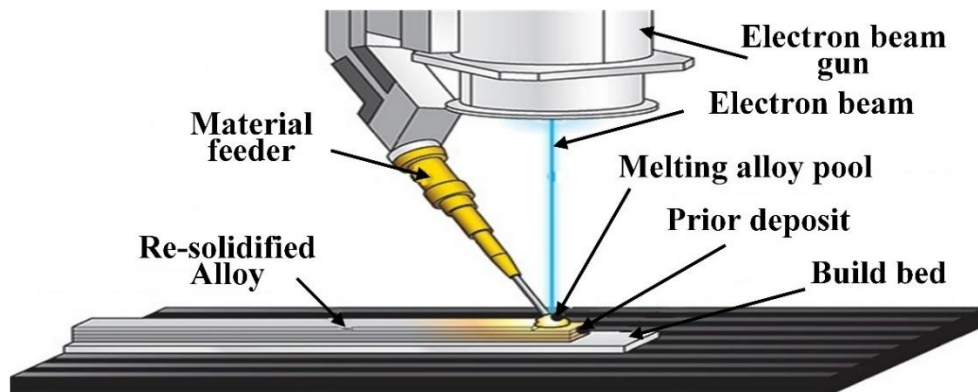


Figure 2.1 Schematic of EBM adapted from Węglowski et al. (2016)

- **Selective laser melting (SLM)**

The SLM technology uses high power-density laser power to melt metal powder material to build products. The schematic of SLM is shown in Figure 2.3. The high power-density laser beam is controlled by the scanner to melt the powder type metal material on the fabrication powder bed. When one layer is built, the roller pushes the material from supply system to the build bed thereby preparing the next layer. Finally, the producing part is built successively. The main supply materials of this AM technology is powder type, such as Ti-6Al-4V, 316L, and stainless steel (Sing et al., 2018). The SLM tends to produce parts with near full density (up to 99.9% relative density). While, this AM technology is commercialised, there are still many research and industrial challenges, such as balling effect, extensive cracking, limited flow

ability of ceramic, and the required high preheating of the chamber (Moritz and Maleksaeedi, 2018).

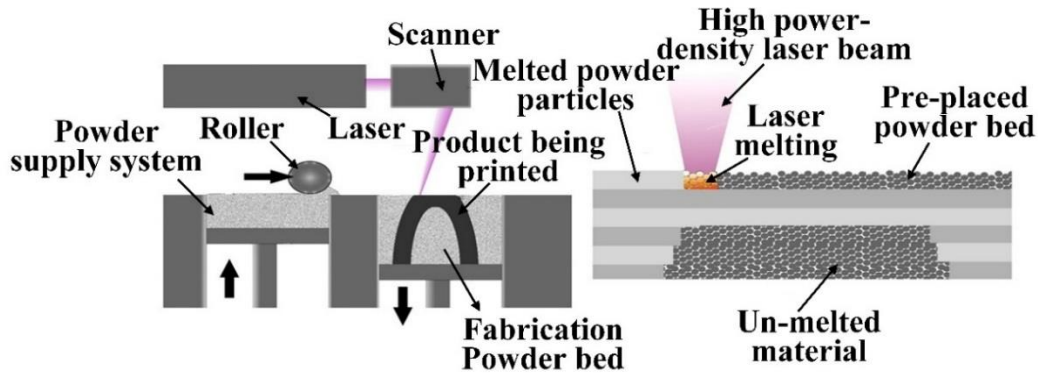


Figure 2.2 Schematic of SLM adapted from Gross et al. (2014)

- **Selective laser sintering (SLS)**

The working principle of SLS is similar to SLM. The SLS schematic is shown in Figure 2.4. The significant different between these two AM technologies is the power of the laser and the material used. The SLS uses lower laser power. The main powder type material are non-metallic, such as polyamide and nylon (Chen et al., 2018). Due to the material properties, the SLS normally does not require structures to support the produced part. The un-used powder plays the role of support structure (Sing et al., 2017).

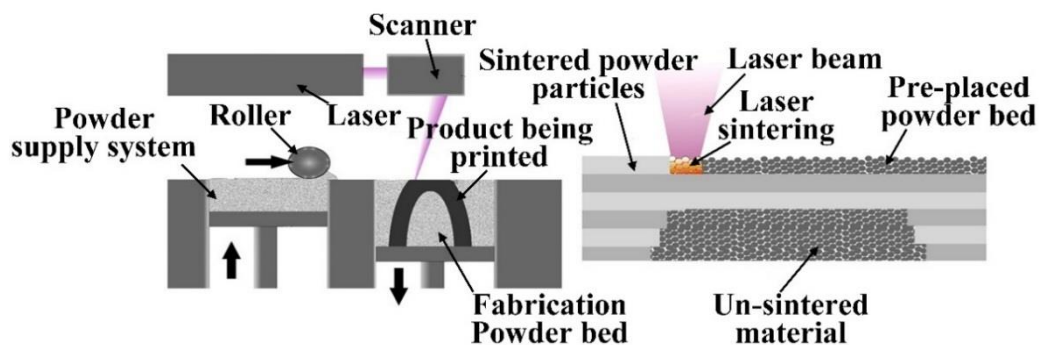


Figure 2.3 Schematic of SLS adapted from Sing et al. (2017)

- **Fused deposition modelling (FDM)**

The FDM fuses thermoplastic filament material by heating printer extruder head's nozzle to build products, which the schematic is shown as Figure 2.5. The beam material is supplied by the motor and melted by heating head. The melting material is then pushed out from the nozzle, which combines solidified part to produce the part. When the part has the suspended structure, the support structure is necessary. The main supply materials of this FDM is also beam type, such as acrylonitrile butadiene styrene (ABS), polycarbonate (PC), etc (Skowyra et al., 2015). This AM technology has been widely used as the personal 3D printer due to its affordable machine price and material.

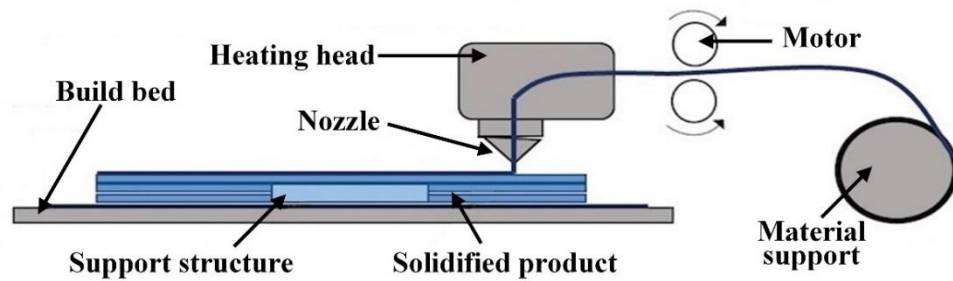


Figure 2.4 Schematic of FDM adapted from Tanikella et al. (2017)

- **Stereolithographic (SLA)**

The FDM uses photo polymerization converts liquid materials (photopolymer) into a solid form which the schematic is shown as Figure 2.6. The photo polymerization is released by light-emitting device and controlled by the scanner to solid the liquid materials. The producing part is pulled out when it is fully built. The main supply material of this FDM is a liquid, such as poly1500 or TuskXC2700T (Lee et al., 2015b). However, this AM system is very expensive, a typical SLA system normally costs about £200,000 (Salonitis, 2014).

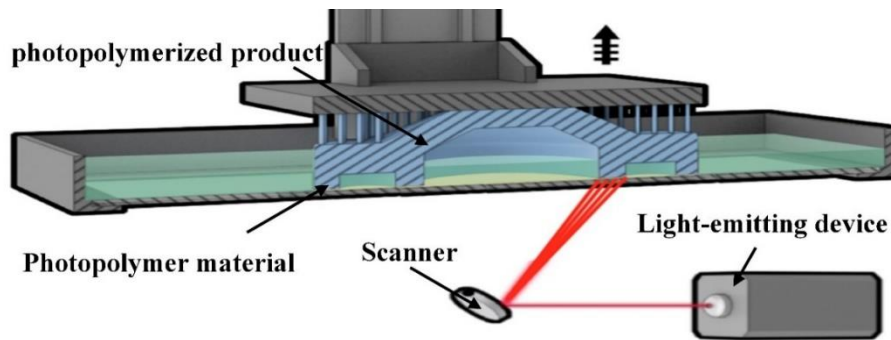


Figure 2.5 Schematic of SLA adapted from Wang et al. (2015).

2.2.2 Data Generation of the AM Process

With the information of five popular AM processes, this section will introduce the standard AM process in the data generation perspective. AM process can be considered as a data generation process starting from the initial order to the product delivery. This process includes six stages, Convert, Locate and orient, Adding support structure, Slice, Build, and Post-process, which is shown in Figure 2.7 (Wang and Alexander, 2016).

Typically, when customers make an order the CAD models are sent to the AM company. In the first stage (Convert), all of CAD (Computer-aided design) models, created by any design software, are converted into a particular format, such as STL (Standard Tessellation Language) format. Then, these models are sent to AM process operators (Sturm et al., 2017). In the next stage (Locate and orient), system operators decide orientations and positions of each part in every production (Sealy, 2011). The location and layout rotation of each product in the building bed depends on the operators' knowledge and experiences. Particularly for multiple part production, the decisions on orientations and positions of the parts are challenging as they need to match several requirements. Sometimes operators have to forego lower priority requirements, such as minimum energy consumption.

AM system software helps operators to add a supporting structure if it is necessary, which is the Support structure stage. Both of the two stages (Locate and orient (Das et al., 2015), and Support structure (Hussein et al., 2013)) generate information about the products orientation, position and supporting structure. The AM aided software

then creates slice files (Slice) for the system to organise the processing paths of each layer (Gross et al., 2014). During the production process (Build), sensors generate sensing data to represent the working and environment information. Before shipping to the customer, the products need to be cleaned and checked. Unfused powders and support structures are removed in the Post-process stage. In this stage, material usage and product accuracy data is obtained.

Consequently, the whole data generation process creates a considerable volume of data from multiple data sources, up to one trillion voxels of information with dozens of attributes (Dehoff, 2015):

1. **Process operation data** (Steed et al., 2017, Uhlmann et al., 2017) is the data generated by the parameter settings which is controlled by process operators e.g., many factories: scan speed, scan power, and laser power rate. Generally, operators follow the induction training to set these parameters. They may also decide to modify them sometimes.
2. **Working environment data** (O'Regan et al., 2016, Uhlmann et al., 2017, Zhao and Rosen, 2017) represents the working environment of the system during production, e.g., environment temperature, and chamber temperature. This data normally is collected from the monitoring system of AM machines. It will depend on how the monitoring system was designed. In many cases, the machine owners still build-up an extra monitoring platform for collecting more data from working environment.
3. **Design-relevant data** (Diegel et al., 2010, Hällgren et al., 2016, Sturm et al., 2017) is collected from design for AM, e.g., part orientation, part height, and part geometry. It can include part design (CAD models), process planning (part layout of the building bed) and material design (multi-material parts). This data depends on the technique requirement and human experiences.
4. **Material condition data** (Han et al., 2015, Meredig, 2017) is represented the material condition, e.g., material density, material humidity, and material melting point. With the different material condition, the finished parts can show very

different performance, which have been paid attention to by many materials researchers.

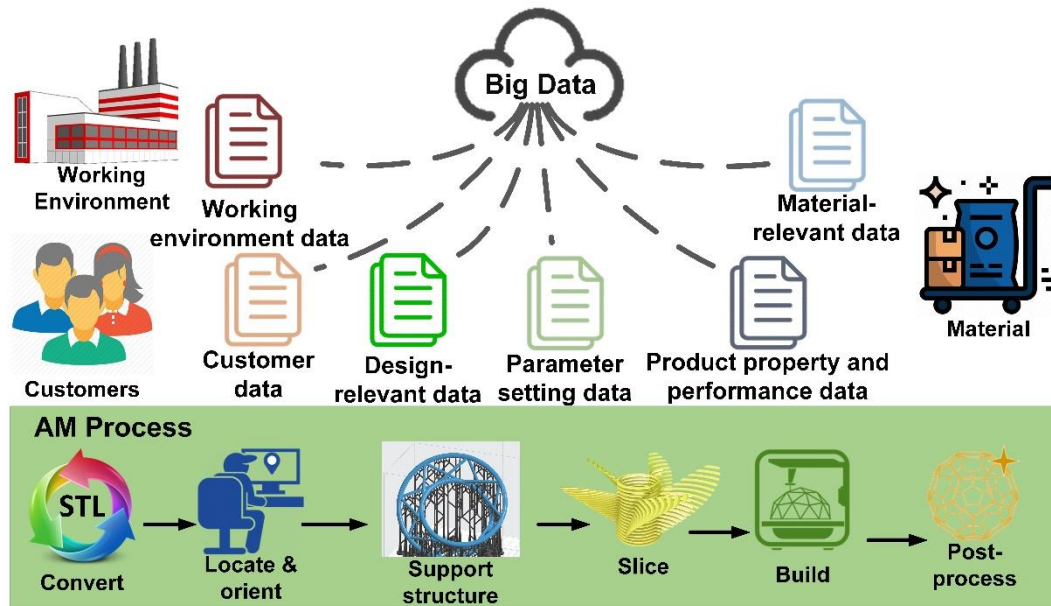


Figure 2.6 data generation process in AM system

The four primary data has mainly constituted a multi-source database of the AM system. While existing studies reveal that design-relevant features have influenced many issues of AM in practice, it has not been given sufficient attention. In the next section, the design for additive manufacturing will be focused and the relevant previous studies will be reviewed and discussed.

2.2.3 Design for Additive Manufacturing (DfAM)

AM provides designers with a unique and far-reaching freedom to optimise their designs, which makes the design of part production and processes more sustainable (Gebisa and Lemu, 2017). The parts produced by AM processes are also generally more complex than conventional manufacturing parts, in terms of geometry and internal structure. The design of these complex parts include additional design freedoms and high product level, especially in part consolidation (Becker and Grzesiak, 2009), part embedded (Gibson and Rosen, 2015), and direct production of assemblies

(Calignano et al., 2014). It is difficult to apply conventional manufacturing design methods to AM production due to such special features.

Current studies on Design for Manufacturing and Assembly (DfMA) typically focus on the standard geometric parts that are produced by conventional manufacturing systems. It makes DfMA methods no longer suitable for use in AM design (Li et al., 2019). Furthermore, there exists an urgent need to provide AM design professionals with a greater range of design and analysis tools for complex part structures and AM processes, Design for Additive Manufacturing (DfAM) has been proposed as a way to address such design problems in AM processes, which has been extensively explored (Tang and Zhao, 2016).

Thompson et al. (2016) reviewed over 300 research articles to summarise the research status, trends, challenges, and opportunities of and for DfAM. The authors of this paper claimed that DfAM was substantially different from conventional manufacturing assembly design in many aspects, such as knowledge, tools, rules, processes, and methodologies. They believed that AM processes require a new design framework because they involve various irregular factors, such as production time, cost, batch size, and so on, in contrast to conventional manufacturing processes. Additionally, the study reviewed a significant number of related works, which covered such topics as part geometry design, process design, and AM material design. Notably, the importance of DfAM was emphasised in cases that examined multiple customised parts produced by AM processes. On top of understanding functional optimisation, understanding sustainable optimisation is another significant objective of reviewing these DfAM studies, and this was highlighted throughout the paper.

Tang and Zhao (2016) published a survey of the sustainability of DfAM. This paper focused on LCA and environmental impacts motivating product designers to optimise AM processes designs. The authors of this survey mentioned that the existing designs methods for AM process primarily focus on fine-tuning product functional performance including size, shape, and topology optimisation. In this survey, several DFAM methods are reviewed and compared as well. For instance, a formal framework was proposed by Rosen (2007) focused on the process, structure property relationship.

This framework considered cellular structure's function and its manufacturability. Another method was proposed by Ponche et al. (2017). In this framework, three main steps of DFAM were pointed out: global analysis, dimensional and geometrical specification design and fulfilment of manufacturing. With these steps, the design process can gradually include manufacturing knowledge. Apart from the methods included in the survey, the DFAM methods are continually discovered and proposed by many other researchers.

Ma et al. (2018) proposed a framework that integrated part lifecycle sustainability with AM product design. In this framework, the AM part lifecycle was described in detail including the part design, production process design, cost and usage control, and end-of-life handling stages. The part and process design was the most critical aspect of their framework and was highlighted throughout it. Factors input into the framework included energy, material support, equipment, and logistics. Process cost, environmental impacts, and potential human toxicity were returned as outputs. To validate this framework, Ma et al. (2018) presented a case study targeted at a gear. This study handled each part of its framework independently, but the described stages—from part design to end-of-life handling—interact, meaning that every stage affects the others. Furthermore, it only produced LCA results without any optimisation.

Gardan and Schneider (2015) introduced a design optimisation method, topological optimisations, for improving the part structure of the SLS process that discovered the knowledge of manufacturing limitation and situation from the SLS process. Further, a unique design structure that can clean unused powders augmented to this method's optimised results. The method was validated by a case study using steel part example by different AM process: FDM, SLS and SLA. However, these optimisations are considered to be unable to match the fabrication capabilities of AM processes; the researchers must examine the process's design methods in more detail (Tang and Zhao, 2016). Moreover, Gebisa and Lemu (2017) pointed out that sustainability is an essential component of DfAM and discussed how current AM processes are not sufficiently energy efficient, as general manufacturing design principles are not suitable for use with them.

Based on this understanding of DfAM, Tang et al. (2016b) proposed a framework that integrates design in LCA assessment with the AM process. This framework used an LCA model to assess the environmental impact of the AM process, and design-relevant data was input into the framework. Moreover, they proposed a design for optimising energy consumption and material used according to this method. The paper also presented a case study validating the framework's performance, using an aircraft engine bracket as the target product. Following their framework's process, creating an optimised engine bracket design for production through AM remained the primary objective and kept the safety factors. The produced design required approximately 47% less material than did the original design; this figure was also lower than those of the optimised designs of conventional manufacturing processes, like the computer numerical control (CNC) process, by 22%. To produce new parts, more than half of the CO₂ equivalents were either for AM or conventional processes. However, this new design only facilitated a production energy consumption approximately 2% lower than that of the original design through both the AM process and the conventional process. It is apparent that reducing energy consumption was more difficult than was optimising other LCA assessment indicators. The framework of Tang et al. is a fundamental architecture for AM process designers who seek to optimise their designs to protect the environment (Tang et al., 2016b).

2.2.4 Short Summary

AM has not only been a popular manufacturing technology for research but has also increasingly been employed by industry. It includes various technologies, such as EBM, SLM, SLS, FDM, and SLA, which produce different material products. Even with the different technologies and working principles, the general data generation of an AM process is similar, which can sense and collect different types of data from the process. It offers an opportunity to data-driven methods for solving problems. The design relevant information becomes interesting for many related researchers. According to the above research on DfAM, it is widely viewed as one of the most necessary aspects of AM systems, especially for sustainability analysis. Additionally, DfAM integrates design features for AM process optimisation. The research on AM

sustainability has become a crucial research topic. In this PhD research, energy consumption is selected as one of the most critical sustainability issues, which is reviewed in the next section.

2.3 AM Energy Consumption Analysis and Impacts

It is now established that AM is regarded as a comprehensive manufacturing system. It is interesting to know the energy consumption of AM processes accurately (Watson and Taminger, 2018). In this section, the energy consumption of different AM technologies is compared to show the range of AM energy consumption. Then, energy consumption impacts are determined from the previous literature. With the focus of design-relevant features, the design-relevant features of AM energy consumption are reviewed.

2.3.1 Energy Consumption Comparison of Different AM Technologies

Based on different working principles shown in the previous section, AM technologies have been applied to a number of different systems with various material supplies, it is interesting that the energy consumption has shown a large difference, as indicated in Table 2.1.

Table 2.1 Energy consumption comparison between different AM technologies

AM technologies	Unit energy consumption (kWh/kg)
EBM (Baumers et al., 2012)	17.0 to 49.1
SLM (Kellens et al., 2010)	26.9 to 38.75
SLS (Sreenivasan and Bourell, 2010)	14.5 to 36.0
FDM (Baumers et al., 2011)	23.01 to 346.4
SLA (Baumers et al., 2011)	20.7 to 41.4

By understanding the working principles of these five AM technologies, there are several interesting points shown with the energy consumption. For instance, EBM and SLM both use similar materials. But their energy consumption rates are different due

to their different working principles. EBM utilises the concentrated beam of electrons to melt metal powder or filament material in order to build products, while SLM utilises the high power-density laser to melt metal powder material to build products. Moreover, SLM and SLS apply a similar technique. However, their energy consumption level shows large difference caused by different material usages. Comparing SLA and SLM, although the working principles and materials are different entirely the energy consumption rates are similar. Furthermore, even using the same technology and the same materials to conduct tests, the changes incurred in terms of energy consumption. Thus, it highlights the difficulty in analysing and optimising the energy consumption of AM systems (Sreenivasan and Bourell, 2010, Gross et al., 2014, Watson and Taminger, 2015, Telenko and Seepersad, 2010). That means the energy consumption of AM processing is challenging to analyse and optimise. Many researchers have shown that energy consumption of AM processing is caused by many different components and impacted by numerous attributes.

According to the above studies, the level of AM energy consumption is typically described as low efficiency in a wide range. The problems regarding AM energy consumption are challenging to researchers due to the complexity of AM processes and various impact factors. In the next section, the energy consumption impacts are determined.

2.3.2 AM Energy Consumption Impact Factors

Table 2.2 has shown the differences in the rates of AM energy consumption caused by many different components and impacted by numerous attributes. Based on the system understanding and manufacturing experience, research has found correlations between energy consumption and various processing attributes of AM processes, such as processing, product design, and material attributes.

Table 2.2 Energy consumption related attributes of AM systems in literature

Literatucre	Processing attributes	Product design attributes	Material attributes
Sreenivasan and Bourell (2010)	Scan speed; Laser power rate; Build platform size	N/A	Material powder density

Gross et al. (2014)	Layer thickness; Laser beam radius; Scan speed; Laser power	Part orientation	Material powder absorption
Watson and Taminger (2015)	Feedstock and recycling transported distance; Build platform size	Volume of deposited material	N/A
Telenko and Seepersad (2010)	N/A	Z-height	Material powder density
Baumers et al. (2011)	Processing procedures; Build time	Part geometry; Z-height; Capacity utilisation	N/A

In Table 2.2, literatures have shown various models for examining energy consumption in AM systems. However, the impacts are inconsistent because many correlations exist. Thus, it is difficult to identify all related attributes of AM process energy consumption from a single study or experiment. Specifically, Sreenivasan and Bourell (2010) applied a basic energy consumption function, where the voltage and the current are the main inputs. In their study, system power is calculated from 1000 watts to 2500 watts, and the heater system is highlighted as the largest energy consumer. Furthermore, this article shows that scan speed, laser power rates, build platform size, and material density impact the energy consumption in the targeted AM system. However, energy consumption modelling was not established in this paper.

Watson and Taminger (2015) built an energy consumption model by considering the impact of the process and product design attributes, such as the feedstock and recycling transported distance, build platform size, and the volume of deposited material. But, in this paper, the energy consumption model was suggested without any experimental validation. In another paper, Telenko and Seepersad (2010) compared the differences in energy consumption between SLS and injection moulding (IM). They also revealed the correlations between energy consumption and build height and material density, which were obtained from the experimental results. A Similar methodology had been also applied by Baumers et al. (2011). In this research, the energy consumptions of two SLS machines were compared. They defined an AM process with 3 phases of energy consumption, which are warm-up, building, and cooling down. Furthermore, the authors indicate that product geometry could have an essential impact on energy consumption in the AM system. From these studies, some researchers consider

processing attributes are more closely related to energy usage. They contain scan speed, layer thickness and building time. While, product design attributes, such as part orientation, the products of height, are also defined as critical energy-relevant factors in AM systems, which are reviewed in next section with more details.

2.3.3 Design-relevant Impacts on AM Energy Consumption

It is highlighted that the design-relevant data highly depends on human's activities, which includes two categories, part design data and process planning data. These two types of data are determined by part designers and process operators. However, design-related impacts are often overlooked due to their complexity.

Zhang et al. (2018a) believed that a bio-inspired part design could improve sustainability through functionality improvements, the reduction of material usage and energy consumption, and the introduction of smaller environmental impacts. They applied this idea to the part design stage in the AM process and proposed a conceptual model for redesigning areas of the AM process. This model integrated DfAM principles with bio-inspired design aspects, such as material features, production process parameters, and product functionality. A case study was conducted which compared three different part filling structures (diamond, honeycomb, and bone) using an SLS process. The bone structure was considered the bio-inspired structure in this study, and many factors relating to the structures, such as their physical properties, basic stress analysis results, energy consumption rates, and other LCA assessments, were compared. Notably, the energy consumption of the bone structure was found to be lower than that of the honeycomb structure by 8% and that of the diamond structure by 12%. The bio-inspired geometrical design highlighted in this paper provides a solution for the structural design of the AM process which reduces energy consumption and maintains product functionality.

Aside from parts' filling structures, other design-relevant factors also draw researchers' attention. Panda et al. (2016) pointed out that slice thickness and part orientation are two significant factors in determining AM energy consumption. An optimised framework based on genetic programming was proposed to develop the relationship

between energy consumption, slice thickness, and part orientation. In their experiment, slice thickness varied between 0.02 mm and 0.10 mm in intervals of 0.02 mm and part orientation varied between 0° and 45° in 5° intervals. Other process parameter settings were kept the same. Based on this approach, energy consumption can be predicted with an error rate of 3.45%. Based on the idea that slice thickness and part orientation are two important aspects of AM energy consumption, Paul and Anand (2012) also conducted several experiments on part orientation. In these experiments, three geometric primitives (a cube, a cylinder, and a functional part) were built in three slice thicknesses (0.03 mm, 0.05 mm, and 0.10 mm) and three part orientations (0°, 30°, and 45°). The energy consumption of the production process was then monitored. For each geometric primitive, energy consumption decreased as slice thickness increased and orientation degree decreased. However, it is difficult to compare the amount of energy consumed in the production of these three geometric primitives because these experiments monitored total energy consumption rather than the unit energy consumption of each process. According to the above studies, filling structure, slice thickness, and part orientation impact AM energy consumption. However, only a single part was built in each AM production experiment, which happens rarely in current AM production processes (particularly SLS and SLM).

Baumers et al. (2012) claimed that differences in energy consumption are revealed between processes in which a single part is built and processes in which multiple parts are built. In their study, six AM systems, including SLS, SLM, electron beam melting (EBM), and fused deposition modelling (FDM), were tested and compared; each system produced both a single part and multiple parts within a single production process. On average, building multiple parts costed approximately 25% less energy than did the production of single parts, and the SLS system was found to use 97% less energy than the other systems examined in this study. However, it is difficult to draw a conclusion on the energy consumption behaviours of these systems based on these experiments alone. Further, each experiment used the part design that was based on the single-part production process to generate a multiple-part production process design. In an AM process, various part designs are combined and built together to produce a suitable process design. Moreover, the chosen process plan varied in terms

of orientation and part positioning for each AM technology that was used; this was not addressed in the paper. Therefore, due to the complex process and various impacts, it is necessary to apply real data rather than experimental data to analyse and model AM energy consumption.

2.3.4 Short Summary

According to the above related works and previous research of the AM technologies and energy consumption analysis, the issue of AM energy consumption analysis is a crucial research problem. However, manufacturing is currently moving into the next industrial revolution, Industry 4.0, which allows the production equipment to sense and collect more data from AM systems (Shrouf et al., 2014). With more data being sensed and collected, the behaviour of energy consumption in AM systems tends to be predictive by advanced data analytics. Advanced data analytics, as a range of approaches, was researched in this thesis, especially machine learning and deep learning. In the next section, the conventional machine learning algorithms and deep learning algorithm are introduced, and the relevant previous research is reviewed.

2.4 Advanced Data Analytics

Advanced data analytics refers to a group of technologies which are applied to data to solve the critical problem. Sometimes it is not a specific technology but rather a combination or integration of several methods to gain information, build predictive model, and discover the relevant knowledge (Bose, 2009). Different technologies provide various function and solution for the research or industrial problems. For example, the data mining and data integration generally is used for discovering the pattern recognition and identifying the relationships. Evolutionary and Swarm Algorithms (EAS) normally focus on the multi-objective optimisation problems. Neural networks can anticipate decisions and assist in predictive analytics (Brook Wu et al., 2006). In some conventional machine processing, energy is significantly consumed which is able to be reduced by optimising several parameters and features, such as tool path of machining (Hu et al., 2018) and changing the multi-objective feature sequencing.

2.4.1 Process Optimisation by Advanced Data Analytics

One of the most powerful functions of advanced data analytics is to optimise the manufacturing process. Especially, the evolutionary and swarm algorithms (ESA) is a group of optimisation technologies, such as genetic algorithms (GA) and particle swarm optimisation (PSO). In this section, several research cases of process optimisation are reviewed.

Bensingh et al. (2019) introduced a hybrid approach that combines artificial neural networks (ANN) and PSO to optimise the injection modelling process parameters. In their study, the injection modelling process produced a bi-aspheric lens. The quality of the lens and its upper process capability was the model's optimisation validation metrics, and it was represented through the three main measures of each side of the bi-aspheric lens: radius of curvature, surface roughness, and waviness. In this study, seven parameters were optimised to improve the quality of products. An ANN based model was used to predict lens quality based on the injection modelling process parameters. Training and testing data were collected from the 44 experiments conducted over the course of the study. Based on the ANN prediction model, PSO was applied to optimise the parameters of the NN structure, including its number of neural layers, to improve the model's performance.

Moreover, the optimised results were compared to the GA- optimised ANN, and the proposed approach was found to return fewer errors and present a faster convergence speed than traditional PSO. The optimisation provided by PSO was proven to be better than that of GA. However, one of the six main outputs, the waviness of the shallow profile, was predicted with a substantial error larger than the mean error of the original values. With the similar idea, Perhinschi and Perhinschi (1997) modified standard GA to base on the floating-point representation of the chromosome and appropriate genetic operators to solve controller design problem of autonomous air-vehicle. Five parameters were optimised in this research by using the modified GA method.

Wang and Hsu (2008) proposed a GA-based, hybrid grey theory method to forecast high technology industrial output, which high technology industry is the rapidly

progressive technology with various demand and high investment. In the high technology manufacturing, factors such as production techniques, market demand and investment capital influence the development trends, making it difficult to forecast. In their study, as the traditional grey forecasting model is unreliable, the grey theory was used for predicting the output of the high technology industry, and the GA was used to minimise the prediction error of the model parameters. The results showed that the GA-based method achieved higher accuracy and a lower error rate compared to the Bayesian genetic model and the grey forecasting model. Besides, in the pharmaceutical industry, GA can provide a solution for some problems, like facility layout optimisation.

Janahiraman et al. (2018) introduced a hybrid method that integrates extreme learning machine with PSO to optimise CNC processing and product surface roughness. Two stages were identified as essential in their paper: modelling and optimisation. PSO was used for optimisation. Three inputs were used for modelling: cutting speed, feed rate, and cut depth. A difference of 24% was found to exist between the predictive results returned by this model and the real-world results. Additionally, it identified optimal parameter settings. Task scheduling presents another problem that is often solved by PSO methods.

Hamamoto (1999) introduced GA-based methods to optimise the facility layout design in pharmaceutical factories, which considered many objectives, such as operation cost, maintenance cost, material handling cost, and throughput rate. In this research, two facility layout methods are used, growth method and band layout method. Moreover, GA also shows the exceptional performance in machining. Yildiz (2013) introduced a hybrid differential evolution algorithm for selecting the optimal milling process parameters such as depth of cut, feed rate and cutting speed. This method compares the GA-based hybrid to other evolutionary algorithm-based methods. The achievement of the process is verified by using two objective functions, which are unit production time and unit production cost. The comparison of the algorithms focuses on the economic aspect rather than other aspects such as product quality and tool wear. Furthermore, GA can also optimise a nonlinear programming model.

Zhang et al. (2018b) published an article addressing the digital array radar (DAR) task scheduling problem, which was defined as an N-P problem and was, therefore, difficult to solve using only the meta-heuristic method. In this study, an integer programming optimisation model was built to establish the DAR task structure and was formed of multiple aspects. In addition, a hybrid PSO was proposed for improving efficiency in task scheduling schemes. This study adopted chaotic sequences and Shannon entropy equation to improve the quality of the initialised points and the convergence speed. When compared to three other scheduling optimisation methods (the online interleaving algorithm, GA-PSO, and the HPF algorithm), the proposed optimisation method obtained the highest successful scheduling ratio from the same number of targets. PSO improved when the initialised point and convergence speed coefficients were changed. The study was championed by many other researchers as one of the most important studies for PSO improvement. For example, Kennedy (2011) suggested setting the convergence coefficients as 2.05 and the initial coefficient as 0.7298 to improve the convergence speed of PSO. In next section, the focus is to AM process, some relevant researches are reviewed.

2.4.2 Advanced Data Analytics for AM

According to the data generated from AM process, current related research only uses a part of the data in this multi-source database, which is mostly collected from the process operation and the working environment. Steed et al. (2017) pointed out that it was essential to analyse process data to understand AM process. Thus, a software, called Falcon, was developed for a better exploratory visual analysis of the large, irregular and multivariate time-series data that are generated from AM process. Falcon software displayed data from system monitoring files with a clear visualisation. It allows users to check the data across multiple views and provides users with basic data analysis results, including the mean, quartile, and variance. Falcon software also showed product imagery to users helping people to understand the building condition of every single layer. However, their research focused on a single AM process which failed to reveal general knowledge of AM systems. O'Regan et al. (2016) proved some correlations between building environment and product voids and residual stress after

summarising critical process parameters and data in an SLM system. They found that most attributes that impacted the product voids and residual stress were represented and displayed as different types of data in system monitoring files by the target system. However, they did not establish any data analytical model in this paper, which was indicated as a future work.

It is well-known that AM processes are complex due to its high levelled automation and customization. Issues of AM process normally related to many impacts, which is a big challenge to researchers. Deep learning, as the most popular technology of machine learning, is considered to solve problems of complex system, such as AM process. Uhlmann et al. (2017) introduced a data analytical method, using neural networks to build a classification model, for assessing selective laser melting (SLM) process. This approach focused on the quality of product to classify products into three categories, perfect products, defective products and unfinished products. Data was collected from machine process log files and sensor log files, which included 16 different features, such as platform temperature, chamber temperature, layering time and process pressure. The neural network was used as one of the modelling algorithms, which showed merits compared to other conventional machine learning methods, such as nearest neighbour, Bayes classifier, and support vector machine (SVM). The highest predictive accuracy, showing by neural network model, is about 90%. They pointed out that more system behaviour knowledge could be discovered when more related data was collected and used, and data analytical methods could be optimised by expanding input data. This result proved that deep learning technology is suitable for AM process predictive problems comparing to other machine learning algorithms.

Shevchik et al. (2018) also paid close attention on the quality issues of AM process. They claimed that quality monitoring of AM process is lack of attention. In their paper, the acoustic emission was treated as the index of product quality. The acoustic signals of a SLM system are recorded by sensors. This type of data was shown as the light microscope images that presented the energy densities. These energy densities were classified as three different levels that represented three types of product quality (poor medium and high part qualities), which were able to observe on microscope images. Using these images as inputs, a spectral CNN was designed to build the classification

model. The classification accuracies were over 80%, specifically, poor quality is 89%, medium quality is 85% and high quality is 83%. This study using the leading-edge method, CNN, to solve the problem of AM process, which was claimed as a novel approach in research of AM process.

The AM process condition is another focus of attention, which deep learning technologies are often applied as solutions. Xiong et al. (2013) proposed a neural network structure to predict the process condition of a gas metal arc welding (GMAW) based AM process. In their study, a laser vision sensor was used with composite filtering technique to measure the bead width and height. These two measurements were inputs of the proposed neural network and process condition parameters were predicted, which were welding speed, wire feed rate, and arc voltage. The results of these predictions were acceptable. Specifically, predictive error of welding speed was 19.26%, error of wire feed rate was 22.69%, and error of arc voltage was only 1.19%. The second part of their study was predicting the bead geometry (width and height) using the welding speed, wire feed rate, and arc voltage. The error of width and height was only about 1% to 2%. Their study established a relationship between process variables and the bead geometry by using deep learning technology. Current research about deep learning for AM process tends to pay attention on the issues of quality detective and process monitoring. However, this leading-edge technology, especially CNN, can solve more than them. Combining product design model, CNN is a functional tool to extract product features that are too abstract to be represented by some specific attributes.

Vahabli and Rahmati (2017) also focused on modifying part orientation and layer thickness to improve the surface roughness. In their study, the target AM technology was FDM. They tried six different analytical models to build the relationship between surface roughness and the inputs, layer thickness and part orientations. By comparing the results of different models, the authors proposed a hybrid model to predict the surface roughness and it had shown its merits. The method was also validated by producing various parts with different material, parameters, and machines. This prediction model can help the AM operators to modify the layer thickness and part orientation for improving the surface roughness.

With the same interests, Asadollahi-Yazdi et al. (2018) believed the optimising parameter settings for AM process can improve the process. In their research, the layer thickness and part orientation were determined as the main target of the optimising parameters. By optimising these two important parameters, three objective functions were focused, production time and material mass, surface roughness, and mechanical behaviour (Ultimate Tensile Strength (UTS)). In this paper, the authors used the Non-dominated sorting genetic algorithm-II (NSGA-II) as the optimisation approach which was introduced by Deb et al. (2002) for solving multi-objective optimisation problems. In Asadollahi-Yazdi's paper, it can be proved that the production time, material mass, roughness and UTS of AM were influenced by layer thickness and part orientation. Apart from genetic algorithm, the PSO was another popular evolutionary algorithm.

PSO is one of the most famous evolutionary algorithms used to solve continuous, non-linear, multi-objective optimisation problems (Kuo and Lin, 2010, Tang et al., 2016a). Theoretically, the traditional PSO method works by sending out a swarm of particles to search for the best result according to the required limitations; each particle represents a feasible solution to the given problem (Zou et al., 2019). PSO was also used to solve AM process optimisation problems (Yusup et al., 2012). Ye et al. (2018) proposed a PSO-based method for optimising AM processes which features stochastic finite element analysis (SFEA). SFEA was used to model the output value, which was the residual stress in thin-walled parts. PSO was used to find the maximum value of the target within the limitations. The proposed method began by extracting the process parameters, such as layer thickness, melting temperature, scanning speed, and hotbed temperature flux, from the process. Also, the CAD part design model was considered a potential input variable for the SFEA model. The results of their case study were reasonable, and their research involved collecting part design data to characterise one of the essential process factors. This emphasises the necessity of carrying out further DfAM research.

Raju et al. (2018) proposed a hybrid PSO method integrated with bacterial foraging optimisation (BFO) to solve mechanical and surface quality problems of AM processes, such as those introduced by varying hardness, flexural modulus, tensile strength, and surface roughness. Four parameters were considered for input into the simulation

model: layer thickness, support material, model interior, and orientation. The model was built through multiple linear regression. Two types of part design were printed to model data collection, and 18 samples were produced for each. Three parameter setting combinations were used to uncover the best solution to each mechanical and surface quality problem. The PSO–BFO algorithm was then used to find the best parameter settings. This study exemplifies the advantages PSO can offer AM parameter optimisation and how it can be easily integrated with other algorithms for exceptional results. However, the authors selected the constant inertia weight and cognitive factors for the proposed PSO–BFO model without providing an explanation of either choice.

2.4.3 Short Summary

Advanced data analytics is a group of powerful data-driven technologies, such as GA and PSO, especially in the industrial big data environment. The big data provide sufficient historical data and information for mining the patterns. Technologies like machine learning and deep learning have the capability to learn and discover knowledge from data. With the optimisation methods, manufacturing processes are improved by optimising the relevant parameters.

2.5 A Critical View

In summary, five different AM technologies were presented in detail in section 2.2.1. With the understanding of AM systems, the data generation process of AM was displayed, and then the DfAM was focused as one of the interesting, relevant research topics. Following the knowledge of AM, the AM energy consumption analysis was introduced, which includes the comparison between different AM technologies, impacts, and design-relevant features. In order to solve the problems, advanced data analytics was selected as the leading technology. In section 2.4, the core advanced data analytics technologies were introduced, and the research cases of process optimisation were reviewed. At the end of the section, the research how advanced data analytics work on AM process was reviewed as well.

From these related works, the AM energy consumption analysis is proved as an interesting and significant research issue, which is able to be solved by advanced data analytics. It is also considered as an implementation of achieving an Industry 4.0 level manufacturing system.

Chapter 3 A Framework for AM Energy Consumption Analytics under Industry 4.0

3.1 Introduction

With rapid advancements in the industry, technology, and applications, many concepts have emerged in manufacturing. It is generally known that the far-sighted term ‘Industry 4.0’ was published to highlight a new industrial revolution. Many manufacturing organizations and companies are researching this topic. However, the achievement criteria of Industry 4.0 are yet uncertain. There is still a long way to go to improve manufacturing up to the required level to match all concepts with all dimensions, especially consciousness. Moreover, industry and academia demand a complete structure of these technology applications to show the development of manufacturing with the different levels of performance, which will be introduced in next section. AM is one of the most popular applications of Industry 4.0. Although AM systems tend to become increasingly automated and worry less, the issue of energy consumption still attracts attention, even in the era of Industry 4.0 (Frank et al., 2019).

In this chapter, a framework is designed for modelling, predicting, and managing the energy consumption of AM processes. This framework is designed by following the standard industrial data mining process, which is explained in Appendix A.1. The main sections of the framework are inspired by the 5C structure for Industry 4.0, which includes data collection, data transformation, data analytics and intelligent function

delivery (Lee et al., 2015a). In addition, the proposed framework includes the core elements of the AM process, which are reviewed in Section 2.2.

The framework includes four sections, Data sensing and collection section, Data Integration section, Data analytics section, and Information and Knowledge section. The framework demonstrates a comprehensive structure for building an Industry 4.0 level manufacturing from the hardware level to intelligence level, which the AM process is focused as the target system. At the end of this chapter, the experimental setup of this PhD research is introduced.

3.2 A Framework of AM Energy Consumption Modelling Prediction, and Management under Industry 4.0

According to the literature review in the last chapter, the AM system has some concepts, such as digitalisation, communication, standardisation, flexibility, and customisation. However, it does still not achieve the lower level of Industry 4.0 (Atzori et al., 2010). In order to upgrade AM systems matching the requirement of Industry 4.0 in the respective of energy analysis, a framework is proposed in this section. In this framework, an AM system is integrated. The production design, operators, and materials statement are integrated with AM machine to generate an energy model. In the model, plenty of data is collected, where information and knowledge can be discovered. Based on this design principle an IoT based framework is designed which is shown in Figure 3.1 (Qin et al, 2017).

In this framework, there are four sections, which are: The Data sensing and collection section, the Data Integration section, the Data analytics section, and the Information and Knowledge section. These four section are closely interlinked, and each section consists of several components

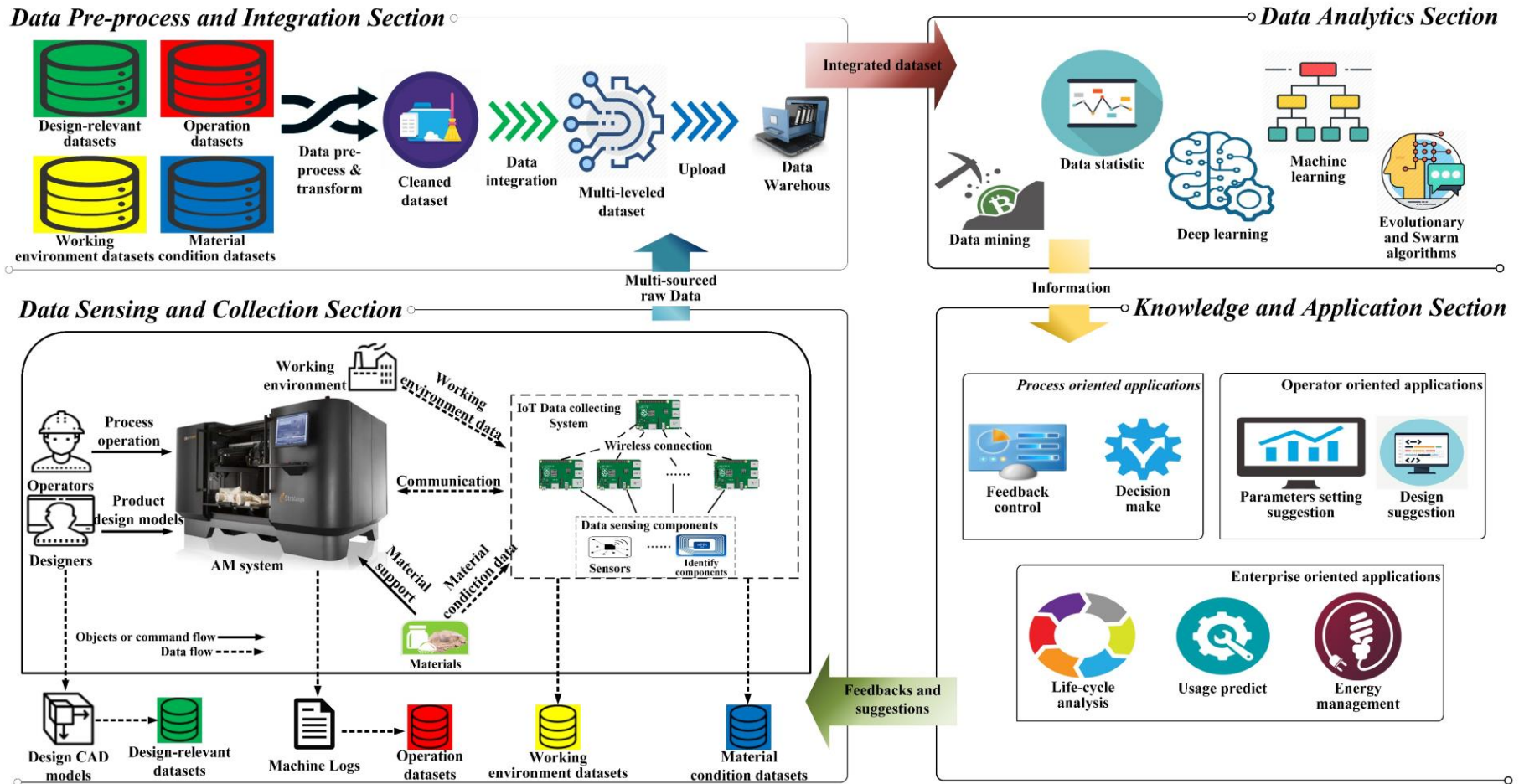


Figure 3.1 A Framework of AM energy consumption modelling, prediction, and management

3.2.1 Data Sensing and Collection Section

The Data sensing and collection Section is known as the AM production status and processing environmental condition where the target AM system, materials, operators, products, and other environmental factors are included. It is obvious that the AM system and other associated physical objects typically carry lots of relevant data invisibly. With different sensors and components, this invisible data is able to be extracted (Gajski et al., 1994). However, in this section, the digital data sets are only generated and collected as the raw datasets, which means this type of datasets tends to be unreadable, being represented as massive and meaningless strings of numbers. According to the previous work of AM system data generation, this section considers four types of premier datasets, design-relevant datasets, operation datasets, working environment datasets, material condition datasets.

The AM system is the main object of this research, as the majority of energy is consumed by it. Most current AM systems have embedded sensors in them obtaining various processing data collected during operation. This data is generally represented in the machine logs, which is created after each production. In addition, to achieve the integrated function, the IoT technology has become one of the best solutions, generate horizontal integration, end-to-end digital integration, and vertical integration in manufacturing systems (Kagermann et al., 2013). In this section, the IoT technology will be used to sense and collect the extra data for collecting other relevant data, which will be integrated in the energy model. The IoT based data collection system includes data sensing components, i.e. sensors, identify components and collection and transformation devices, i.e. embedded development boards. In next chapter, the data sensing and collection will be introduced comprehensively.

3.2.2 Data Pre-process and Integration Section

As mentioned in last section, the raw datasets are typically unreadable and massive. The first mission on the Data pre-process and integration section is data cleaning and transfer. By applying the data cleaning and transfer, the raw data is cleaned without missing value and outliers. All datasets are transferred into the standard data format,

which can be accessed by the database software, programming application, and basic analysis software. The most important step on this layer is data integration.

The data is collected from different resources, such as product design, working environment, operation parameter setting and IoT data sensing and collecting system. These data carry different information representing different features, which involve various and dimensions and tend to be nested as a multiple hierarchical structure. The features of these dataset structure are rarely independent (Rajeswaran and Blackstone, 2018). This data may be difficult to integrate using typical data integration methods, such as the extract, transform, and load (ETL) technique (Yin and Kaynak, 2015). Under this comprehensive data environment, it is very challenging to integrate the multi-source data which includes the multiple hierarchical structure for building the prediction model (Cavalheiro and Carreira, 2016). In this section, this nested data will be integrated by a novel technology which will be discussed in next chapter with more technical details. Also, the integrated data is upload to the data warehouse for the storage, which allows people to access the database in the local and cloud.

3.2.3 Data Analytics Section

When the integrated data is obtained from the previous section, Data pre-process and integration section, the integrated data is used for several advanced data analytics technologies, such as data statistic, data mining, machine learning, deep learning, and evolutionary and swarm algorithms, with different purpose.

For example, by applying data statistic, basic statistical analysis is obtained, which gives people a general idea of how the data is shown as for every collected feature and target values. With the data mining technology, the relationship between system energy consumption and related attributes can be found. The hidden information is exploited. Machine learning and deep learning technologies can build the energy consumption model which can predict the energy consumption of the AM system. The evolutionary and swarm algorithm can help to optimise relevant parameters and design for reducing the energy consumption. Overall, in this section the valuable information of AM energy consumption is discovery by several advanced technologies which

assist people in modelling, predicting and managing energy usage and making the correct decisions.

3.2.4 Knowledge and Application Section

In the Knowledge and application section, the discovered information is shown as different implementations and applications. The performance and applications can be divided into three sections; Process orientated applications, Operator orientated applications, and Enterprise orientated applications based on differently oriented objects.

In the section of processing orientated applications, AM processing receives the feedback controlling signals, which then changes the settings of the relevant parameters for reducing the energy consumption. These decisions change parameter are made by the IoT framework relying on the information and knowledge analysed from the preceding layer. Operators and designers are able to obtain the system energy consumption behaviour from the production energy recorded, and by predicting the future energy use from the Operator oriented applications. The information will be presented to them virtually and graphically; which can guide operators to utilize the system economically. In addition, they can also receive production design suggestion for improving the design. The enterprise manager is more interested in the system life-cycle analysis, energy sustainability analysis, and energy management which can also be delivered as the enterprise oriented applications.

This framework focuses on AM process energy consumption which creates a new method of energy consumption analysis in the age of Industry 4.0. This framework involves numerous related factors which integrate different attributes within the data and cloud-based database. Benefits from the data mining and big data analysis technology. Valuable information and knowledge about AM process energy consumption are generated and presented to people intelligently and some decisions are made by framework and control system automatically. This framework is able to match Industry 4.0 required capabilities, which is regarded as an application of Industry 4.0 (Qin et al., 2016).

3.3 Feasibility Study Setup

3.3.1 Introduction of the Experimental SLS Machine

In the last decade, SLS has become a mainstream AM system. This system sinters powdered material to build products using lasers. Figure 3.4 displays a schematic layout of the SLS process as an example of the AM systems, which is the main target AM system of this PhD research. In Figure 3.2, it is seen that the system consists of many different types of power consuming systems, such as laser system, heating system, build platform system, feed and recycle system and miscellaneous (Kellens et al., 2011, Sreenivasan and Bourell, 2010).

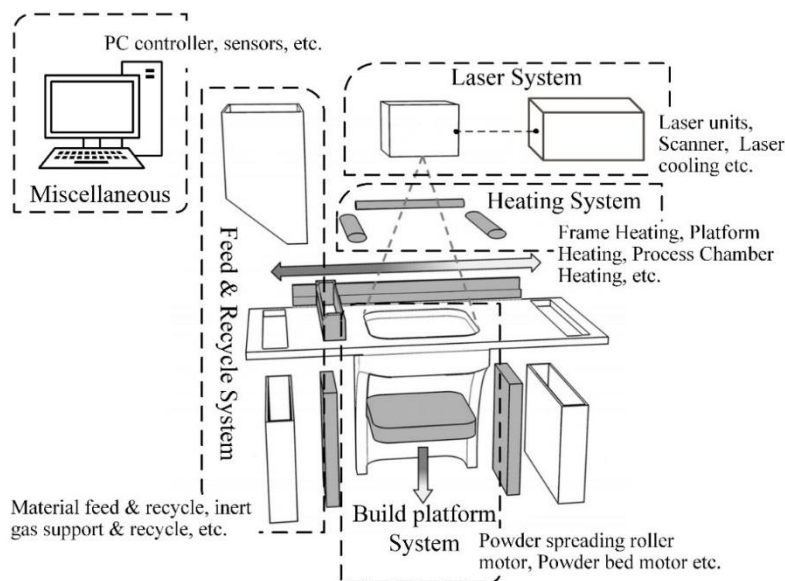


Figure 3.2 Main power drains of SLS process adopted from Watson and Taminger (2015)

Each energy consuming system has included several power consumers. For example, the heating system, consisting of frame heating, platform heating, and process chamber heating, is responsible for the major of energy consumed in this process. In addition, the laser units, scanner, and laser cooling system are three main power components in the laser system, with the laser cooling system consuming the most of energy in this subsystem. The main energy usages of the build platform system are driving the motors. Feed and recycle system includes the material and inert gas feed and recycle process. There are also controllers, electrical elements, and sensors

supporting the system controlling and monitoring functions in such an SLS system, which are also a main part of energy consumers (Kellens et al., 2010).

In this research, the EOS P700 is the target SLS system which is located in School of Engineering at Cardiff University. The EOS P700 has a build envelope, maximum size is 740* 400* 590 mm (x, y, and z), and the effective build envelope size is 700* 380* 580 mm (x, y and z). This significant build platform allows multiple part, sometimes more than hundreds, producing at the same time. In the chamber, two parallel blades are built as the recoater to make sure the powder can be placed on the building bed equally.

The EOS P700 consists of two 50W CO₂ lasers which can sinter nylon materials (PA2200 and PA3200GF). To produce the entire volume of parts, it also has two powder storage areas that can store 40 to 80 kg powder material for guarantying the material supply. Normally, each production takes less 24 hours; this depends on the building volume. Figure 3.3 shows the EOS P700 in the working environment (Soe, 2012).



Figure 3.3 Experiment machine in working environment

PA2200 is the original polyamide-12 material without any fillers, and PA 3200GF contains 40% glass beads for enhancing stiffness. The general material properties and thermal properties are shown in Table 3.1. the melting point of both two material is about 172-180 °C, and the density of laser-sintered part of PA2200 is 0.93 g/cm³, PA3200GF is 1.22 g/cm³.

Table 3.1 Material data collected from the support company material sheet

Material properties	PA2200	PA3200GF
Average grain size	56 μm	57 μm
Bulk density	0.45 g/cm ³	0.63 g/cm ³
Density of laser-sintered part	0.93 g/cm ³	1.22 g/cm ³
Melting point	172-180 °C	172-180 °C
Vicat softening temperature B/50	163 °C	166 °C
Vicat softening temperature A/50	181 °C	179 °C

3.3.2 Unit Energy Consumption of the AM Process

The understanding of AM energy consumption is helpful to be determined before introducing the unit energy consumption. The unit energy consumption (E_U) is shown as the following equation:

$$E_U = \frac{E_T}{M_T} \quad (3.1)$$

In the equation 3.1, the M_T is the product weight of a total build. E_T represents the total energy consumption of each build, which is denoted as following, where n is the number of energy consumers (E_e), such as heating system, layer system, build platform system feed, and recycle system, in the system, T is the total time of each process (Qin et al., 2017). It is highlighted that an AM system typically consists of these kinds of consumers, although they may be different in different AM technologies. In addition, when the entire process is considered, involving pre-process and post-process, E_e should include more consumers of pre-process and post-process. In this paper, the energy consumers (E_e) focus on the energy consumers in the AM system

(Yosofi et al., 2019). The total energy consumption of each build is shown as equation 3.2. E_e is monitored by system monitoring system.

$$E_T = \sum_n \left(\int_0^t E_e \right) \quad (3.2)$$

From the above equations, the unit energy consumptions of all existing builds have been calculated. Figure 3.6 is the unit energy consumption frequency histogram of all tracking builds which was collected from Aug 2016 to Apr 2019 with more than a hundred builds. It is noticeable in the histogram that over 80% builds consume the unit energy from 120 kWh/kg to 600 kWh/kg. However, the energy consumption of each build shows differently even in this range.

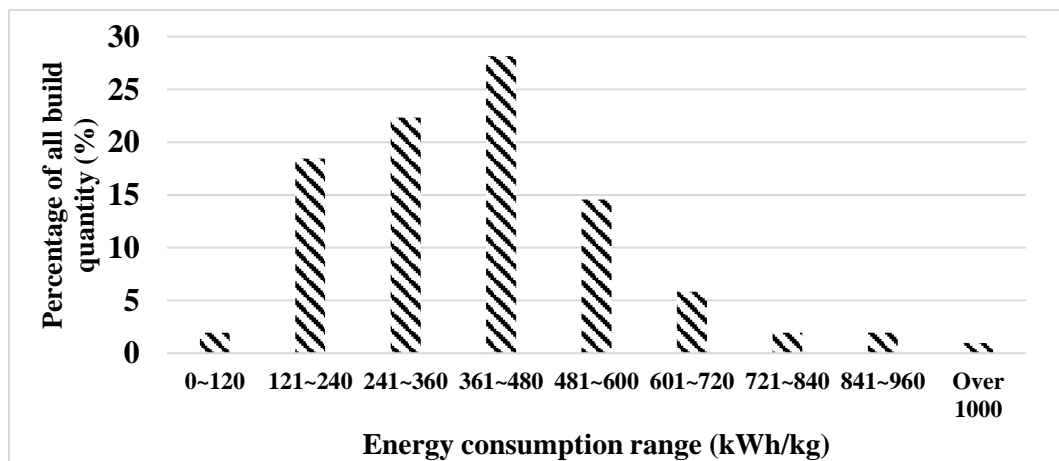


Figure 3.4 Energy consumptions frequency histogram

Table 3.2 shows the basic statistic information including the value of maximum, minimum, mean, standard deviation, 1st quartile, 3rd quartile, and median. The range of the energy consumption is significant which a big standard deviation, 496.8285 kWh/kg. The media is lower than mean value means majority energy consumption is between minimum value and mean value.

Table 3.2 Basic information of the unit energy consumption of experimental machine

	Maximum	Minimum	Mean	Standard deviation	1 st quartile	3 rd quartile	Median
Unit Energy Consumption (kWh/kg)	107.2829	3468.4256	483.1233	496.8285	278.3328	505.1319	386.5819

3.3.3 Evaluation Metrics

In this research, the model performance is mainly evaluated by Root-mean-square-error (RMSE) and Model correlation coefficient (MCC), and all the results are obtained by five-fold cross validation (Wong, 2015). The RMSE is used to measure the difference between the predictive value and the actual value, which denotes as:

$$e_{RMSE} = \sqrt{\frac{\sum_{i=1}^n (p_i - a_i)^2}{n}} \quad (3.3),$$

where p_i is the predictive value, a_i is the actual value that is the unit energy of each build (E_U) in this research (Han et al., 2011).

Another performance validation method is the MCC, represented as:

$$MCC = \frac{S_{PA}}{\sqrt{S_P S_A}} \quad (3.4)$$

$$S_{PA} = \frac{\sum_i (p_i - \bar{p})(a_i - \bar{a})}{n-1}; S_P = \frac{\sum_i (p_i - \bar{p})^2}{n-1}; S_A = \frac{\sum_i (a_i - \bar{a})^2}{n-1} \quad (3.5),$$

where \bar{p} is the average value of the predicted values, and \bar{a} is the average value of the entire actual values.

3.4 Summary

In the era of Industry 4.0, AM processes are necessary for the whole manufacturing production industry. Energy consumption has become a big concern with the rapid growth of the product volume. It is an indispensable component of the power source reduction, environment protection, and process life cycle analysis. Current AM energy consumption analysis methods were reviewed in Section 2.3. These methods are difficult to obtain reasonable results because the energy consumption problem is a multi-attribute convergence problem. The Industry 4.0 solution is designed for solving this type of problem. Based on this purpose and relying on this classification, a framework was designed for AM energy consumption modelling, prediction, and management. Using this IoT framework, the energy consumption of the AM process is going to be modelled, predicted, and managed which assists AM engineers, researchers and enterprise managers in solving the energy problem of the process. This framework collects, integrates, and analyses data from the entire production environment. The relevant information and knowledge is discovered. The results are shown intelligently for different processing participants dependent upon their roles in the system.

Chapter 4 Multi-source Data Analytics for AM Energy Consumption Modelling

4.1 Introduction

In the AM data generation process, which has been reviewed in Chapter 2, process, material, design and environmental attributes, including evident and hidden energy consumption related factors, can be digitalised and connected in a virtual world (Gubbi et al., 2013) using IoT techniques (Qin, 2017). Depending on the different data sources, this data is defined as the multi-source data (Yager, 2004), which are often used to build data mining models for ascertaining the AM system relevant information and knowledge (Boyes et al., 2018). Unfortunately, multi-source data is generally collected by different methods from various data sources (Chan et al., 2018). This data involves various features and dimensions, which tend to be nested as a multiple hierarchical structure. The features of this data structure are rarely independent (Rajeswaran and Blackstone, 2018). This data is difficult to integrate using typical data integration methods, such as the extract, transform, and load (ETL) technique (Yin and Kaynak, 2015). Under this large data environment, it is very challenging to integrate the multi-source data, which includes the multiple level structure for building the prediction model (Cavalheiro and Carreira, 2016). Integrating and modelling this multi-source data of the AM system to predict energy consumption becomes a crucial research question for AM development.

This chapter proposes a hybrid multi-source data integration and analytics approach for AM energy consumption modelling based on IoT, clustering, and deep learning techniques in the AM system. In Section 4.2, the multi-source data collection is described with the methodology and the experimental. The experimental data is collected from a SLS system, which is also used for the validation of the proposed modelling approach. In section 4.3, a hybrid approach is proposed, where the multi-source data is integrated and modelled by a clustering based deep learning approach to predict AM energy consumption. So, in section 4.4, the proposed approach is validated, compared with the conventional machine learning modelling approaches and discussed to reveal the performance.

4.2 Multi-source Data Sensing and Collection

In order to integrate the multi-source data and build the energy consumption model for AM systems, an IoT application is utilised to sense and collect the multi-source data from several relevant data sources of an AM system, such as production process operation, product design, working environment and materials condition. In this section, the method of data sensing and collection is described and the hardware setup of data sensing and collection for a real-world AM system is introduced.

4.2.1 Multi-source Data Sensing and Collection for an AM Process

To analyse the energy consumption of an AM process, the data is collected from four primary sources: production operation, working environment, product design and materials. In the context of IoT, there are three main data collection methods, such as system monitoring files, design CAD models, and IoT application, to collect data from these four data sources in an AM process. The data sensing and collection process is illustrated in Figure 4.1.

In Figure 4.1, system operation data and working environment data are collected from the machine embedded sensors, which are represented as a series of numbers in the system monitoring files. These numbers can be temperature, voltage, current, and gas concentration, where data pre-processing is necessary before model building.

Furthermore, the data collected from system monitoring files is not enough to present the comprehensive aspects of a working environment (Chong and Kumar, 2003). In this research, extra working environment data is sensed and collected using an IoT data collecting platform. This IoT platform is structured on single-board computers, such as Raspberry Pi and MBed devices, to connect sensors (Min et al., 2007, Zhou et al., 2017, Risteska Stojkoska and Trivodaliev, 2017), and the target AM system. This connection builds a wireless data sensing and collection network (Pereira et al., 2018, Yashiro et al., 2013).

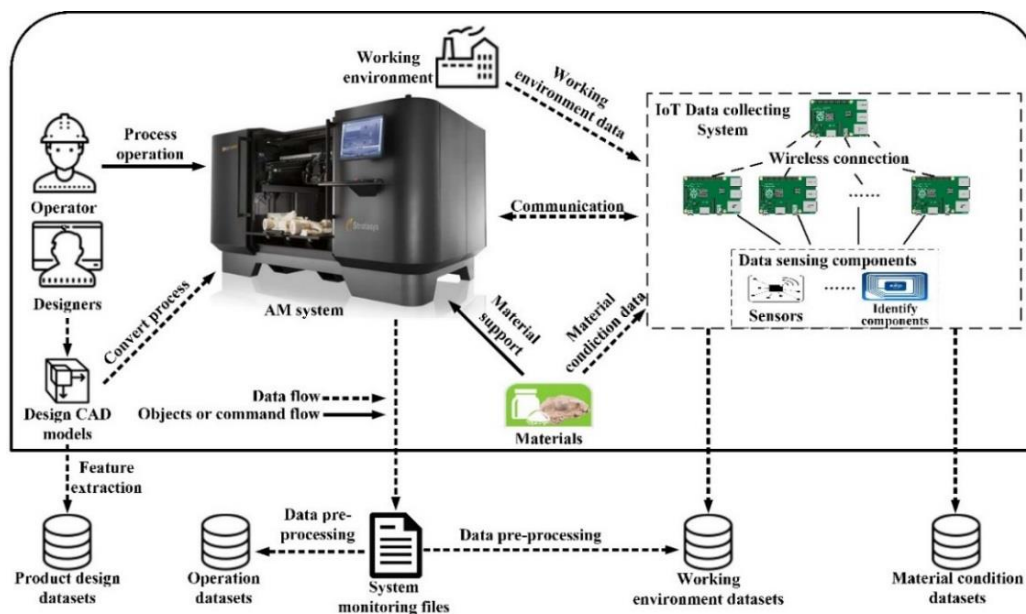


Figure 4.1 Multi-source data sensing and collection using IoT for an AM process

Besides, product design CAD models can be shown as various formats depending on CAD design software and saving templates (Diegel et al., 2010, Hällgren et al., 2016). By converting process, these design CAD models are converted to STL format, which has mentioned in the chapter 2. To obtain design-relevant information, such as geometric information, spatial location information, spatial proportion information, these design CAD models need to be analysed by software, such as SolidWorks, Autodesk CAD, or AM software (Han et al., 2000, Babic et al., 2008). The details of data requirements and data sources are introduced in next section.

4.2.2 Hardware Setup of Data Sensing and Collection for the Target System

In this project, to validate the above data sensing and collection approach, data was collected from a real-world AM process, EOS P700 (a SLS system) which is described in last chapter. As mentioned before, the data is collected from four main data resources, part design, working environment, process production, and material. This data is collected through three collection methods in the project, system monitoring files, IoT data collecting system, and product design CAD models. This section will show how the data is collected and the details of collected data.

- **System monitoring file**

The EOS P700 system automatically generates two monitoring files in each build. One file, called Job file, recorded parameter settings of each process. This file can be viewed by a parameter view software (EOS-Formats) (Tomsoftware, 2015), which is shown in Figure 4.2.

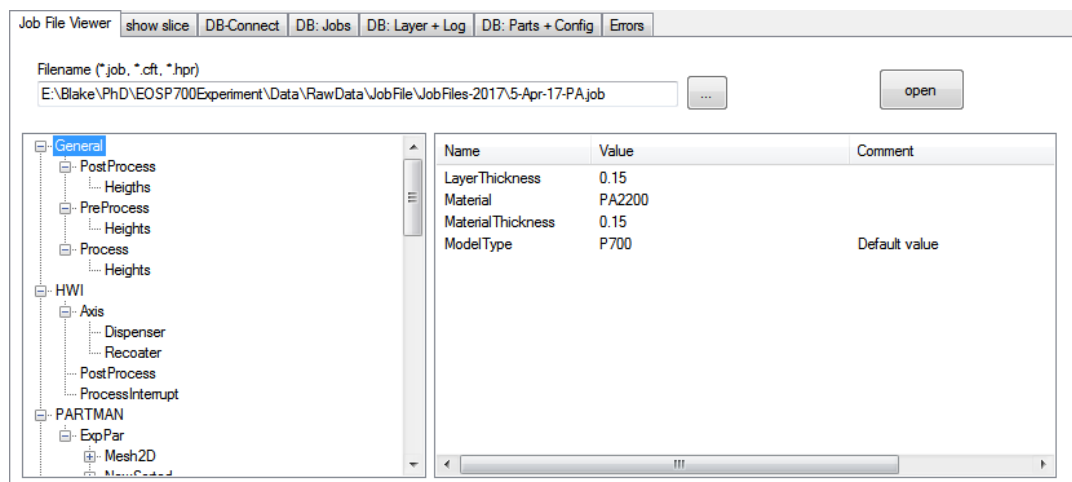


Figure 4.2 Parameter setting features viewed by EOS-Formats software

By using this software, seven parameter setting data were collected from the Job file, maximum and minimum value of dispenser, recoater speed, power of laser for sintering, scan speed of laser for sintering, scan space of laser for sintering, and scan angle between each layer. The details of the data is shown in Table 4.1 which the data attribute name and description. This data was typically given by system technicians

before starting production process, which was not changed during process. However, technicians would change some parameters between builds depending on working condition. This data was categorised into a build-level dataset which means the data is considered as the same value for each build.

Table 4.1 Data description of Job file

Data attributes	Data description
DispenserMax	The maximum value of dispenser measured in ‘%’.
DispenserMin	The minimum value of dispenser measured in ‘%’.
RecoaterSpeed	The recoater speed measured in ‘mm/mim’.
HatchPower	The power of laser for sintering measured in ‘%’.
HatchSpeed	The scan speed of laser for sintering measured in ‘mm/s’.
HatchWidth	The scan space of laser for sintering measured in ‘mm’.

Also, during each production process, the system automatically generated another monitoring file, called Report file, which included eleven production process data attributes. This data was collected for every production layer by various sensors that are embedded within the system, such as working time of each layer, laser sintering time and cumulative recoating time, frame temperature, chamber temperature, platform temperature, scanner temperature, and oxygen level, which the details of the data is determined in Table 4.2.

Table 4.2 Data description of Report file

Data attributes	Data description
ChamberTemperature	The building chamber temperature measured in ‘°C’.
FrameTemperature front	The front-frame temperature measured in ‘°C’.
FrameTemperature back	The back-frame temperature measured in ‘°C’.
FrameTemperature left	The left-frame temperature measured in ‘°C’.
FrameTemperature right	The right-frame temperature measured in ‘°C’.
PlatformTemperature	The working platform temperature measured in ‘°C’.
ScannerTemperature	The scanner temperature measured in ‘°C’.
PyrometerTemperature	The Pyrometer temperature measured in ‘°C’.
O₂Level	The oxygen percentage in the working chamber measured in ‘%’.
EnergyDeviation	The energy deviation percentage of the system.

The data size of each Report File was different depending on heights of building products, which meant more layers that were produced, more significant of the data was generated. This data was classified into a layer-level dataset. These monitoring files were formatted as RPT files by the system, which were typical machine report files. In this case study, these RPT format files were converted to standard comma-separated values (CSV) data format which was popular in many data analytics areas. Benefit from completed monitoring system in EOSP700, there was not any missed or abnormal data in the monitoring files. Table 4.3 shows a screen shot of an RPT file opened by CSV data format. Based on the data description and the data collection principle of system monitoring system, the data in Report files is collected once per layer, which is represented as the layer-level datasets.

- **IoT data collecting system**

A part of data cannot be collected from working environment and material condition only via system monitoring files. In this research, an IoT platform was introduced to sense and collect more data from working environment and material condition according to the data sensing and collection process in the section 4.2.1. This IoT platform was designed using the Raspberry Pi (RPI), and it connected multiple RPIs and the AM system via a wireless communication by an Ad-Hoc network. The network allowed nodes to be dynamically added and removed from the system.

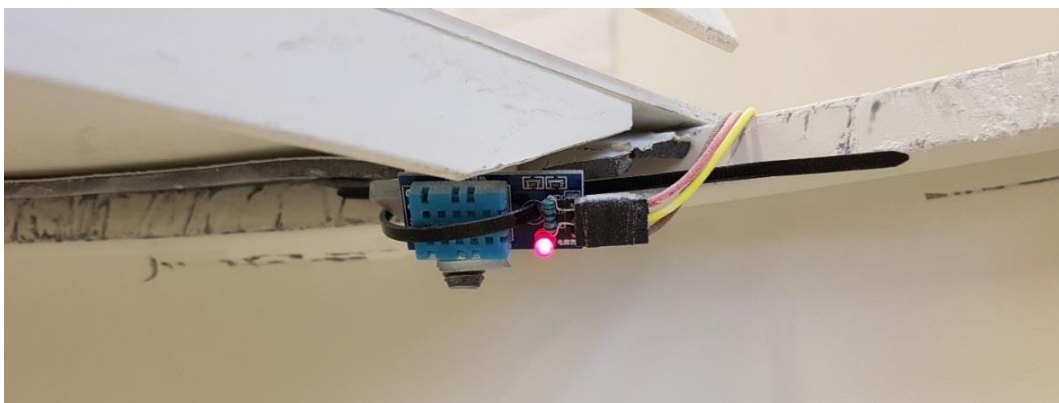


Figure 4.3 DHT11 sensor located in the material cylinder

This system is entirely self-sufficient with no external infrastructure required. Notably, three RPIs were connected, and one of them was linked to the EOS P700 controlling

system. Several temperature and humidity sensors, the DHT11 Sensor were set up on this wireless IoT platform to collect external data and identify the type of used material. Figure 4.3 shows the working environment of a DHT11 sensor sensing the temperature and humidity of the material. The core coding of sending and receiving data by RPIs is shown in Appendix C.1 and B.2. Figure 4.4 shows one of three RPIs collecting the data of the sensors.



Figure 4.4 An RPI collecting the data of sensors

By using the RPI based IoT platform, more working environment and material condition data were sensed and collected, like lab temperature, humidity, controlling system temperature and humidity, material powder temperature and humidity, and proportion between new powder and recycled powder with the data attribute name and description is shown in Table 4.4. The IoT data is collected once per layer, which belongs to layer-level data.

	A	B	C	D	E	F	G	H	I	J	K	L	
1	Date	Time	Z-Height [mm]	t_at_BREC	t_at_BEXP [ms]	t_at_BNLA [ms]	ChamberTemperature[°C]	FrameTemperature front[°C]	FrameTemperature back[°C]	FrameTemperature left[°C]	FrameTemperature right[°C]	Platform Temperature[°C]	Scanne
2	16/12/2016	15:33:11	0.15	4	115710	115819	176.43	144.9	144.9	144.9	144.9	144.7	
3	16/12/2016	15:35:07	0.3	153	41795	41905	175.93	144.9	144.9	144.9	144.9	144.9	
4	16/12/2016	15:35:49	0.45	153	39732	39843	176.07	145.2	144.9	145.2	144.9	144.9	
5	16/12/2016	15:36:29	0.6	153	37873	37984	176.29	145.2	145.2	144.9	145.2	144.9	
6	16/12/2016	15:37:07	0.75	153	37763	37874	176.29	144.9	145.2	144.9	145.2	145.2	
7	16/12/2016	15:37:45	0.9	153	37873	37983	176.5	144.9	144.9	144.9	144.9	145.2	
8	16/12/2016	15:38:23	1.05	153	36466	36577	175.78	144.9	144.9	145.2	144.9	145.2	
9	16/12/2016	15:38:59	1.2	153	35904	36015	175.93	144.9	144.9	144.9	144.7	145.2	
10	16/12/2016	15:39:35	1.35	153	36451	36562	175.85	145.2	144.9	144.9	144.9	145.4	
11	16/12/2016	15:40:12	1.5	153	35873	35983	175.93	145.2	144.9	144.9	144.9	145.2	
12	16/12/2016	15:40:48	1.65	153	36467	36577	175.93	144.9	145.2	145.2	145.2	145.4	
13	16/12/2016	15:41:25	1.8	153	35904	36015	176.07	144.9	145.2	144.9	145.2	145.4	
14	16/12/2016	15:42:01	1.95	153	36451	36562	176.07	144.9	145.2	144.9	145.2	145.4	
15	16/12/2016	15:42:37	2.1	153	34592	34702	176.14	144.9	145.2	144.9	144.9	145.4	
16	16/12/2016	15:43:12	2.25	153	34482	34593	176.07	144.9	144.9	145.2	144.9	145.4	
17	16/12/2016	15:43:46	2.4	153	34576	34687	176.14	145.2	144.9	144.9	144.9	145.4	
18	16/12/2016	15:44:21	2.55	153	34482	34593	176.14	145.2	144.9	144.9	144.9	145.4	
19	16/12/2016	15:44:56	2.7	153	34591	34702	176.22	144.9	144.9	144.9	144.9	145.4	
20	16/12/2016	15:45:30	2.85	153	34498	34609	176.22	144.9	144.9	145.2	145.2	145.4	
21	16/12/2016	15:46:05	3	153	34591	34702	176.29	144.9	144.9	144.9	145.2	145.4	
22	16/12/2016	15:46:40	3.15	153	34482	34593	176.22	144.9	145.2	144.9	145.2	145.4	
23	16/12/2016	15:47:14	3.3	153	34560	34671	176.29	145.2	145.2	144.9	145.2	145.4	
24	16/12/2016	15:47:49	3.45	153	34498	34608	176.29	145.2	144.9	145.2	144.9	145.2	
25	16/12/2016	15:48:24	3.6	153	34560	34671	176.29	145.2	144.9	144.9	144.9	145.2	
26	16/12/2016	15:48:58	3.75	153	34482	34593	176.43	144.9	144.9	144.9	144.7	145.2	
27	16/12/2016	15:49:33	3.9	153	32607	32719	176.29	144.9	144.9	144.9	144.9	145.4	
28	16/12/2016	15:50:06	4.05	152	32528	32639	176.29	144.9	144.9	144.9	144.9	145.2	
29	16/12/2016	15:50:38	4.2	153	32592	32702	176.43	144.9	144.9	145.2	145.2	145.2	
30	16/12/2016	15:51:11	4.35	153	32513	32624	176.43	145.2	145.2	145.2	145.2	145.2	
31	16/12/2016	15:51:44	4.5	153	32623	32734	176.5	145.2	145.2	144.9	145.2	145.2	
32	16/12/2016	15:52:16	4.65	153	32514	32624	176.5	145.2	145.2	144.9	145.2	145.2	
33	16/12/2016	15:52:49	4.8	153	34576	34687	176.5	144.9	144.9	145.2	144.9	145.2	
34	16/12/2016	15:53:24	4.95	153	34514	34624	176.5	144.9	144.9	144.9	144.9	145.2	

Table 4.3 Screen shot of an RPT file opened by CSV data format

Table 4.4 Data description of wireless IoT system

Data attributes	Data description
TempNewPowder	The new powder temperature measured in ‘°C’.
HumNewPowder	The new powder humidity measured in ‘%’.
TempRecyPowder	The recycle powder temperature measured in ‘°C’.
HumRecyPowder	The recycle powder humidity measured in ‘%’.
LabTemperature	The lab temperature measured in ‘°C’.
ControlTemperature	The control system temperature measured in ‘°C’.
ControlHumidity	The control system humidity measured in ‘%’.

- **Product design CAD models**

Another build-level data was collected from product CAD models, which include product design information. In this research, the SLS system produce a wide range of parts and components from complicated mechanical parts to building models. 13 product design features were recognised from product design CAD models and shown in Table 4.5. More information about design-relevant data collection is introduced in the next chapter, section 5.3.

Table 4.5 Data decryption of design-relevant data

Data attributes	Data description
AverFillingDegSingle	The average filling degree of single part measured in ‘%’.
FillingDegWhole	The filling degree of the whole build measured in ‘%’.
AverRateLWSingle	The average rate between length and width of single part measured in ‘%’.
AverRateLHSingle	The average rate between length and height of single part measured in ‘%’.
AverRateHWSingle	The average rate between height and width of single part measured in ‘%’.
AverRateLWWhole	The rate between length and width of the whole build measured in ‘%’.
AverRateLHWhole	The rate between length and height of the whole build measured in ‘%’.
AverRateHWWhole	The rate between height and width of the whole build measured in ‘%’.
BottomArea	The bottom area measured in ‘mm ² ’.
HeightBuild	The entire height measured in ‘mm’.
NoPart	The number of printing products.
HightPart	The average height of produced parts.

Overall the data for this research is collected from four main data resources. Three data collection methods are used, and two levelled data types are introduced, build-levelled and

layer-levelled data. The comprehensive data description including data attribute name, description, sources, categories, collection methods is displayed in Table 4.6. For integrating this data and building the model of AM energy consumption, the approach of multi-source data integration and energy consumption modelling is proposed in next section

4.3 AM Energy Consumption Modelling using Multi-source Data

In this research data is collected from the monitoring files, product design models, and the IoT data collecting system. Four main types of data, process operation data, working environment data, product design data, and material condition data, are created.

4.3.1 Multi-source Data Integration

In an AM process, it is obvious that these four multi-source data are contained with either, build-level or layer-level data. Specifically, during each build, process parameter settings are constant. The relevant data is collected once at each build. This data is classified into the build-level dataset. Also, work environment, and material condition may keep changing all the time during a working process. This type of relevant data is collected many times during a build, specifically several times or once per layer, which is categorised into the build-level dataset. To integrate the multi-source data and build an energy consumption prediction model, this research proposes a hybrid approach shown in Figure 4.5.

Table 4.6 Data description including data sources, categories, and collecting methods

Data attributes	Data description	Data sources	Build-levelled data	Layer-levelled data	Collection methods
DispenserMax	The maximum value of dispenser measured in ‘%’.	Process operation	Yes	No	Machine log
DispenserMin	The minimum value of dispenser measured in ‘%’.		Yes	No	
RecoaterSpeed	The recoater speed measured in ‘mm/m’.		Yes	No	
HatchPower	The power of laser for sintering measured in ‘%’.		Yes	No	
HatchSpeed	The scan speed of laser for sintering measured in ‘mm/s’.		Yes	No	
HatchWidth	The scan space of laser for sintering measured in ‘mm’.		Yes	No	
HatchAngle	The scan angle between each layer measured in ‘°’.		Yes	No	
AverFillingDegSingle	The average filling degree of single part measured in ‘%’	Product design	Yes	No	Product design model
FillingDegWhole	The filling degree of the whole build measured in ‘%’.		Yes	No	
AverRateLWSingle	The average rate between length and width of single part measured in ‘%’.		Yes	No	
AverRateLHSingle	The average rate between length and height of single part measured in ‘%’.		Yes	No	
AverRateHWSingle	The average rate between height and width of single part measured in ‘%’.		Yes	No	
AverRateLWWhole	The rate between length and width of the whole build measured in ‘%’.		Yes	No	
AverRateLHWhole	The rate between length and height of the whole build measured in ‘%’.		Yes	No	
AverRateHWWhole	The rate between height and width of the whole build measured in ‘%’.		Yes	No	
BottomArea	The bottom area measured in ‘mm ² ’.		Yes	No	
HeightBuild	The entire height measured in ‘mm’.		Yes	No	
NoPart	The number of printing products.		Yes	No	
HightPart	The average height of produced parts.	Yes	No		
RateNewRecy	The rate between new and recycle powder, measured in ‘%’.	Material condition	Yes	No	Wireless IoT platform
TypeMaterial	The type of material.		Yes	No	
TempNewPowder	The new powder temperature measured in ‘°C’.		No	Yes	
HumNewPowder	The new powder humidity measured in ‘%’.		No	Yes	
TempRecyPowder	The recycle powder temperature measured in ‘°C’.		No	Yes	
HumRecyPowder	The recycle powder humidity measured in ‘%’.		No	Yes	
LabTemperature	The lab temperature measured in ‘°C’.	Working environment	No	Yes	Machine log
ControlTemperature	The control system temperature measured in ‘°C’.		No	Yes	
ControlHumidity	The control system humidity measured in ‘%’.		No	Yes	
t_at_BNLA	The time of each production layer measured in ‘s’.		No	Yes	
ChamberTemperature	The building chamber temperature measured in ‘°C’.		No	Yes	
FrameTemperature front	The front-frame temperature measured in ‘°C’.		No	Yes	
FrameTemperature back	The back-frame temperature measured in ‘°C’.		No	Yes	
FrameTemperature left	The left-frame temperature measured in ‘°C’.		No	Yes	
FrameTemperature right	The right-frame temperature measured in ‘°C’.		No	Yes	
PlatformTemperature	The working platform temperature measured in ‘°C’.		No	Yes	
ScannerTemperature	The scanner temperature measured in ‘°C’.		No	Yes	
PyrometerTemperature	The Pyrometer temperature measured in ‘°C’.		No	Yes	
O₂Level	The oxygen percentage in the working chamber measured in ‘%’.		No	Yes	
EnergyDeviation	The energy deviation percentage of the system.		No	Yes	

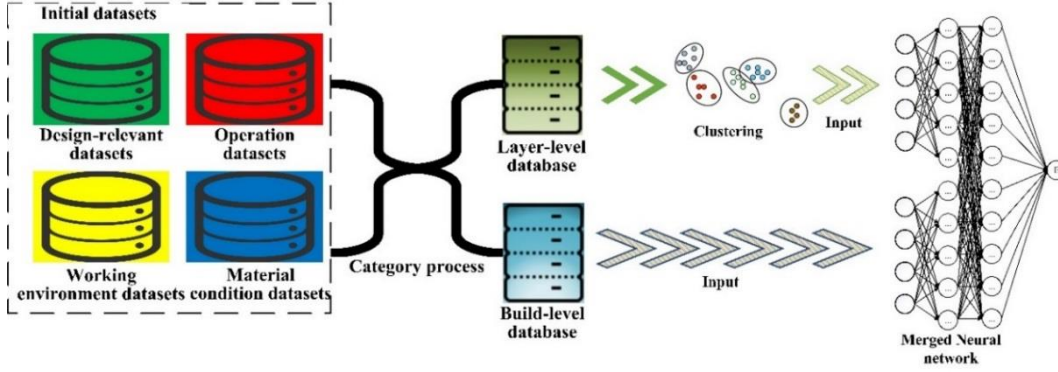


Figure 4.5 Multi-source data integration and modelling process

It is evident that each build contains layers of differing numbers, largely depending on the height of the products. Therefore, the size of each layer-level dataset is varied, and consisting of format for every dataset is necessary. In this research, the clustering method is introduced to unify layer-level database format.

The L_{ni}^j is a raw layer-level dataset for each build, where j is the j^{th} build (j is between 0 to J , which J is the total number of builds). n is the number of layers for each build, i is the number of features collected for layer data. Because every build includes various layer number depending on the height of build, n is different between different j . For every L_{ni}^j .

$$CL_{ci}^j = f_C(L_{ni}^j) \quad (4.1)$$

f_C is the clustering function to discover the number of C centre points (CL_{ci}^j). In each build, the layer-level raw dataset (L_{ni}^j) represents a dataset with the number of n indexes and the number of i features. With the algorithm, each L_{ni}^j will be clustered into C clusters, and minimize the total Euclidean distance, between cluster centre and each point. So, in each build, a centre points dataset (CL_{ci}^j) can represent an original layer-level dataset. Then, combining all the CL_{ci}^j into a resided dataset, representing as L_{ic}^j . The L_{ic}^j is one input part of the merged neural network that is structured as Figure 4.10. The B_k^j is a build-level database which is the other input part of the merged neural network, which k is the number of features in the build-level database

4.3.2 Merge Neural Network for Multi-source Data Modelling

This merged neural network (MNN) includes three sections, layer-level section, build-level section and full-connected section, shown in Figure 4.6. The L_{ic}^J is the input of the layer-level section and the B_k^J is the input of the build-level section. The full-connected section is connected to the layer-level and build-level sections.

Specifically, the neurons of a layer-level section are described using the equations (4.2):

$$u_L = \sum_1^l w_{Lic} C L_{ic}, y_L = f_l(u_L + \Delta b_l) \quad (4.2)$$

w_{Lic} is the weight of each neuron on each layer-level section, l is the number of neurons on each layer-level section, y_L is the output of each neuron, which is the input of next layer, f_l is the activation function of a layer-level section, and Δb_l is the bias.

The neurons of a build-level section are denoted as a set of equations (4.3):

$$u_B = \sum_1^b w_B B_k, y_B = f_b(u_B + \Delta b_b) \quad (4.3)$$

w_B is the weight of each neuron on each build-level section, b is the number of neurons on each build-level section, y_B is the output of each neuron, which is the input of next layer, f_b is the activation function, and Δb_b is the bias.

With the full connection layer, neurons are represented as:

$$u_f = \sum_1^F (w_{fi} y_l + w_{fi} y_b), y_f = f_f(u_f + \Delta b) \quad (4.4)$$

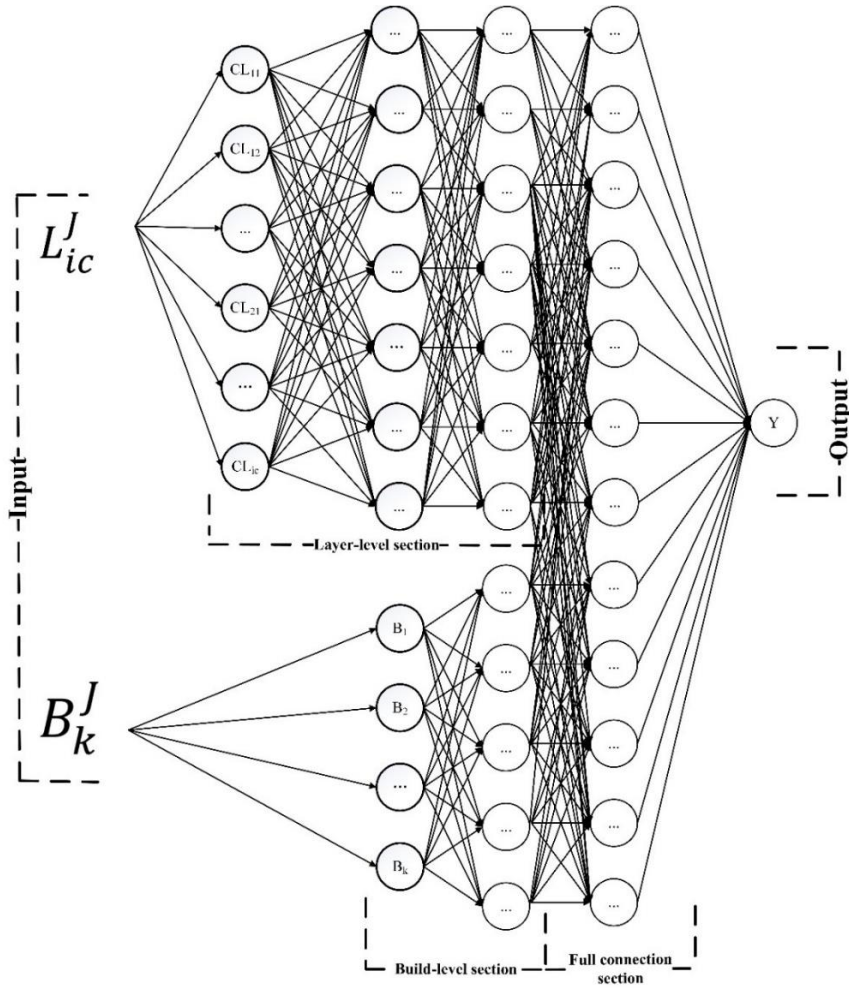


Figure 4.6 Merged neural network structure

w_{fi} is the weight of each neuron on each full connection section, F is the number of neurons, which $F = \sum fi$, y_f is the output of each neurons, which is the input of next layer, f_f is the activation function of, and Δb is the bias of full connection section. This hybrid approach fuses clustering and deep learning techniques, the levelled multi-source data is integrated and modelling to predict target values. In next section, the proposed approach is validated by the real case of the SLS system.

4.4 Evaluation of AM Energy Modelling using Multi-source data

In this section, results focus on validation of the proposed method. Several comparisons were raised for verifying performances of the proposed approach. Firstly,

this case study introduced three ML methods as benchmarks. In this section, results from three machine learning methods are presented using results from single level datasets and multi-level datasets.

4.4.1 Results of Conventional Machine Learning (ML) Approaches

These three ML algorithms are linear regression (LR), k -nearest neighbours (k -NN), decision tree (DT), which are popular in academia, industry, and business (Han et al., 2011). LR was the first ML algorithm to predict energy consumption in this case study. Using this algorithm, outputs were expected to be a linear combination of inputs. In this project, results from the ordinary least squares regression were taken as the LR results. k -NN is one of the most straightforward supervised machine learning, which is applied to both classification and regression (Altman, 1992). DT is a first classifier structure like a flowchart. Every internal node, branch and leaf node of a DT represents an attribute, a result, or a class label, respectively, and the topmost node is called the root. Depending on attribute values, unknown tuple is classified within each leaf node storing the class information, which contains the classification rules of a DT models (Pedregosa et al., 2011). Five-fold cross-validation was used to avoid the flag problems like overfitting or selection bias (Kohavi, 1995). All these conventional machine learning algorithms were programmed in the Python language with Scikit-learn package, the codes are shown in Appendix B.3.

The experiments were run with 3 types of input datasets for the conventional machine learning algorithms, layer-level datasets, build-level datasets, and combined datasets. For the layer-level datasets, the clustering was used for equalling the dimensions due to the layer number was different between each build. For clarity, the data was collected from over a hundred builds including thousands of product design models, and each build contained the different number of layers from 20 to 3500. Accordingly, the cluster number was set from 1 to 20 for the layer-level datasets. Figure 4.8 shows the MCC results of three conventional machine learning algorithms with which the layer-level data is used.

Figure 4.7 shows the MCCs of three ML methods. It is obvious to see the maximum MCC, the best MCC results, appear when the cluster number is one for all three ML methods. Comparing the three ML methods, linear regression obtained the best result (0.530) with k -NN close to it. DT did worst job for MCC which was 0.316. The worst result of DT is 0.032 which was also the lowest MCC of all results.

Moving to RSME, Figure 4.8 shows the RSME of conventional ML methods. Generally, the trend of RSME is same as MCC when cluster number is changed. The minimum values of RSME of three ML methods were obtained when cluster number is set as one. The lowest RSME is get from k -NN (51.901 kWh/kg) which is also very stable when cluster number is changed. LR involved the largest RSME (1436.755 kWh/kg) and when the cluster number is changed the results of LR changes dramatically. The RSME of DT is also stable however, the minimum RSME of DT (99.584 kWh/kg) is larger than the best results of other two results. The entire results are shown in the Appendix B.1.

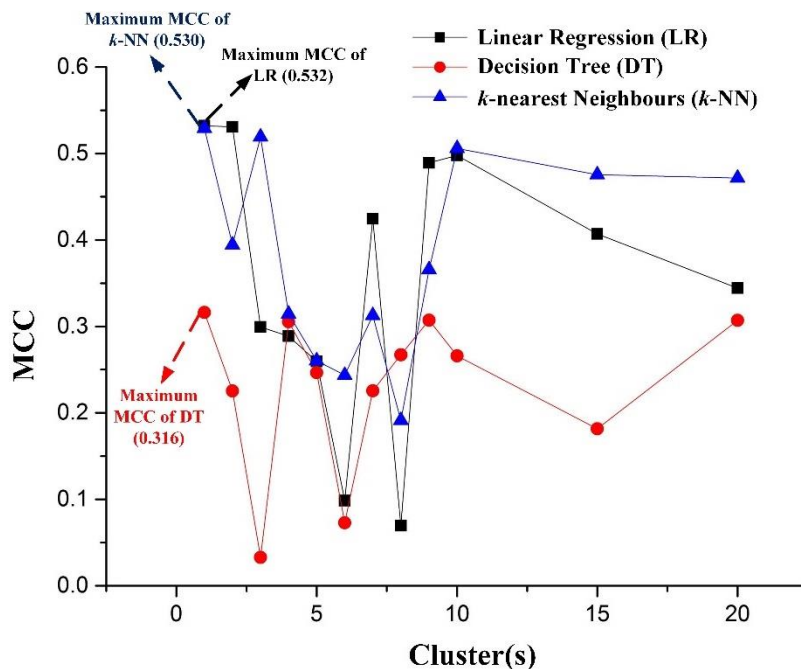


Figure 4.7 MCC of three ML methods using layer-level datasets

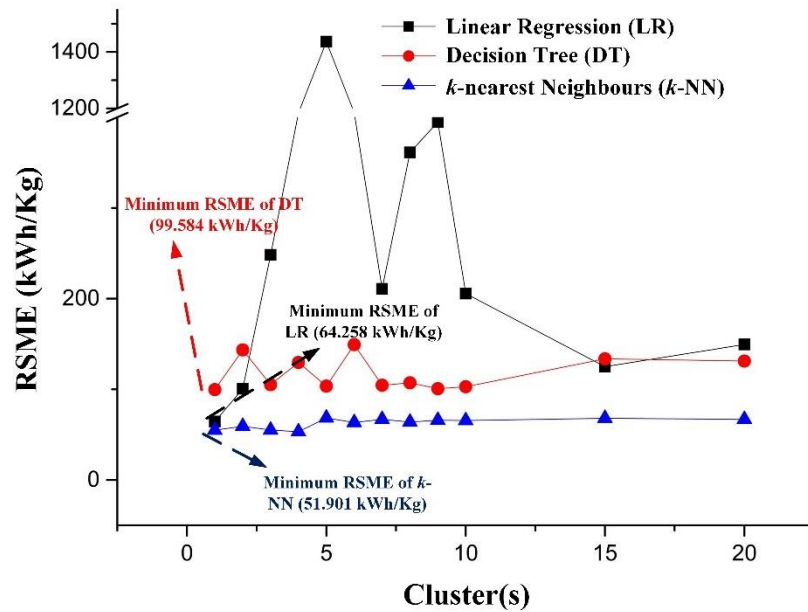


Figure 4.8 RMSE of three ML methods using layer-level datasets

Next, the MCC and RSME of three ML methods by using build-level datasets are displayed in Table 4.7. Comparatively, the MCC of DT is the largest value (0.687), however, the RSME of DT is also the largest. The k -NN obtained the lowest RSME value (42.215 kWh/kg). And the MCC is 0.526 which is lower than best results about 0.162. It is hard to tell which the best modelling method is by only using the build-level dataset. The entire results are shown in the Appendix B.2.

Table 4.7 MCC and RSME results of three ML method using build-level dataset

	Linear regression	Decision tree	k -NN
MCC	0.573	0.687	0.526
RSME (kWh/kg)	115.056	102.704	42.215

In order to combine the layer-level and build-level dataset and apply the conventional ML methods, the centre point values of the cluster (one cluster to represent layer-level data) was used to join with build-level data. Table 4.8 shows the results (MCC and RSME) of the combined datasets.

Table 4.8 MCC and RSME results of combined datasets

	Linear regression	Decision tree	<i>k</i> -NN
MCC	0.607	0.691	0.541
RSME (kWh/kg)	86.822	59.585	44.168

All these three ML methods have improved by integrating the layer-level and build-level datasets, especially the RSME of DT has reduced about 50%. Overall, comparing these three methods, it is difficult to say which one is the best method for modelling the target AM system energy consumption. Considering all the results, the highest MCC is 0.691 which the DT was applied, and the combined datasets were used. And the lowest RSME is 42.215 kWh/kg which the *k*-NN was applied and the build-level datasets were used.

4.4.2 Results of the Multi-source Data Modelling

In this section, the results of proposed approach are presented. Results using the layer-level dataset and considering the number of clusters from 1 to 20 are shown in Figure 4.9. An artificial neural network was applied as the prediction model. Parameter settings of the neural network are highly depended on different training and testing dataset. With a different dataset, neural network structures tended to be different for obtaining the best performance. All neural networks used two types of activation: (1) for the output layer, scaled exponential linear activation was applied, and (2) for the remaining layers, the ReLU activation was used. The mean squared error was used to represent the loss. Supported by a popular Python package, Keras, the Adam optimiser was used (LeCun et al., 2015b). The codes are shown in Appendix C.4.

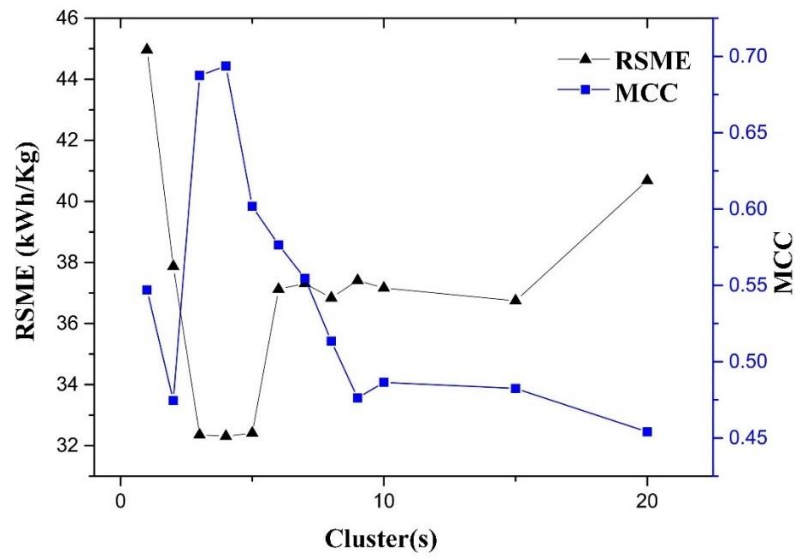


Figure 4.9 Results comparison between a different number of the cluster

With the different number of clusters represents the layer-level dataset, MCCs and RMSEs show an irregular pattern. The best result appears when choosing 4 clusters with the highest MCC (0.694) and lowest RMSE (32.306 kWh/kg). Also, the results of 3 and 5 clusters take the second and third best place. Specifically, with 3 clusters, the MCC is 0.687 and RMSE is 32.353 kWh/kg, and with 5 clusters, the MCC is 0.602 and RMSE is 32.414 kWh/kg. It is also needed to be highlighted that the highest RMSE is 44.965 kWh/kg with only one cluster. When the number of clusters is increased more than 5, RMSEs start to increase. MCCs is reduced when the number of clusters is more than 4, and the lowest is 0.454 when 20 clusters are chosen. Moreover, when only using build-levelled datasets as input dataset the MCC is 0.753, and the RMSE is 62.955 kWh/kg. It is interesting to know the prediction performance when integrated these two datasets by using the proposed method.

Table 4.9 Results comparison applying MNN using the build-level dataset and layer-level dataset with different the number of clusters (3 to 5)

	3 Clusters	4 Clusters	5 Clusters
MCC	0.786	0.803	0.685
RMSE (kWh/kg)	25.906	25.460	28.406

From Table 4.9, it appears that choosing to apply 4 clusters representing the layer-level dataset prediction performance is the best. This case study uses 3 to 5 clusters as the layer-level input dataset separately. When 4 clusters represent the layer-level data and integrating with build-level data is used, the best result is obtained with the highest MCC (0.803), and lowest RMSE (25.460 kWh/kg). Comparing with all other results from any above input datasets and prediction models, this result is the best.

4.4.3 Discussion

According to the results from the last section, energy consumption of the AM process is predicted accurately by using the proposed method. A few interesting points are necessary to discuss from the results. Firstly, the prediction accuracy varies with different number of clusters. When layer-level data are clustered as 3 to 5 clusters, the best results are obtained. It is interesting to note that the AM production process can also be divided as 3, 4 or 5 energy phases regarding Baumers et al.'s (2011) research. This finding indicated that the clustering centre points are able to represent the entire production process. It also proves the correctness of Baumers et al.'s suggestion. Secondly, by using the ML algorithms, it is difficult to show that expanding input datasets can yield better results. With the results obtained by either datasets (layer-level dataset, build-level dataset or both datasets), the deep learning based algorithms, including typical neural networks and proposed clustering based MNN, show merits compared to the results of benchmark algorithms in this case study. The deep learning methods have presented a good performance for building the relationship between the target and high dimension data input. However, with the integrated input datasets, typical ANNs cannot easily be applied to model the target values, while the proposed clustering based MNN structure is able to integrate different levelled datasets and predict AM energy consumption precisely. To build the predictive model of AM energy consumption, multi-source data cannot be applied entirely. Because some data is generated during the process, only the historical data is allowed to be used, such as working environment data. Therefore, the multi-source data have to be analysed, whilst considering the data sensing time point.

4.5 Summary

The approach, proposed in this chapter, is based on a review of related research indicating the significant meaning of data-driven methods in industrial sustainability domain. In contrast to the existing published research, a hybrid approach has been proposed fusing IoT, clustering, and deep learning techniques. In this chapter, the multi-source data generated from an AM process are sensed and collected by IoT techniques. This data includes process operation data, working environment data, material condition data and product design data, which is categorised into two level datasets, layer-level dataset, and build-level dataset. By applying a clustering-based MNN to integrate this multi-level multi-source data, the AM energy consumption is predicted accurately. Comparing with other research regarding AM energy consumption analysis, this method can predict the energy consumption of each production rather than measure a range of energy usage, which provides an accurate value of energy consumption. In addition, this approach is suitable for not only one AM technology, but also other typical AM technologies. In the actual industrial scenario, this can be very helpful to implement data analytics when the multi-source data is collected. In the next chapter, the multi-source features are analysed for determining the energy consumption prediction method.

Chapter 5 Design-relevant Data Analytics for AM Energy Consumption Prediction

5.1 Introduction

To recap within the standard data generation of AM processes, four primary datasets can be generated and collected; process operation dataset, design-relevant datasets, working environment dataset, and material condition dataset. In the previous chapter, the energy consumption model was built based on this multi-source data. However, the multi-source data cannot be used entirely for the prediction, as working environment dataset is generated during the process. Design-relevant dataset plays a significant role in the model built in multi-source data, and it is generated before the production. It is well known that the design-relevant data has the highest randomness compared with the other three primary datasets. In addition, according to the interview held with the AM technicians, the design-relevant information changes in every build. The data values can be significantly different when the location and orientation of each part changes. However, there are currently no comprehensive guidelines for AM part designer and operators to optimise their design and ensuring decisions. The input data is decided before the production, and the predictive energy consumption can be known before the system starts. With the help of the proposed energy consumption prediction, the energy is able to be controlled by changing the part designers' and process operators' design and decision, in terms of optimising the design-relevant data.

The design information based prediction approach relies on the modelling introduced in chapter 4. In Section 5.2, the multi-source features are analysed first to determine the critical features for energy consumption. By comparing correlation between these impacts features and energy consumption, design-relevant features are selected for AM energy consumption prediction. Next, design-relevant data is analysed to attempt to identify patterns. After describing these patterns, the proposed AM energy consumption prediction approach is presented, in which design-relevant data is the main input dataset. A case study is provided in section 5.3, which validates the performance of the proposed approach.

5.2 AM Energy Consumption Prediction

This section will display the weights of each feature in the multi-source data model for determining the importance of each feature for AM energy consumption modelling. Considering the data generation time point and the weights of impact features, the design-relevant features are selected for AM energy consumption. Then, this introduces the design-relevant data collected from the target AM system (EOS P700) for determining the general patterns of design-relevant data in the SLS process. After the analysis, the AM energy consumption prediction approach is proposed.

5.2.1 AM Energy Consumption Impact Feature Comparison

The energy consumption model is based on the merged neural network of multi-source data, which the weight of each input feature can be extracted from the first layer of neural network. The weight is a representation of the importance for the target value that is energy consumption. Tables 5.1, 5.2, 5.3, and 5.4 show the weights used for each data source.

Table 5.1 shows the weights of process operation features. The hatch speed has the largest weight compared to other process operation features, which means the hatch speed is the most significant feature in the process operation feature. The total weight is 0.1034 which is lower than the average weight compared to other classes of features. The data of these features is decided before the production. From the interview of

technicians, these decisions are basically based on the manufacturer handbook which is generally fixed. Any change of these feature would need to be evaluated before it is implemented.

Table 5.1 Weights of process operation features

Feature name	Weight	Feature name	Weight
DispenserMax	0.0089	DispenserMin	0.0096
RecoaterSpeed	0.0134	RecoaterPower	0.0158
HatchSpeed	0.0207	HatchWidth	0.0137
HatchAngle	0.0072	<i>Total weight</i>	0.1034

The weights of design-relevant features are shown in Table 5.2. The total weight is 0.4635 which is the highest value of four classes of energy consumption impact features. In filling degree of whole build obtains the largest weight in the entire design-relevant features. These features will be discussed in next section in terms of the reason of collection and more details of each feature. It is highlighted that the design-relevant features are determined before the production process.

Table 5.2 Weights of design-relevant features

Feature name	Weight	Feature name	Weight
AverFillingDegSingle	0.0345	AverRateLWWhole	0.0309
AverRateLWSingle	0.0384	AverRateLHWhole	0.0323
AverRateLHSingle	0.0390	AverRateHWWhole	0.0334
AverRateHWSingle	0.0444	BottomArea	0.0396
HeightPart	0.0368	HeightBuild	0.0386
FillingDegWhole	0.0560	NoPart	0.0396
<i>Total weight</i>	0.4635		

In this research, six material condition features considered with which the type of material has the largest weight in the energy consumption modelling. The total weight is only 0.0826 which is the smallest weight compared to other feature classes. The material condition is considered as the lowest impact for energy consumption in this research. However, there are much more material condition features are not considered in this research. In addition, the material condition does change much in the lab

environment, which will show much different results when the production is happened in real industrial environment.

Table 5.3 Weights of material condition features

Feature name	Weight	Feature name	Weight
RateNewRec	0.0097	HumNewPowder	0.0114
TypeMaterial	0.0184	TempRecyPowder	0.0129
TempNewPowder	0.0137	HumRecyPowder	0.0106
<i>Total</i>	<i>0.0826</i>		

The working environment features have obtained the second place of importance for energy consumption modelling, which the total weight is 0.3505. The weight of platform temperature is the largest weight. Although the working environment impact AM energy consumption significantly, it cannot be considered as the prediction input features. Because this data is generated during the production, the prediction is made for the energy consumption. From the weight values, the manufacturer should focus the analysis of heating system. These features can impact AM energy consumption without any doubt.

Table 5.4 Weights of working environment features

Feature name	Weight	Feature name	Weight
LabTemperature	0.0146	FrameTemperature left	0.0403
ControlTemperature	0.0127	FrameTemperature right	0.0329
ControlHumidity	0.0102	PlatformTemperature	0.0426
t_at_BNLA	0.0114	ScannerTemperature	0.0269
ChamberTemperature	0.0292	PyrometerTemperature	0.0264
FrameTemperature front	0.0383	O ₂ Level	0.0135
FrameTemperature back	0.0367	EnergyDeviation	0.0145
<i>Total weight</i>	<i>0.3505</i>		

By analysing the importance of energy consumption impact features. The design-relevant features are focused for AM energy consumption prediction in this research. Before proposing the prediction method, the patterns of design-relevant feature is determined by analysing some examples of CAD model for the target system.

5.2.2 Pattern Analysis of Design-relevant Data

A number of examples of the CAD model will be shown in the section. These examples are chosen from the system CAD model database that was created over the last two years. Figure 5.1 shows two examples of product CAD models. From these two examples, a sort of characteristics were identified and noted:

1. The overall complexity of the part made by SLS can be very different. It could be a complicated mechanical part or a well-designed special model.
2. The part design can consist of many different geometric features. Some of them are more of a standard shape and form, while others can be a one-off with unique features.
3. In one build, to be more process efficient, it often consists of different designs in different shapes and forms designed by different designers, but to be made together in one build.

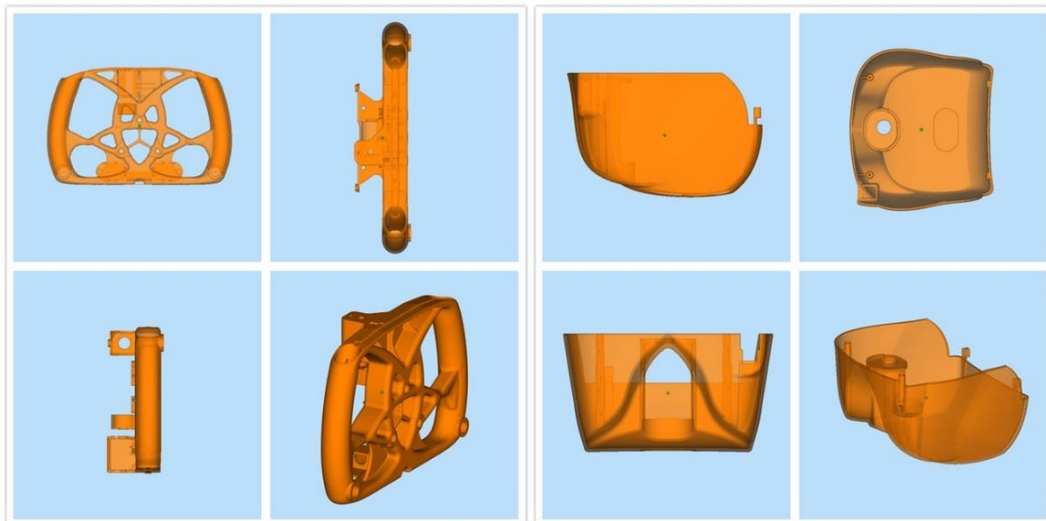


Figure 5.1 Two examples of products made by target SLS system

The two parts shown in Figure 5.1 were collected from the same production which is displayed in Figure 5.2 (a). In this production operation, totally, 17 items were produced where these 17 parts were originally from several orders. Generally, the number of parts made in every SLS production can be very different. In some cases, it

made 3 to 4 parts in one built, while others can produce more than one hundred parts simultaneously. Figure 5.2 (b) shows another production example where 28 items were made together. Both builds shown in Figure 5.2 (a) show respective SLS production particularly from the viewpoint of product design and process planning.

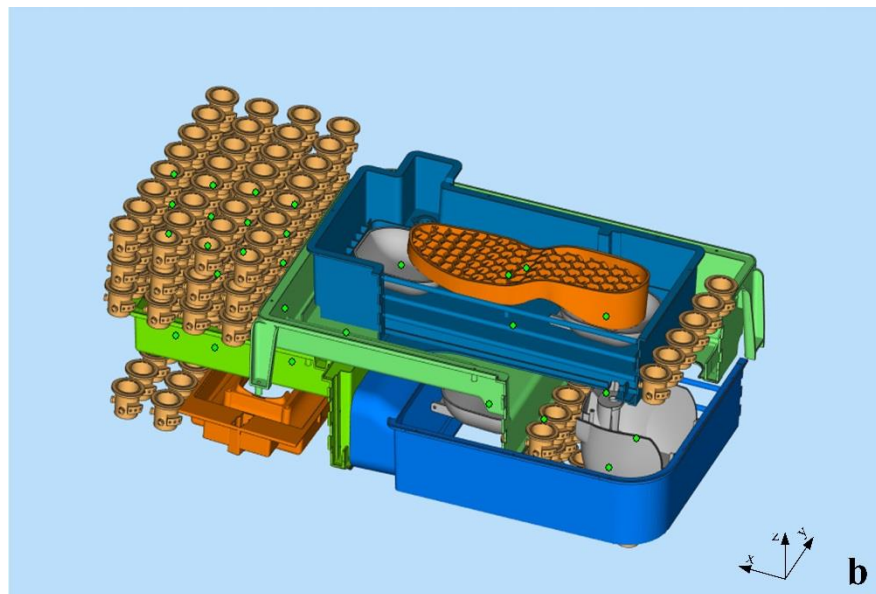
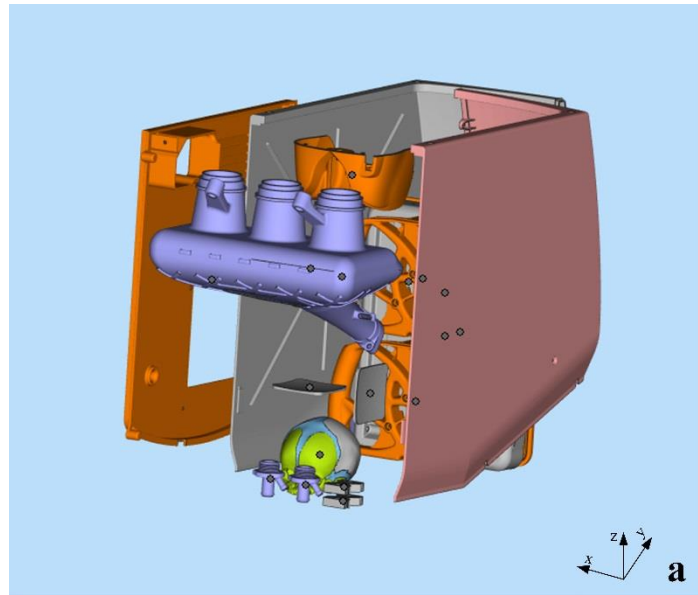


Figure 5.2 CAD models of another SLS production

Observing and comparing above two SLS productions shown in Figure 5.2, a few points concerning production characteristics are noted:

1. Each SLS operation produces a wide range of parts and components in terms of both quantity and geometric profiles.
2. The parts and components produced in each production can have very different product features represented in CAD models.
3. The exact position (location) and rotation of every single part and component in the bed are determined by SLS technicians.
4. The products are often randomly chosen from customers' orders. This means for parts contained in a specific order, they can appear in different SLS productions.

Based on the interview with a number of SLS technicians at School of Engineering, Cardiff University, it is often the case that technicians decide the type, quantity, position and rotation of parts and components to be produced in each production. Their decisions largely depend on the size of SLS building platform and technicians' past experience. While critical process-related information, for example, concerning SLS system energy spending, has been highlighted in literature, technicians and designers have not really considered such critical inputs during their production planning. Therefore, it is imperative that such critical aspects of the process, e.g., energy consumption, can be reflected during design phase or in production planning.

In the next section, the design-relevant data of AM process is focused as the main input, and based on the proposed energy consumption modelling approach, an energy consumption prediction method is proposed

5.2.3 Energy Consumption Prediction based on Design-relevant Data

In order to predict energy consumption for AM systems based on the design-relevant data, a deep learning based approach is proposed in this study. The proposed AM energy consumption modelling process is shown in Figure 5.3.

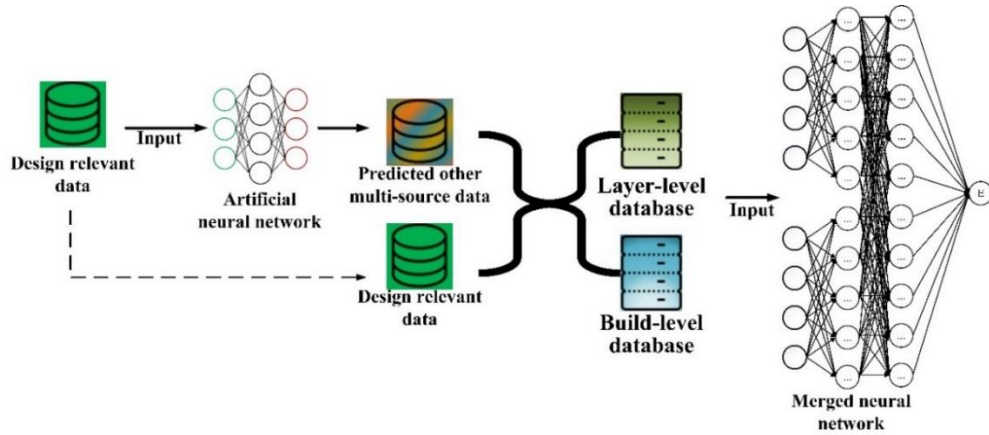


Figure 5.3 AM energy consumption modelling based on design-relevant data

Firstly, the design-relevant data (D_i) is used for predicting the process data. The process data includes various datasets, such as working environment dataset, process operation dataset (parameter setting data), and material condition dataset. Each of these datasets can also involve different data attribute. For example, the process operation dataset consists of the parameter settings of laser powder, scan space, scan speed, and scan angle. It is noticed that a different system may involve different attributes. More details of multi-source data analytics for AM energy consumption has been introduced and discussed in our previous paper (Qin et al., 2018). The first deep learning based prediction model $f_p(*)$ is built using the design-relevant data and historical process data (L_j), shown as follows:

$$L_j = f_p(D_i) \quad (5.1)$$

$$E_U = f_m(D_i, L_j) \quad (5.2)$$

By using the design-relevant data and the predicted multi-source data that predicted by equation (5.1), these two datasets consist a complete multi-source dataset which can be classified into two levelled datasets (Qin et al., 2018). Then the merged neural network $f_m(*)$ is used for integrating the predicted other multi-source data and design-relevant data and predicting energy consumption (E_U), which is donated as equation

(5.2). The details of the merged neural network ($f_m(*)$) are explained in the Chapter 4. This energy consumption modelling is based on deep learning techniques, and two neural networks are applied in the approach. The design-relevant data is used as the primary input data.

Generally, the design features of the AM process are defined by two group people, part designers and process operators (Chergui et al., 2018). The design-relevant data is then categorised as two datasets, part-design dataset, and process-planning dataset, which is donated as:

$$D_i = [PD_g, PP_h] \quad (5.3)$$

where PD represents the part-design dataset which the number of g features, PP is the process-planning dataset which the number of h feather.

5.3 Evaluation of AM Energy Consumption Prediction using Design-relevant Data

This research has collected design-relevant data from August 2016 until April 2019, including over a thousand product CAD models and spanning more than a hundred productions. These parts are ordered by different companies and designed by various part designers. Each production process produces a wide range of parts in terms of geometric profiles. Also, these parts are placed in different locations with various orientations which are generally determined by operators. These decisions normally depend on system operators' experiences of AM process planning. It is obvious that every build of this AM process can be very different, in terms of not only the part number and geometric profiles but also the process planning factors, such as part position and rotation. In this section, the design-relevant data used in the target system was used for building energy consumption modelling. The performance of the proposed model was compared to the one of multi-source data modelling and benchmarks.

5.3.1 Design-relevant Data Description

In this case study, several design-relevant features were extracted to describe the produced models. The original data of these design-relevant features was extracted from the CAD models. To recognise these features, an AM analysis software was applied in this case study, called Autodesk Netfabb. The user interface of the software is presented as Figure 5.4. The CAD models shown in the figure were built on 15th September 2017. The whole production had 26 different part which were ordered by five different companies or organisations. As discussed in last section, the parts built in the same production involves significantly different patterns and characteristics.

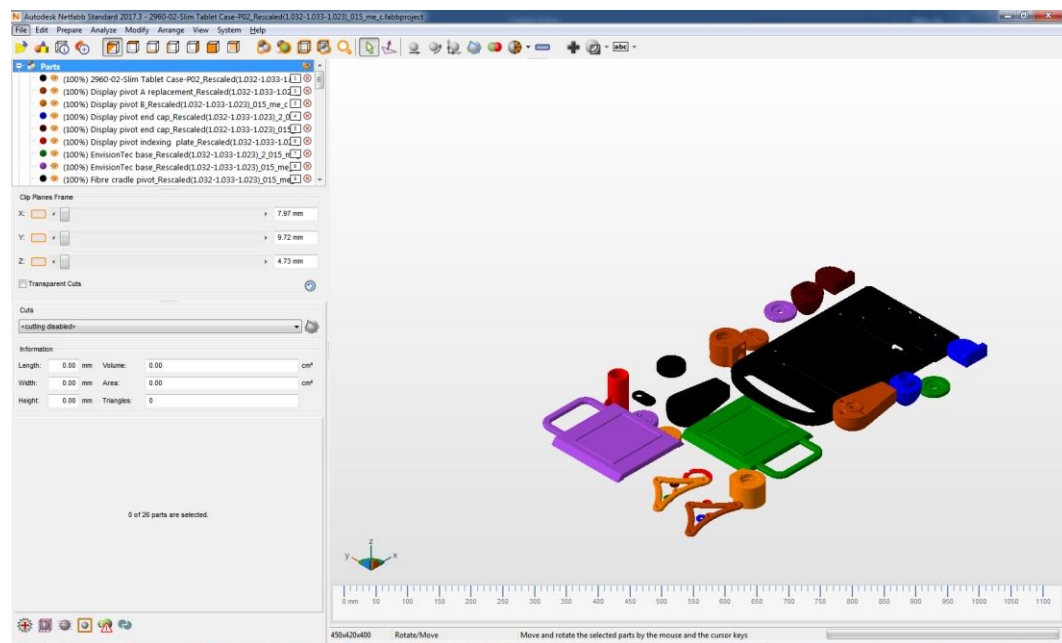
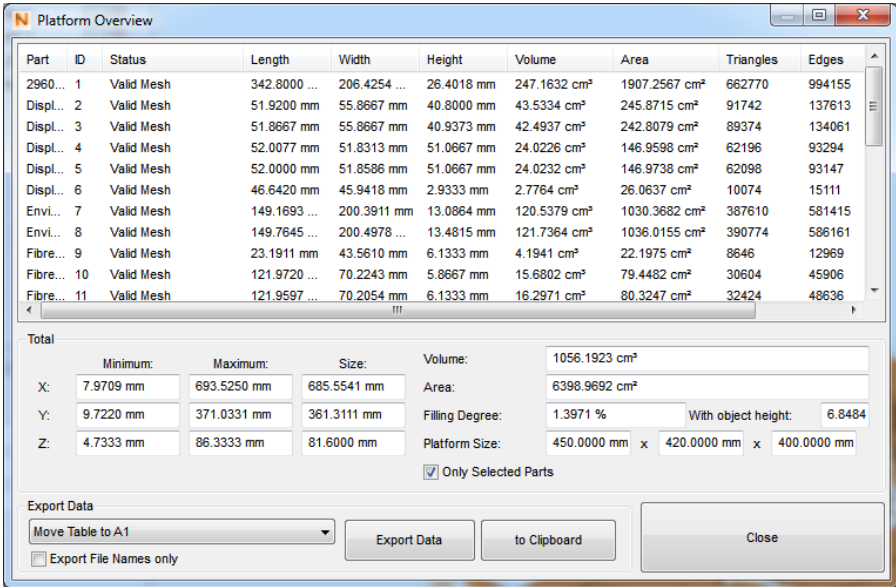


Figure 5.4 Autodesk Netfabb interface for collecting design-relevant data, example built on 15th September 2017

In order to represent these patterns and characteristics, this research used Autodesk Netfabb software to analyse the models. From the software several data or information is extracted, such as the envelop size (three dimensions) of each part and the entire build, the filling degree of entire build, and the area size of the entire build. The interface of design information analysis is shown as Figure 5.5. The information can be exported as the datasets, which allows calculations to be done to obtain more

design-relevant data. The code of generation design-relevant data is shown in Appendix B.5.

With this information, more design-relevant data is calculated, which includes average filling degree of a single part, average rates between three dimensions of a single part, and rates between three dimensions of a whole build. By using this programming, twelve design-relevant features are collected in this case study. The details of design-relevant data is shown at Table 5.5. The entire design-relevant dataset is shown in the Appendix A.2.



The screenshot shows the 'Platform Overview' window in Autodesk Netfabb. It contains a table with 11 columns: Part, ID, Status, Length, Width, Height, Volume, Area, Triangles, and Edges. Below the table is a 'Total' section with various statistics and a 'Platform Size' section with dimensions and a 'Filling Degree' field. There are also 'Export Data' and 'to Clipboard' buttons.

Part	ID	Status	Length	Width	Height	Volume	Area	Triangles	Edges
2960...	1	Valid Mesh	342.8000 ...	206.4254 ...	26.4018 mm	247.1632 cm ³	1907.2567 cm ²	662770	994155
Displ...	2	Valid Mesh	51.9200 mm	55.8667 mm	40.8000 mm	43.5334 cm ³	245.8715 cm ²	91742	137613
Displ...	3	Valid Mesh	51.8667 mm	55.8667 mm	40.9373 mm	42.4937 cm ³	242.8079 cm ²	89374	134061
Displ...	4	Valid Mesh	52.0077 mm	51.8313 mm	51.0667 mm	24.0226 cm ³	146.9598 cm ²	62196	93294
Displ...	5	Valid Mesh	52.0000 mm	51.8586 mm	51.0667 mm	24.0232 cm ³	146.9738 cm ²	62098	93147
Displ...	6	Valid Mesh	46.6420 mm	45.9418 mm	2.9333 mm	2.7764 cm ³	26.0637 cm ²	10074	15111
Envi...	7	Valid Mesh	149.1693 ...	200.3911 mm	13.0864 mm	120.5379 cm ³	1030.3682 cm ²	387610	581415
Envi...	8	Valid Mesh	149.7645 ...	200.4978 ...	13.4815 mm	121.7364 cm ³	1036.0155 cm ²	390774	586161
Fibre...	9	Valid Mesh	23.1911 mm	43.5610 mm	6.1333 mm	4.1941 cm ³	22.1975 cm ²	8646	12969
Fibre...	10	Valid Mesh	121.9720 ...	70.2243 mm	5.8667 mm	15.6802 cm ³	79.4482 cm ²	30604	45906
Fibre...	11	Valid Mesh	121.9597 ...	70.2054 mm	6.1333 mm	16.2971 cm ³	80.3247 cm ²	32424	48636

Total

Minimum: 7.9709 mm Maximum: 693.5250 mm Size: 685.5541 mm Volume: 1056.1923 cm³

X: 9.7220 mm Y: 371.0331 mm Z: 86.3333 mm Area: 6398.9692 cm²

Filling Degree: 1.3971 % With object height: 6.8484

Platform Size: 450.0000 mm x 420.0000 mm x 400.0000 mm

Only Selected Parts

Export Data: Move Table to A1 Export Data to Clipboard Close

Export File Names only

Figure 5.5 Information shown by Autodesk Netfabb

These features were divided into two classes, the part-design-relevant features, and the process-planning-relevant features. The part-design-relevant features are determined by part designers, and the process-planning-relevant features are determined by process operators. Specifically, the part filling degree, the average geometry ratios of three dimensions, and the average part height are the part-design-relevant features. The totally filling degree of the whole build, the total geometry ratio of three dimensions, the bottom area, the height of the build, and the number of produced parts are the process-planning-relevant features.

Table 5.5 Design-relevant feature description.

Part-design-relevant features		Process-planning-relevant features	
Feature names	Feature description	Feature names	Feature description
Part filling degree (%)	The average ratio between the actual volume and the envelope volume of each part.	Total filling degree (%)	The ratio between the actual volume and the envelope volume of the whole build.
Geometry ratio (wl)	The average ratio between the width and length of each part.	Total geometry ratio (wl)	The ratio between the width and length of each part.
Geometry ratio (hl)	The average ratio between the height and length of each part.	Total geometry ratio (hl)	The ratio between the height and length of the whole build.
Geometry ratio (wh)	The average ratio between the width and height of each part.	Total geometry ratio (wh)	The ratio between the width and height of each part.
Part height (mm)	The average height of each part.	Bottom area(cm²)	The bottom area of the whole build.
		Height (mm)	The height of the whole build.
		Number of Parts	The total number of parts of the whole build.

Additionally, the basic statistical information of this dataset is shown in Table 5.6, including the value of the maximum, minimum, average, and standard deviation for each design-relevant feature. These design-relevant features can represent the behaviours of the part designers and the process operators. Furthermore, the target AM process have included a wide range of design-relevant feature and energy consumption. It is interesting to note that the standard deviation of the ratio between the width and the length of the whole build is only 0.0303. The reason is that the AM process operators generally filled the bottom of the building plate entirely. When the build chamber is fully filled, the ratio between the chamber width and its length is about 0.66.

Table 5.6 The basic statistic information of the design-relevant data

	Part filling degree (%)	Geometry ratio (wl)	Geometry ratio (hl)	Geometry ratio (wh)	Part height (mm)	Total filling degree (%)	Total geometry ratio (wl)	Total geometry ratio (hl)	Total geometry ratio (wh)	Bottom area (cm²)	Height (mm)	Number of Part
Minimum	2.1237	0.0713	0.0319	0.2637	15.4958	1.4895	0.4664	0.0461	0.6448	1228.4154	29.5429	2
Maximum	41.4006	7.8088	8.3898	28.1925	321.0955	22.7305	0.6530	0.8246	10.8877	2655.0434	570.6848	115
Average	15.9732	1.1709	0.5615	3.3402	65.4453	8.6514	0.5361	0.2688	2.9369	2359.5735	180.2767	27
1st Quartile	9.0960	0.6422	0.2527	1.5174	35.7571	4.9704	0.5244	0.1551	1.5724	2240.7884	100.8143	11
Median	13.6305	0.9597	0.3965	2.2560	50.6216	7.6354	0.5374	0.2250	2.3545	2476.7168	153.3181	20
3st Quartile	23.0468	1.2183	0.6034	3.3602	80.4060	11.3647	0.5443	0.3388	3.4840	2568.2663	228.1132	38
Standard deviation	9.1083	1.0374	0.8547	3.7172	48.0987	4.5723	0.0303	0.1642	2.1445	295.5327	114.5861	22

5.3.2 Results of Energy Consumption Prediction based on Design-relevant Data

Based on the validation metrics that are shown in Chapter 3, the results of three energy prediction models, which are the ANN model using design-relevant data directly, the proposed model, and the multi-source data model, are displayed in Table 5.7. The proposed model is compared to the previous energy consumption prediction model (Qin et al., 2018) and the model that only uses design-relevant data. The MCC of the proposed energy consumption model that is introduced in this chapter is 0.7908, and RSME is 23.2163 kWh/kg. According to Energy consumption model shown in last chapter, the MCC of energy consumption prediction model using multi-source data is 0.8030, and the RSME is 20.2271 kWh/kg. The comparison of the proposed model and the previous model reveal that, although the proposed method has not obtained the best results (Panda et al., 2016), it is still acceptable with only 0.0122 MCC and 2.9892 kWh/kg RSME differences.

It is highlighted that the RSME of the proposed model is over 50% less than the model using an ANN model to predict energy consumption directly. Furthermore, the proposed model is better than the performance of the benchmark models that were compared in the previous paper. The performances of benchmark models are shown in the previous paper, which the MCC and the RMSE of the Linear regression are 0.607 and 115.056 kWh/kg; the MCC and the RMSE of the Decision tree are 0.691 and 59.585 kWh/kg; the MCC and the RMSE of the k -nearest neighbour are 0.541 and 44.168 kWh/kg, which has been obtained from last chapter.

Table 5.7 The prediction results of the three models

Prediction model	MCC	RSME (kWh/kg)
ANN model using design-relevant data	0.7012	69.5732
Proposed energy consumption prediction model	0.7908	23.2163
Multi-source data predict energy consumption	0.8030	20.2271

Moreover, the weights of the design-relevant feature are extracted from the merged neural networks. The weights displayed in Table 5.8. The most substantial one (0.1254)

is the weight of the total filling degree. Also, there exist other four weights which are higher than the average weight, the geometry of width and height, the bottom area, the height of the whole build, and the geometry of height and length. These five features are considered as the most critical features that can significantly impact the prediction of AM energy consumption in this case study.

Table 5.8 The weights of the design-relevant features extracted from the merged neural networks.

Part-design-relevant features		Process-planning-relevant features	
Feature name	Weight	Feature name	Weight
Part filling degree (%)	0.0744	Total filling degree (%)	0.1209
Geometry ratio (wl)	0.0828	Total geometry ratio (wl)	0.0667
Geometry ratio (hl)	0.0841	Total geometry ratio (hl)	0.0697
Geometry ratio (wh)	0.0958	Total geometry ratio (wh)	0.0720
Part height (mm)	0.0793	Bottom area(cm ²)	0.0853
		Height (mm)	0.0832
		Number of Parts	0.0854
Total weight	0.4164	Total weight	0.58353

5.3.3 Discussion

Energy consumption was predicted using a deep learning-based prediction model developed based on previous work. The purpose of this chapter is to build the model by using design-relevant data. The data was collected before the AM process began, which indicates that AM energy consumption could be predicted prior to the production process commencing. The performance promotion of the proposed model is 1.52% MCC lower and 4.98% RSME higher compared to the results of Chapter 4. Although it did not match the performance of the multi-source data prediction model, it can predict the energy consumption before the process. The performance of the proposed model was worse than that of the multi-source data prediction model within a reasonable range of error. It performs better than the model that used neural networks directly and other benchmark algorithms used in the last chapter. AM energy consumption was predicted using a deep learning-based prediction model developed based on our previous work.

The data was collected before the AM process began, which indicates that AM energy consumption is predicted prior to the production process commencing. Comparing to our previous study, this modelling and prediction method proposed in this paper has been improved, which provides an opportunity to understand and reduce the AM energy consumption before the process.

Generally, other relevant researches focused on impacts of one or two design-relevant features, such as thickness and part orientation, for AM energy consumption, and examined the relationship through the experimental focusing on certain values of features. However, with the rapid development of AM technology, AM tends to produce multiple parts in one production, especially for SLS and SLM systems (Chergui et al., 2018). It is hard to analyse the system only based on one or two features that describe the single part, like part orientation. Also, the AM produced part generally is complex because of the special structure and design. Therefore, it is necessary to consider more design features, which represent the design information precisely. In addition, only applying the experiment is difficult to validate this complex issue that should involve significant variants of each feature. Comparing to the other relevant researches reviewed in Section 2, the proposed approach involves more AM design-relevant features, including part design features and process planning features, which are able to represent the design condition of multiple part production. These two types of design-relevant features are proposed based on the review of DfAM research, which stands on both perspectives of part designer and process operators. Furthermore, the proposed method was built and validated by a large sum of historical data, including thousands of CAD models in over a hundred builds. Different from other relevant studies, this method covers much more variables of each feature according to the actual production.

Moreover, two types of design-relevant features, part design relevant features and process planning features, are used in this research, which have not covered the entire area of DfAM. Another future work in this research is to collect more design-relevant data. For example, material design can be one type of important feature as the multiple material AM production is a trend in both academia and industry (Thompson et al.,

2016). Furthermore, testing experiments should be applied to validate the simulation results in the future

5.4 Summary

The focus of this chapter has been on the prediction of AM process energy consumption. With the model built in the last chapter and feature analysis of all energy consumption features, the design-relevant features are selected as the best optimiser for reducing the AM energy consumption. In this chapter, the design patterns are discovered from several examples of AM produced product, especially for multiple part production, such as SLS and SLM. It is more complicated than the single part production. Also, according to the literature of DfAM, the determined AM design patterns follow the essential characteristics of DfAM.

Then, the design-relevant data based energy consumption prediction is proposed, which is exemplified in an SLS process. The energy consumption prediction approach based on deep learning technology has been proposed that uses design-relevant data as input. Design-relevant data is generated before the AM process begins and includes part design data and process planning data, which are determined by part designers and process operators. It appears that the proposed energy consumption prediction approach obtained results similar to those of the previous prediction model using design-relevant data.

Chapter 6 Data-driven AM Energy Consumption Management

6.1 Introduction

In the last chapter, the AM energy consumption has been predicted before producing the parts only based on design-relevant data and historical multi-source data. With the help of energy consumption framework, modelling, prediction, and optimisation, managing energy consumption become possible. Modelling and prediction have been introduced in the last two chapters.

The management process includes framework design, modelling, prediction, and optimisation. In the first section of this chapter, the entire data-driven AM energy consumption management is introduced. It reflects the essential information of previous chapters, and the energy consumption optimisation will be introduced in the second half. This research proposes a deep learning driven energy consumption method. The energy consumption is controlled by optimising the decisions of part designers and process operators using the proposed method. The optimisation method is validated on the target AM system. The results are displayed and discussed in detail.

6.2 Data-driven AM Energy Consumption Management

In order to manage AM energy consumption, it is necessary to model, predict, and optimise energy consumption. In this section, the modelling and prediction are

reflected to enhance the understanding of energy consumption. Furthermore, an optimisation method is introduced in next section.

6.2.1 Process of Data-driven AM Energy Consumption Management

Sufficient relevant data is needed to be collected and analysed to manage the energy consumption in the AM. The framework is necessary to be designed and structured for understanding the process, collecting and integrating the relevant data, and analysing to discover the information and knowledge. In this research, a framework was proposed in for the above aims in chapter 3. From the understanding of the AM, the AM production generates a multi-source data environment, which four types of features have been considered for energy consumption. To integrate this multiple levelled data for energy consumption modelling, a hybrid energy consumption modelling approach was proposed, which is based on the cooperation of IoT, clustering, and deep learning technologies. By analysing the weight of each input features in the energy consumption mode, the importance of each energy consumption impact feature is obtained. Comparing these features, the design-relevant feature and working environment feature are two types of most essential features.

For the prediction, the input data need to be determined before production. The design-relevant features are selected as the core input feature for the prediction. Based on the analysis of AM design-relevant feature and literature of DfAM, twelve design-relevant features are focused, which decided by part designers and process operators. These two types of design-relevant features are determined to rely on the relevant professionals' experience and the capability of the AM system. This research proposed a prediction method which only uses the design-relevant features as the input of prediction, which is based on the multi-source data modelling. Only historical multi-source data is used.

The final step of the AM energy consumption management is to optimise the energy consumption by changing some features or parameters. Based on the reviewed literature and prediction method, the design-relevant features are focused as the

optimised features to manage energy consumption for the AM, which aims to reduce energy consumption to the lowest value. In the next section, a novelty energy consumption optimisation is proposed.

6.2.2 Deep Learning Driven Particle Swarm Optimisation (DLD-PSO)

In this section, the energy consumption optimisation approach is proposed based on particle swarm optimisation (PSO). Among the various optimisation algorithms, PSO is a robust algorithm that is able to solve nonlinear multi-objective problems so as to help relevant professionals for decision-making (Bai, 2010, Moradi and Abedini, 2012, Chen and Huang, 2017).

In this chapter, the AM energy consumption management is explained in detail including energy consumption modelling, prediction, and optimisation. For the optimisation, a novel deep learning driven PSO (DLD-PSO) algorithm is proposed to reduce AM energy consumption. The main factors in DLD-PSO, such as constant inertia weight and cognitive factors, are driven by the deep learning model. A case study validates the approach. In the case study section, four build examples are tested for proving the feasibility of the approach in detail in terms of result comparison, optimisation process and optimisation details. Moreover, only with a reasonable optimisation process, the AM energy consumption can be managed. To fill this research gap, an energy consumption optimisation is proposed based on the PSO. The design-relevant data is the target of optimisation, and the purpose of the optimisation is reducing the energy consumption. In the next two subsections, the proposed optimisation approach is introduced in detail.

Generally, the searching speed of the particles is adjusted by equal parameters in conventional PSOs (Kennedy, 2011, Kim and Son, 2012). These parameters are defined by constant inertia weight and cognitive factors (Shi, 2001). However, since each relevant feature may have various types of relationship with the optimised target, it is necessary to introduce variable particle searching speed based on the correlations between each feature and the optimised target. Deep learning, as an advanced machine

learning technique, has shown its merits in prediction modelling based on high-dimensional and large-scale data (LeCun et al., 2015a). It has also shown its sensitivity to correlate the relevant features, which is represented by neuron activity (Kim et al., 2016). If this functional characteristic can be adapted to drive PSO, each feature will use a different searching speed in order to achieve the optimised value. If this is possible, it not only improves the convergence speed but also enhances the global best of PSO.

- **Objectives of DLD-PSO**

To initialize the particles, the restriction of each design-relevant feature is necessary to identify. Due to the high-relevance between these features and design, it is essential to identify the sources of the design. The purpose of managing the AM energy consumption is to minimise the energy usage of the AM process. Define the objective function as:

$$\text{Min } [f_m(D_i, L_j)] \quad (6.1),$$

where the $f_m()$ is the merged neural network, and D_i , and L_j are referred to the function 5.2.

$$s. t. : PD_{min}^m \leq PD_m \leq PD_{max}^m \quad (6.2)$$

where the PD_{min}^m and PD_{max}^m are the minimum and maximum of the part-design dataset that is determined by part designers.

$$PP_{min}^n \leq PP_n \leq PP_{max}^n \quad (6.3)$$

The PP_{min}^n and PP_{max}^n are the restriction of the process-planning dataset that is determined by process operators.

- **Process of DLD-PSO**

The DLD-PSO is applied to solve the AM energy management and optimisation problem in this study. The optimisation process is shown in Figure 6.1.

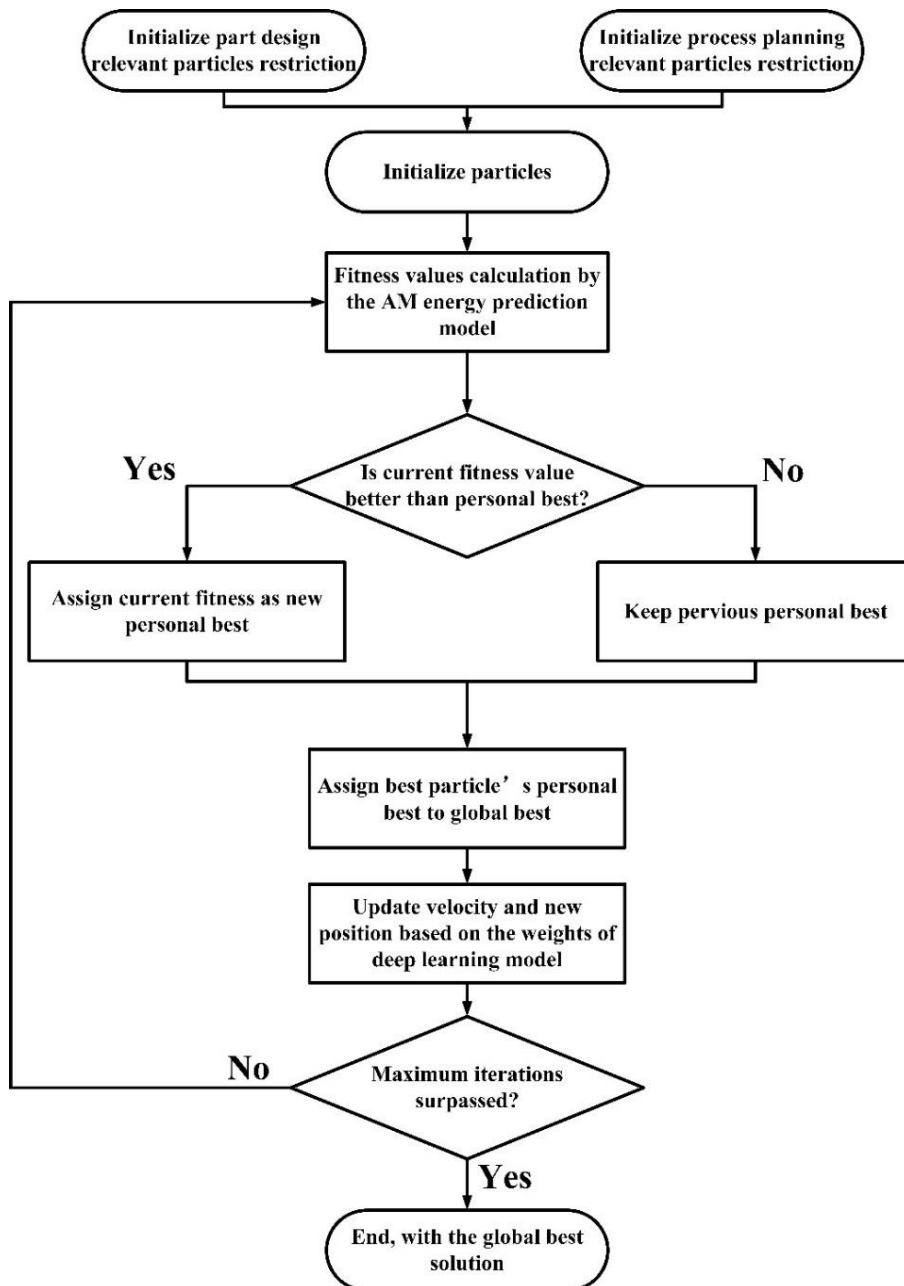


Figure 6.1 The process of the DLD-PSO

Before starting the optimisation, the particle restriction is initialized by part designers and process operators respectively. In the restriction, the initial particles are generated. The fitness values are calculated by the function (2). Then, the fitness value of each particle is compared for find the best values, lowest energy consumption, which is defined as the personal best (p_{best}). Once the new personal best is targeted, the global

best particle (g_{best}) is also found from the best particle's personal best. After that, new particles in each interval is expressed by the following equation :

$$v_i(t + 1) = W * (w_0 * v_i(t) + C_1 * [p_{best}(t) - D_i(t)] + C_2 * [g_{best}(t) - D_i(t)]) \quad (6.4)$$

$$D_i(t + 1) = D_i(t) + v_i(t) \quad (6.5)$$

where v_i is the iteration velocity; w_0 is the inertia weight; C_1 and C_2 are cognitive factors. These two factors determine the cognitive speed when the particle is personal best and globe best.

$$w_k^e = [w_1, w_2, \dots w_K] \quad (6.6)$$

$$W = [w_d^1, w_d^2, \dots w_d^e] \quad (6.7)$$

After training the deep learning model, weights of all neurons (w_d^i) are defined by the optimiser function. k is the number of neurons on the first layer that is connected to the input layer. Each neuron on the first layer is fully connected to all the neurons on the input layer, which have the number of i features. Each weight in the W has represented the weight of a feature of the design-relevant dataset. The W is based on the prediction model. It affects one of the most critical factors of PSO, the changing velocity v_i . Once the optimisation process achieves the maximum number of iterations, the process ends, and the global best of the particle is considered as the optimised results. In Section 3.3, the validation methods were presented.

6.3 Evaluation of DLD-PSO

In this section, the proposed energy consumption management/optimisation method is validated by a feasibility study. It is highlighted that the main purpose of energy consumption management in this feasibility study is reducing energy consumption, which is based on most actual situations.

Four build examples are selected in the feasibility study. According to the details of these four examples and system capability, the restrictions are determined before the optimisation process. The optimisation processing is shown as three types of optimisation, which the results are compared. At the end of this section, optimised design-relevant features are displayed.

6.3.1 Introduction of AM Built Examples for Energy Consumption Management

The actual energy consumption frequency histogram is displayed in Figure 6.2. It is noticeable that over 80% of builds consume unit energy ranging from 120 kWh/kg to 600 kWh/kg. However, energy consumption of each build shows differently even in this range. The standard deviation is 496.8285 kWh/kg which is larger than the average (about 450 kWh/kg). Due to the computing capability, it is necessary to select different examples from the entire range of energy consumption for the simulation. In order to display the reasonable and convincing optimised results, this case study selects four examples that have different energy consumption, which were the Build No. 1 (111.3531 kWh/kg), Build No. 2 (427.1967 kWh/kg), Build No. 3 (632.4544 kWh/kg), and Build No. 4 (1514.6010 kWh/kg). The design-relevant data of these four examples is shown in Table 6.1, and the CAD models are displayed in Figure 6.2.

These four examples are selected from the entire order database on different date. The required parts were ordered by several different companies or originations, which are designer by different designers and CAD software. The CAD models generally converted to STL files, which do not require the source type of file. Design-relevant information of these four examples are various in every feature.

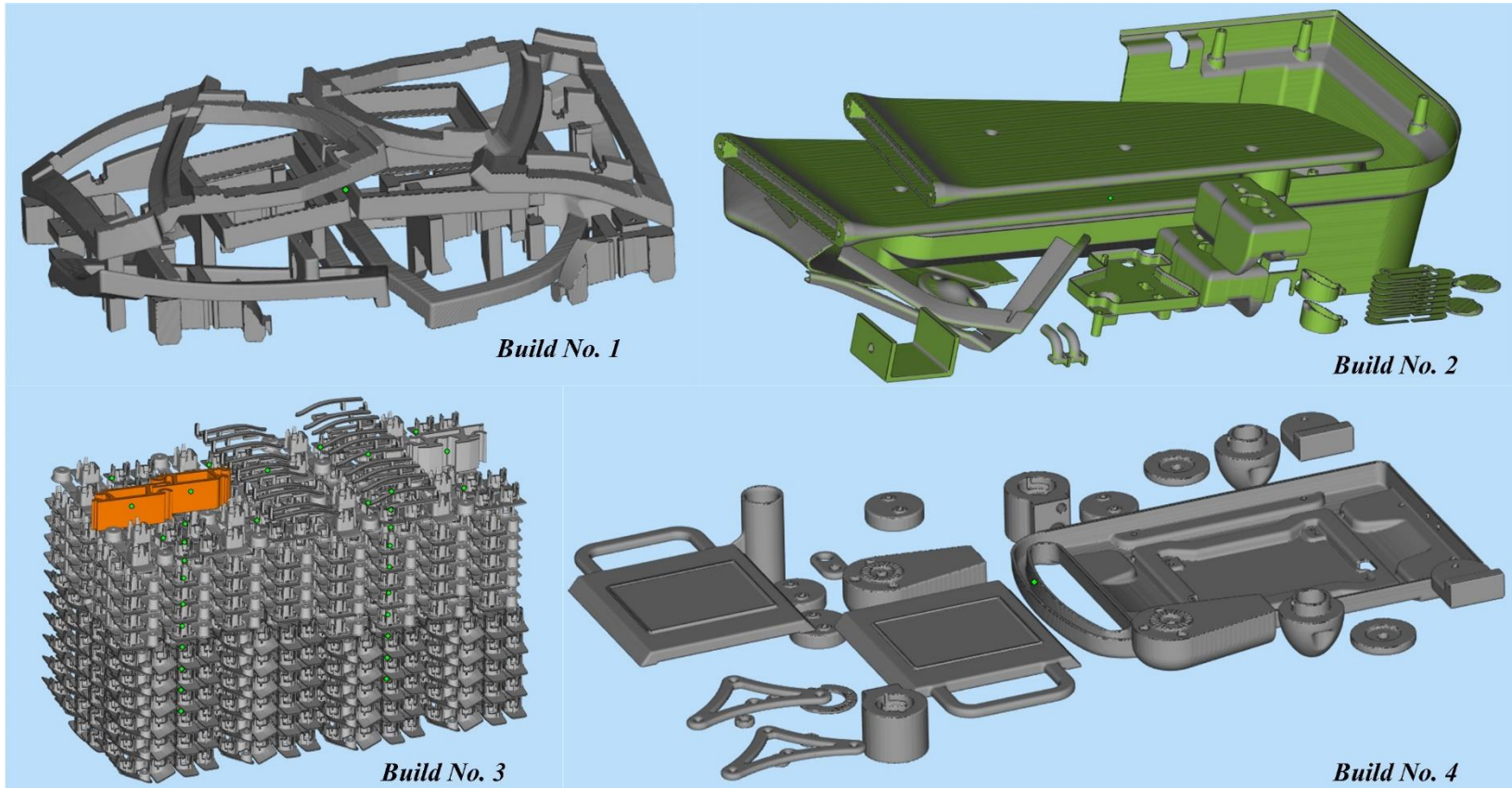


Figure 6.2 The CAD models of the optimised examples

Table 6.1 Examples used for energy consumption management in the different ranges of energy consumption

Build No.	Part filling degree (%)	Geometry ratio (wl)	Geometry ratio (hl)	Geometry ratio (wh)	Part height (mm)	Total filling degree (%)	Total geometry ratio (wl)	Total geometry ratio (hl)	Total geometry ratio (wh)	Bottom area (cm²)	Height (mm)	Number of Part	Energy (kWh/kg)
Build No. 1	25.2876	1.2242	0.9478	1.2916	76.4834	12.6910	0.5360	0.3116	1.7202	2558.3574	215.2757	27	111.3531
Build No. 2	17.1347	0.6876	0.1508	4.5597	31.1093	6.6278	0.5420	0.2178	2.4883	2466.3961	146.9372	30	427.1967
Build No. 3	5.4582	0.9810	0.1761	5.5715	44.0349	4.9138	0.5401	0.6390	0.8452	2613.2170	444.4750	33	632.4544
Build No. 4	41.4006	0.9381	0.2662	3.5245	21.1145	5.2255	0.5270	0.1190	4.4278	2476.9831	81.6000	26	1514.6005

6.3.2 Feature Restriction

Before introducing the results, the design-relevant feature restriction is examined. The restriction is theoretically determined by part designers, process operators, and process capability. According to the interviews of the part designers, and the operators of the target AM process, the historical data and process capability, the restriction of all features for the four examples are displayed in Table 6.3. It still gives the part designers and the AM process operators a wide range of choices to improve their decision for managing energy consumption, which is generally reducing energy consumption.

Table 6.2 The restriction of the design-relevant features in the four optimised build examples

Features	Build No. 1	Build No. 2	Build No. 3	Build No. 4
Part filling degree (%)	23.0 ~ 28.0	15.0 ~ 20.0	3.0 ~ 8.0	39.0 ~ 44.0
Geometry ratio (wl)	1.00 ~ 1.50	0.40 ~ 0.90	0.70 ~ 1.20	0.60~ 1.10
Geometry ratio (hl)	0.70 ~ 1.20	0.05 ~ 0.55	0.05 ~ 0.55	0.05 ~ 0.55
Geometry ratio (wh)	1.00 ~ 1.50	4.30 ~ 4.80	5.30 ~ 5.80	3.30 ~ 3.80
Part height (mm)	60 ~ 90	22.5 ~ 52.5	35.0 ~ 48.0	18.0 ~ 38.0
Total filling degree (%)	10.0 ~ 15.0	5.0 ~ 10.0	3.0 ~ 8.0	3.0 ~ 8.0
Total geometry ratio (wl)	0.30 ~ 0.80	0.30 ~ 0.80	0.30 ~ 0.80	0.30 ~ 0.80
Total geometry ratio (hl)	0.10 ~ 0.60	0.10 ~ 0.60	0.40 ~ 0.90	0.05 ~ 0.55
Total geometry ratio (wh)	1.50 ~ 2.00	2.20 ~ 2.70	0.60 ~ 1.10	4.20 ~ 4.70
Bottom area (cm2)	2000 ~ 3000	2000 ~ 3000	2000 ~ 3000	2000 ~ 3000
Height (mm)	195 ~ 270	143 ~ 225	420 ~ 495	75 ~ 100
Number of Part	15 ~ 35	20 ~ 40	23 ~ 43	16 ~ 36

Moreover, some parameter settings of the neural networks and optimisation algorithms are determined before display the results. All neural networks used two types of activations: 1) for the output layer, scaled exponential linear activation was applied, and 2) for the remaining layers, the rectified linear unit activation was used. The mean squared error was used to represent the loss. Supported by a popular Python package, Keras, the Adam optimiser was used (LeCun et al., 2015b). Based on the dimension of input data, the particles pool size is 100, and the maximum number of iterations is 1000 for the PSOs in this paper (Röhler and Chen, 2011). Basic parameters of the conventional PSO, i.e., constriction coefficient 1 (c_1), constriction coefficient 2 (c_2),

and inertia weight (w_o), are 2, 2, 0.748 respectively, which is commonly used in PSO applications (Yusup et al., 2012)

6.3.3 Optimisation Results of DLD-PSO

Before display the optimisation results, Table 7 shows the comparison between predictive energy consumption and the actual energy consumption for these four builds. The absolute average error of these builds is about 34.3513 kWh/kg, which is close to the RSME of the proposed model (23.2163 kWh/kg). The error will grow when energy consumption increases. The lowest prediction error (+4.9959 kWh/kg) is from Build No. 1, while the actual energy consumption is 111.3531 kWh/kg. The largest error (-78.2030 kWh/kg) of these four examples is Build No. 4, while the actual energy consumption is 1514.6010 kWh/kg.

Table 6.3 The comparison between the predictive and the actual energy consumption

	Build No. 1	Build No. 2	Build No. 3	Build No. 4
Actual energy consumption (kWh/kg)	111.3531	427.1967	632.4544	1514.6010
Predictive energy consumption (kWh/kg)	116.3490	408.2854	597.1588	1436.3987
Error (kWh/kg)	+4.9959 (+4.48%)	-18.9113 (-4.43%)	-35.2956 (-5.58%)	-78.2023 (-5.16%)

Three types of optimisation results are presented depending on the decision of part designers and operators. The part-designer-oriented optimisation is for AM part designer only. The process-operator-oriented optimisation is to optimise the process operators' decision. The designer-and-operator-oriented optimisation considers optimising the decisions of part designers and process operators. Figure 6.2, Figure 6.3, Figure 6.4, and Figure 6.5 display the optimisation results of four build examples using the conventional PSO and the DLD-PSO. Among these optimisation results, the proposed PSO generally obtains better results that require lower energy consumption than the conventional PSO in smaller convergence time.

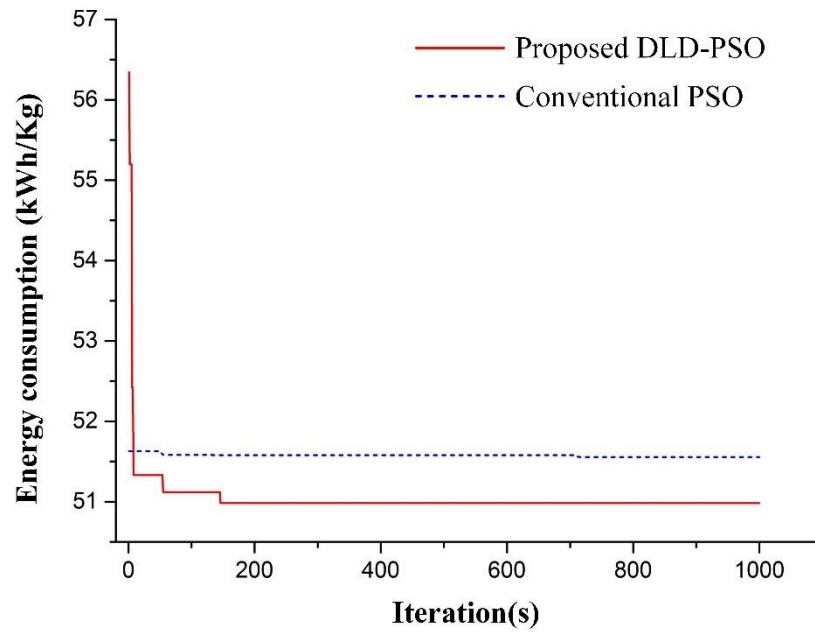


Figure 6.3 Part-designer-oriented optimisation result comparison between the conventional and the DLD-PSO for Build No.1

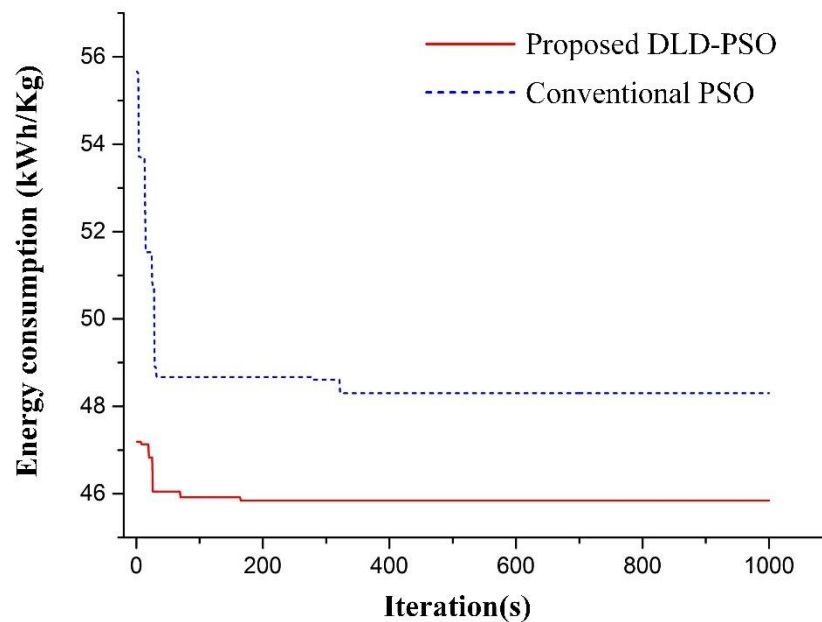


Figure 6.4 Process-operator-oriented optimisation result comparison between the conventional and the DLD-PSO for Build No.1

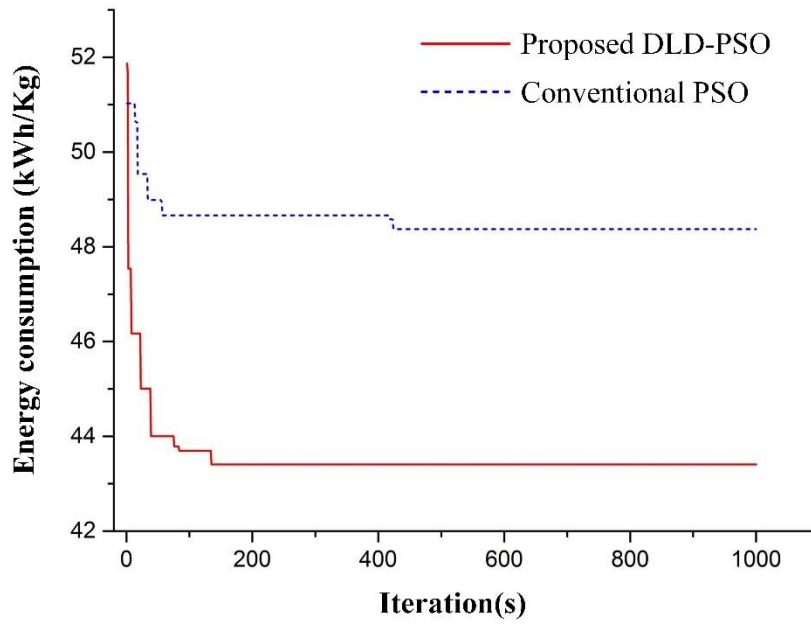


Figure 6.5 Designer-and-operator-oriented optimisation result comparison between the conventional and the DLD-PSO for Build No.1

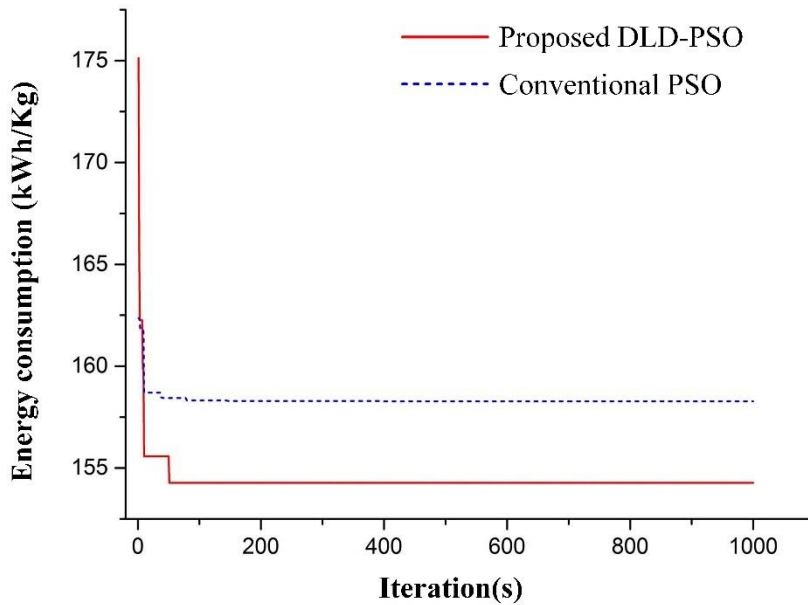


Figure 6.6 Part-designer-oriented optimisation result comparison between the conventional and the DLD-PSO for Build No.2

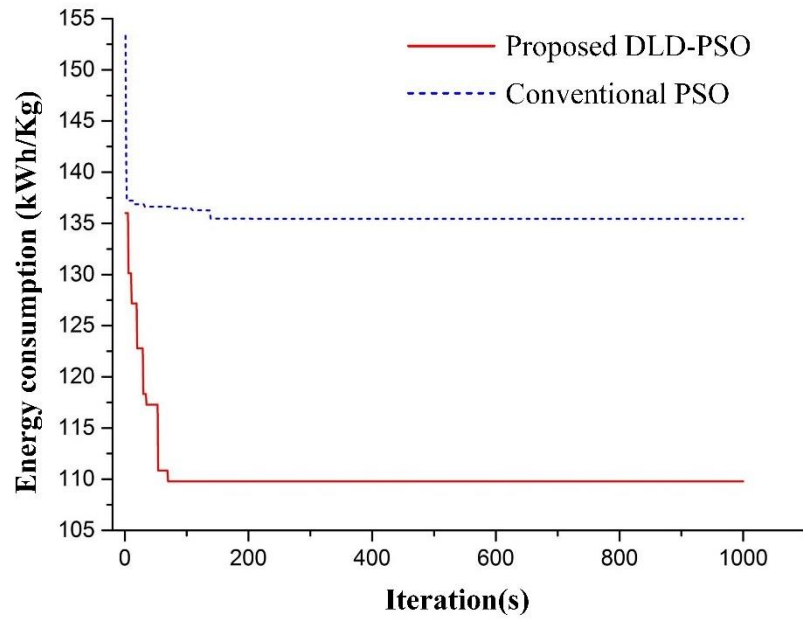


Figure 6.7 Process-operator-oriented optimisation result comparison between the conventional and the DLD-PSO for Build No.2

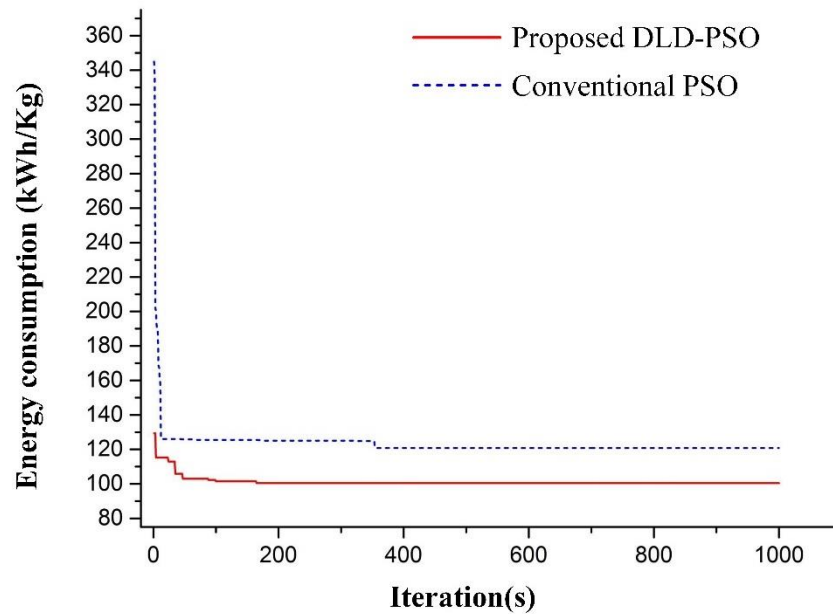


Figure 6.8 Designer-and-operator-oriented optimisation result comparison between the conventional and the DLD-PSO for Build No.2

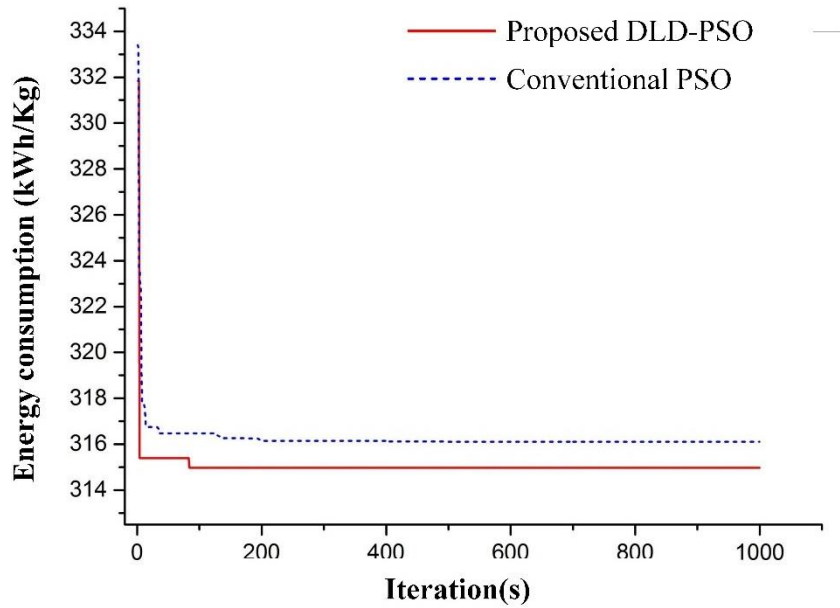


Figure 6.9 Part-designer-oriented optimisation result comparison between the conventional and the DLD-PSO for Build No.3

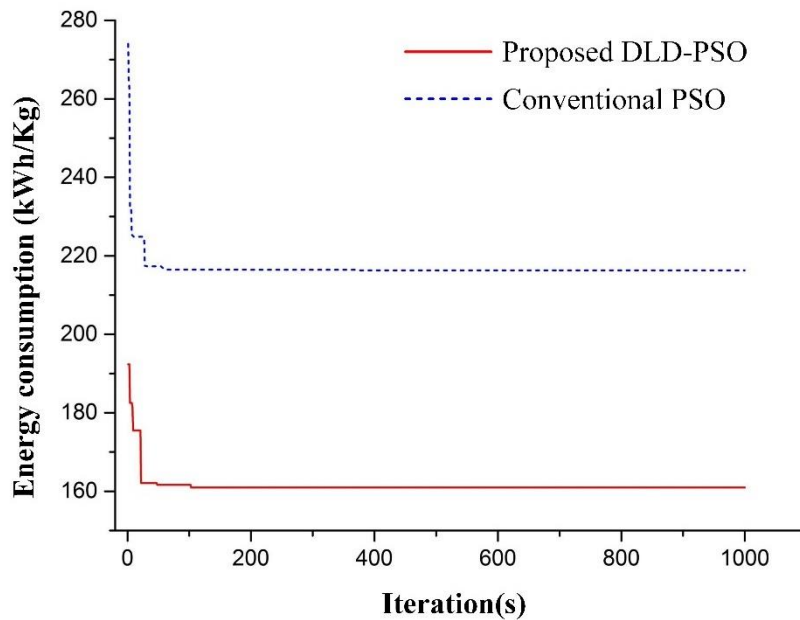


Figure 6.10 Process-operator-oriented optimisation result comparison between the conventional and the DLD-PSO for Build No.3

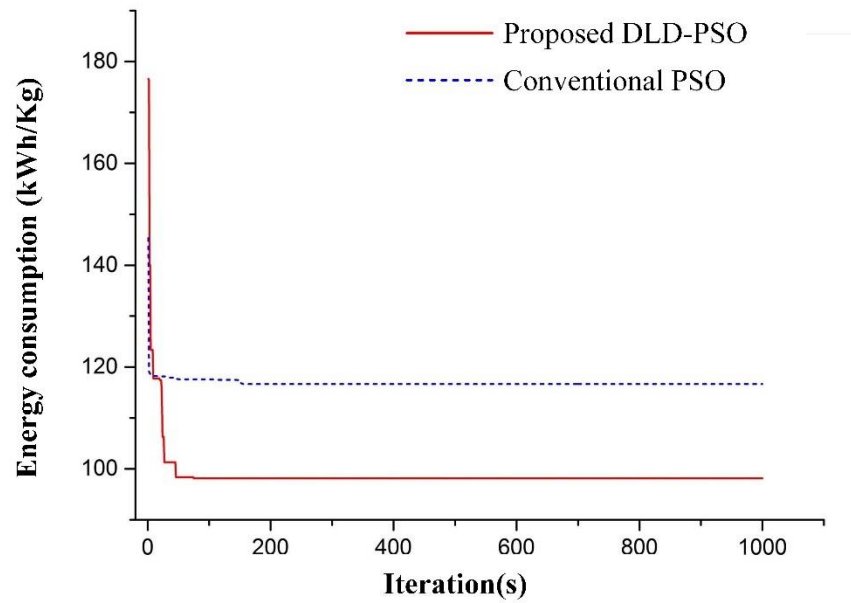


Figure 6.11 Designer-and-operator-oriented optimisation result comparison between the conventional and the DLD-PSO for Build No.3

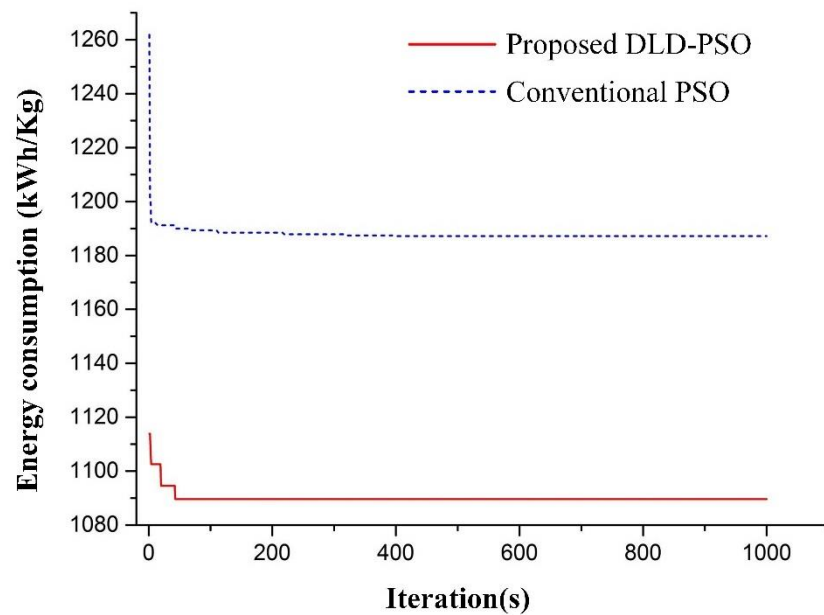


Figure 6.12 Part-designer-oriented optimisation result comparison between the conventional and the DLD-PSO for Build No.4

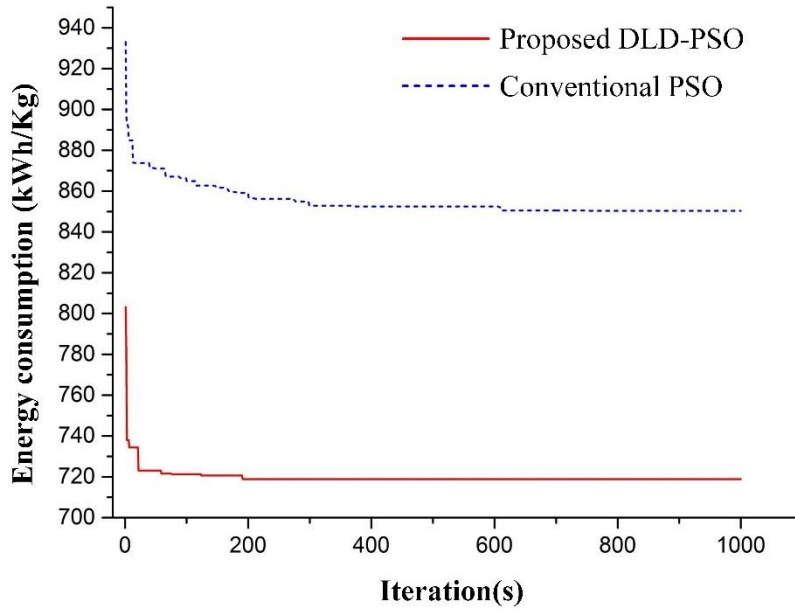


Figure 6.13 Process-operator-oriented optimisation result comparison between the conventional and the DLD-PSO for Build No.4

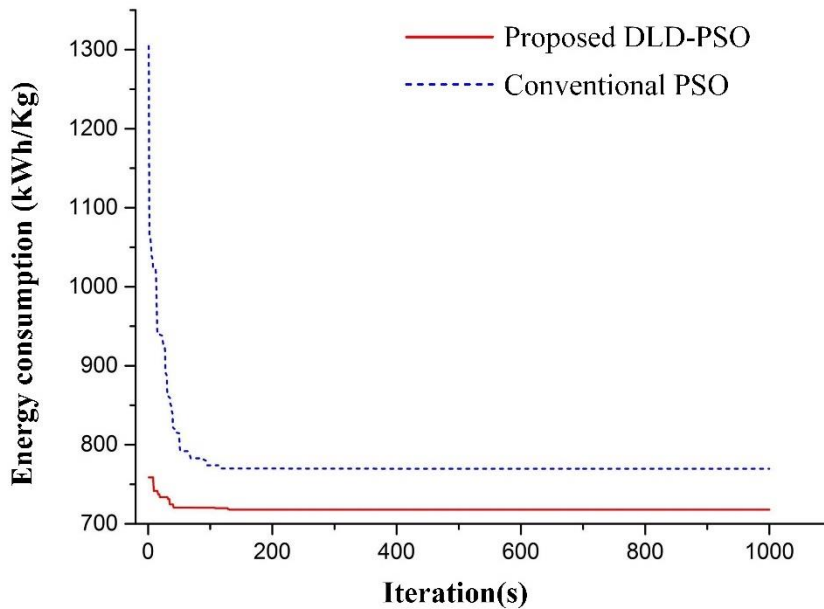


Figure 6.14 Designer-and-operator-oriented optimisation result comparison between the conventional and the DLD-PSO for Build No.4

Table 6.5 shows the optimisation performance of the conventional and the DLD-PSO including the convergence speed, I_v (iteration), and the lowest energy consumption, E_l (wh/g). The average convergence iteration of the conventional PSO is 360 iterations which are significantly larger than the proposed PSO (114 iterations). With the help of deep learning driven weights, the proposed PSO is able to search the globe best faster than the conventional PSO which uses the constant cognitive factors to determine the convergence speed. It is interesting to note that in comparison with each optimisation based on the DLD-PSO, the part-designer-oriented optimisation obtains the best results within the minimal iteration, 82 iterations on average, and process-operator-oriented optimisation have spent more time to get the best results, 134 iterations on average. Moreover, the DLD-PSO optimised energy consumption is generally lower than the conventional PSO optimised energy consumption, which is about 2.14% for the part-designer-oriented optimisation, about 6.62% for the process-operator-oriented optimisation, and about 3.40% for the designer-and-operator-oriented optimisation.

Table 6.4 Comparison between the conventional PSO and DLD-PSO

		Build No. 1		Build No. 2		Build No. 3		Build No. 4	
		I_v	E_l (kWh/kg)	I_v	E_l (kWh/kg)	I_v	E_l (kWh/kg)	I_v	E_l (kWh/kg)
Conventional PSO	Part-designer-oriented optimisation	713	51.5563	147	158.2691	493	316.1101	396	1187.2131
	Process-operator-oriented optimisation	323	48.3003	139	135.4456	375	214.3041	611	850.5141
	Designer-and-operator-oriented optimisation	425	48.3733	355	120.8380	153	116.6745	188	769.9511
DLD-PSO	Part-designer-oriented optimisation	147	50.9837	52	154.2734	85	314.3977	44	1089.6268
	Process-operator-oriented optimisation	166	45.8434	72	109.7810	104	160.9628	192	718.8854
	Designer-and-operator-oriented optimisation	136	43.4054	166	100.4880	76	98.1448	132	717.8302

6.3.4 Optimised Design-relevant Features

Tables 6.6-6.9 show all optimisation results of the DLD-PSO which includes the part-designer-oriented optimisation, initialized as *I*, the process-operator-oriented optimisation, initialized as *II*, and the designer-and-operator-oriented optimisation, initialized as *III*. In addition, Tables 6.6-6.9 include another set of optimised result, initialized as *IV*. Energy consumption of *IV* is calculated by the proposed prediction model through the optimised design-relevant features from *I* and *II*. It is highlighted that the proposed PSO is not applied to generate *IV*. Generally, the most substantial reduction of AM energy consumption appears in the designer-and-operator-oriented optimisation for these four build examples, which reduces the energy usage by 67.92%. Comparing between four examples, the most substantial reduction of AM energy consumption is on the Build No. 3, 83.57% energy usage is reduced in the designer-and-operator-oriented optimisation. Furthermore, the largest average reduction of AM energy consumption reduction of three types of optimisation is 70.24% (Build No. 2). Also, energy consumption reduction of the optimisation *IV* is generally smaller than the designer-and-operator-oriented optimisation.

In Table 6.6-6.9, the most considerable change of the optimised design-relevant feature is the total filling degree, which has changed 45.64% in the process-operator-oriented optimisation and about 38.43% in the designer-and-operator-oriented optimisation. The weight of the total filling degree (0.121) is also the largest compared to the weights of other features. Moreover, the changes in the part-designer-oriented and the process-operator-oriented optimisation are generally more significant than the changes of the designer-and-operator-oriented optimisation. It is interesting to note that the changes in the optimised design-relevant-features grow when original energy consumption increases. Specifically, Build No. 1 cost the lowest energy consumption (116.3490 kWh/kg), and the average change of all features is about 14.39%. In contrast, the most substantial feature change is Build No. 4, which is about 27.29%. The design-relevant feature optimisation process is shown in Appendix B.3 including 12 design-relevant features of four examples.

Table 6.5 The optimised results of Build No.1

		Part filling degree (%)	Geometry ratio (wl)	Geometry ratio (hl)	Geometry ratio (wh)	Part height (mm)	Total filling degree (%)	Total geometry ratio (wl)	Total geometry ratio (hl)	Total geometry ratio (wh)	Bottom area (cm ²)	Height (mm)	Number of Part	Energy (kWh/kg)
I	Optimised results	26.3859	1.2688	0.9897	1.2931	70.94	12.6910	0.5360	0.3116	1.7202	2558.3574	215.28	27	50.9837
	Difference	+1.0983	+0.0446	+0.0419	+0.0015	-5.54	0	0	0	0	0	0	0	0
II	Optimised results	25.2876	1.2242	0.9478	1.2916	76.48	14.0004	0.4606	0.2907	1.6993	2457.3249	252.52	22	45.8434
	Difference	0	0	0	0	0	+1.3094	-0.0754	-0.0209	-0.0209	-101.0325	+37.24	-5.0000	-70.5056
III	Optimised results	25.1556	1.2020	0.9277	1.3054	79.13	13.9552	0.4469	0.2790	1.7620	2424.4020	225.95	19	43.4054
	Difference	-0.1320	-0.0222	-0.0201	+0.0138	+2.64	+1.2642	-0.0891	-0.0326	+0.0418	-133.9554	+10.67	-8	-72.9436
IV	Optimised results	26.3859	1.2688	0.9897	1.2931	70.94	14.0004	0.4606	0.2907	1.6993	2457.3249	252.52	22	48.1260
	Difference	+1.0983	+0.0446	+0.0419	+0.0015	-5.54	+1.3094	-0.0754	-0.0209	-0.0209	-101.0325	+37.2443	-5	-68.2230

Table 6.6 The optimised results of Build No.2

		Part filling degree (%)	Geometry ratio (wl)	Geometry ratio (hl)	Geometry ratio (wh)	Part height (mm)	Total filling degree (%)	Total geometry ratio (wl)	Total geometry ratio (hl)	Total geometry ratio (wh)	Bottom area (cm ²)	Height (mm)	Number of Part	Energy (kWh/kg)
I	Optimised results	16.0894	0.5962	0.3819	4.4716	37.74	6.6278	0.5420	0.2178	2.4883	2466.3961	146.94	30	154.2734
	Difference	-1.0453	-0.0914	+0.2311	-0.0881	+6.63	0	0	0	0	0	0	0	0
II	Optimised results	17.1347	0.6876	0.1508	4.5597	31.11	9.3045	0.5074	0.3162	2.3265	2714.9799	180.05	22	109.7810
	Difference	0	0	0	0	0	+2.6767	-0.0346	+0.0984	-0.1618	+248.5838	+33.11	-8	-298.5044
III	Optimised results	16.6467	0.7105	0.1352	4.5853	36.07	8.9977	0.5169	0.2724	2.4418	2695.2499	165.63	25	100.4880
	Difference	-0.4880	+0.0229	-0.0156	+0.0256	+4.96	+2.3699	-0.0251	+0.0546	-0.0465	+228.8538	+18.69	-5	-307.7974
IV	Optimised results	16.0894	0.5962	0.3819	4.4716	37.74	9.3045	0.5074	0.3162	2.3265	2714.9799	180.05	22	123.9675
	Difference	-1.0453	-0.0914	+0.2311	-0.0881	+6.63	+2.6767	-0.0346	+0.0984	-0.1618	+248.5838	+33.11	-8	-284.3179

Table 6.7 The optimised results of Build No.3

		Part filling degree (%)	Geometry ratio (wl)	Geometry ratio (hl)	Geometry ratio (wh)	Part height (mm)	Total filling degree (%)	Total geometry ratio (wl)	Total geometry ratio (hl)	Total geometry ratio (wh)	Bottom area (cm ²)	Height (mm)	Number of Part	Energy (kWh/kg)
I	Optimised results	7.5168	0.7736	0.4717	5.5533	46.60	4.9138	0.5401	0.6390	0.8452	2613.2170	444.48	33	314.3977
	Difference	+2.0586	-0.2074	+0.2956	-0.0182	+2.57	0	0	0	0	0	0	0	-282.7611
II	Optimised results	5.4582	0.9810	0.1761	5.5715	44.03	7.8365	0.6876	0.4480	0.8012	2698.5380	435.46	29	160.9628
	Difference	0	0	0	0	0	+2.9227	+0.1475	-0.1910	-0.0440	+85.3210	-9.02	-4	-436.196
III	Optimised results	4.1210	0.8763	0.2750	5.5370	44.96	7.3646	0.6292	0.4460	0.8084	2654.8710	443.05	30	98.1448
	Difference	-1.3372	-0.1047	+0.0989	-0.0345	+0.93	+2.4508	+0.0891	-0.1930	-0.0368	+41.6540	-1.43	-3	-499.014
IV	Optimised results	7.5168	0.7736	0.4717	5.5533	46.60	7.8365	0.6876	0.4480	0.8012	2698.5380	435.46	29	101.04134
	Difference	+2.0586	-0.2074	+0.2956	-0.0182	+2.57	+2.9227	+0.1475	-0.1910	-0.0440	+85.3210	-9.02	-4	-496.1175

Table 6.8 The optimised results of Build No.4

		Part filling degree (%)	Geometry ratio (wl)	Geometry ratio (hl)	Geometry ratio (wh)	Part height (mm)	Total filling degree (%)	Total geometry ratio (wl)	Total geometry ratio (hl)	Total geometry ratio (wh)	Bottom area (cm ²)	Height (mm)	Number of Part	Energy (kWh/kg)
I	Optimised results	39.5530	0.8958	0.0878	3.4442	27.71	5.2255	0.5270	0.1190	4.4278	2476.9831	81.60	26	1089.6268
	Difference	-1.8476	-0.0423	-0.1784	-0.0803	+6.60	0	0	0	0	0	0	0	-346.7719
II	Optimised results	41.4006	0.9381	0.2662	3.5245	21.11	7.4449	0.6627	0.3207	4.3755	2725.8123	112.66	32	718.8854
	Difference	0	0	0	0	0.00	+2.2194	+0.1357	+0.2017	-0.0523	+248.8292	+31.06	+6	-717.5133
III	Optimised results	39.9526	0.9038	0.3158	3.6697	25.65	6.8276	0.7046	0.2283	4.3160	2721.7830	121.35	33	717.8302
	Difference	-1.4480	-0.0343	+0.0496	+0.1452	+4.54	+1.6021	+0.1776	+0.1093	-0.1118	+244.7999	+39.75	+7	-718.5685
IV	Optimised results	39.5530	0.8958	0.0878	3.4442	27.71	7.9975	0.7987	0.5500	4.4408	2987.9628	102.53	36	847.1742
	Difference	-1.8476	-0.0423	-0.1784	-0.0803	+6.60	+2.7720	+0.2717	+0.4310	+0.0130	+510.9797	+20.93	+10	-589.2245

6.3.5 Discussion

In the validation of the optimisation performance, four build examples with various energy cost were examined in the case study. The design-relevant features were categorised as two classes: the part-design features, and process-planning features. For optimal results, each feature of these two classes was changed within restriction ranges that was determined by part designers and process operators. The restriction ranges in this case study were determined by part designers, process operators, and SLS process capabilities. It provided these groups of professionals a reasonable range in which to optimise decisions regarding the reduction of AM process energy consumption. Optimisation performance was shown through three types of optimisation oriented toward different professionals.

Generally, the DLD-PSO model obtains the best results faster than conventional PSO method do, in terms of faster convergence speed and lower energy consumption. Moreover, the best results of this model were generally better than those of the conventional PSO model. The process-operator-oriented optimisation through the DLD-PSO model offered a significant improvement over the conventional PSO. It can be seen from the results that the weights of each feature in the deep learning-based prediction model represent the impacts of these features on the target value which is energy consumption in this study. Additionally, the weights driven by the deep learning-based model can help the PSO model find better results faster than conventional PSO model. The performance of the DLD-PSO model was not affected by the prediction model's accuracy, but the convergence speed and result quality of the conventional PSO worsened as the error of the prediction model grew.

In this case study, process-operator-oriented optimisation obtained better results than part-designer-oriented optimisation did. This may be caused by seven features being changed in process-operator-oriented optimisation, and one of them had the largest weight of all the features. Furthermore, designer-and-operator-oriented optimisation consumed the lowest amount of energy—an amount lower than that of part-designer-

oriented optimisation and process-operator-oriented optimisation combined. This means that two types of design-relevant features and energy consumption are not independent from each other in this optimisation method. When an optimisation method accounts for all design-relevant features, the lowest possible energy consumption can be obtained. This requires the cooperation of AM part designers and process operators, which is the main principle of DfAM (Thompson et al., 2016). Though these two groups of professionals work separately, AM energy consumption can still be reduced using the proposed optimisation method. Currently, part designers and process operators may have not realised the relationship between energy consumption and these design-relevant features yet, when they made decisions. However, with the development of the research, these design-relevant features will be highlighted in the AM design software for reducing AM energy consumption in the future.

6.4 Summary

The focus of this chapter has been on the management of AM process energy consumption, which exemplifies the SLS process. The proposed approach is based on a review of related research, indicating the significance of DfAM and PSO in the manufacturing domain. In order to reduce AM energy consumption, the DLD-PSO approach is proposed to optimise design-relevant features. A case study showing the merits of the proposed approach was carried out based on SLS process data. It appears that the proposed energy consumption prediction approach obtained results similar to those of the previous prediction model using design-relevant data. For optimisation purposes, three types of optimisation oriented toward different groups of professionals were introduced. It was found that the DLD-PSO model yields a higher convergence speed and lower energy consumption than the conventional PSO. Four build examples were adopted to validate the proposed optimisation method.

Chapter 7 Achievements and Conclusions

Under the umbrella of Industry 4.0, the intelligent improvement of AM processes is crucial, especially in sustainability. In this PhD research, the AM energy consumption modelling, prediction and management, and advanced data analytics have been explored, which was implemented as an Industry 4.0 levelled application. The framework, modelling, prediction, and optimisation approaches for AM energy consumption are proposed in this research.

This chapter begins with a summary of the main achievements of this research and finishes with the discussion and reflection of this PhD research to re-think and review the entire research process, and to discuss the possible application for thesis contributions.

7.1 Achievements and Conclusion

To summarise the research achievements, it is useful to revisit the original intentions of the research:

The key objective of this research is to pave the way for AM energy consumption modelling, prediction, and management under Industry 4.0.

As mentioned in abstract, the key purpose of this research is to model, prediction, and optimise AM energy consumption, thereby to manage it. This motivation was explored

in at the beginning of this thesis and is underpinned by a discussion of the background of Industry 4.0, industry sustainability and the current state of additive manufacturing and its energy consumption. Despite significant media and academics have paid attention on the growing potential, there has been little empirical research regarding the intelligent modelling, prediction, and management of energy consumption on AM processes in the age of Industry 4.0.

To determine the state-of-the-art research, the literature review was provided the relevant technologies and relevant research, through which the research questions were developed within the overall aim of the research. Firstly, five state-of-the-art AM technologies were reviewed in detail, including working principles, schematic, support materials, and so on. The standard data generation, design for additive manufacturing, and process optimisation of the AM process were then discovered. With the understanding of AM, energy consumption and its impacts were examined in this chapter as well, especially for design-relevant features. At the end of this chapter, several advanced data analytics technologies were introduced and reviewed, which included data mining, machine learning, deep learning, and evolutionary algorithms. Based on the reviews of previous relevant research and study, modelling, predicting, and managing AM energy consumption to achieve the requirement of Industry 4.0 by using advanced data analytics technologies is theoretically feasible.

Following the understanding of related works, a novel opinion of Industry 4.0 and manufacturing was introduced. Summarising various perspectives, the main concepts of future manufacturing have been identified to inform the research aim. In common with the entire industry, there was a gap between recent industry and the achievement of Industry 4.0. With this finding, a categorical classification of Industry 4.0 was presented, which identifies how different intelligence level technologies were acted within three automation of production systems. From this classification, it was clear that the future of current manufacturing was developing in the direction of Industry 4.0. Base on this guidance, the research targeted on AM energy consumption analysis. In order to build a smarter AM process, which can model, predict, and manage energy consumption intelligently, a framework was proposed. This framework included four different layers, which covered the entire data analytics process, from data collection

to knowledge implementation. This chapter answered the research question 1, which was shown in chapter 1.

To collect and integrate multi-source data from AM systems, an IoT based data sensing and collection method was provided based on the standard AM data generation process. Four datasets were collected, which were shown as various data format and structure. Relying on the domain knowledge and clustering technology, a hybrid multi-source data integration, and modelling approach was proposed in this chapter, fusing IoT, clustering, and deep learning techniques. A case study was carried out based on SLS process data collected, which has shown the merits of the proposed approach. Experimental results indicated that the proposed approach tended to yield better performance when integrating the multi-level multi-source data. Especially, comparing with other research regarding AM energy consumption analysis, this method can predict the energy consumption of each production rather than measure a range of energy usage, which provided an accurate value of energy consumption. In the actual industrial scenario, this can be very helpful to implement data analytics when multi-source data was collected.

Among from all of energy consumption impact features, the design-relevant features were selected for predicting the energy consumption due to high relationship to energy consumption and optimisability. The design-relevant features were explored and discussed in chapter firstly, which a couple of AM build examples. The build examples were collected from the real AM production, which was with by different companies. The design-relevant features were examined as the complex and highly based on human's experience and behaviours. An energy consumption prediction approach based on deep learning technology had been proposed that used design-relevant data as input. Design-relevant data was generated before the AM process begins and included part design data and process planning data, which were determined by part designers and process operators. It appeared that the proposed energy consumption prediction approach obtained results similar to those of the previous multi-source data prediction model. Energy consumption can be predicted before the process only based on the CAD models, which were designed and decided by part designers and process operators.

The proposed energy managing approach was inspired by the understanding of AM energy consumption knowledge, which included framework, modelling, prediction, and optimisation. Apart from the proposed framework, modelling, and prediction approaches, a deep learning based energy consumption optimisation approach was proposed to optimise design-relevant features, which is call DLD-PSO. A case study showing the merits of the proposed approach was carried out based on SLS process data. Three types of optimisation oriented toward different groups of professionals were introduced. It was found that the DLD-PSO model yields a higher convergence speed and lower energy consumption than the conventional PSO. Four build examples were adopted to validate the proposed optimisation method. The best results were obtained to generate the recommendations for part designers and process operators. Finally, this approach was a data-driven approach which can also be developed to help other AM technologies.

7.2 Discussion and Reflection

This PhD research has answered all of the research questions raised in chapter one. The achievements and contributions have been highlighted in the last section. The concepts of Industry 4.0 inspired the research. After reviewing the main visions, concepts, and examples of Industry 4.0, there are gaps between the Industry 4.0 levelled manufacturing system and current manufacturing system. This research firstly published a categorical classification which provided a roadmap to help develop an Industry 4.0 manufacturing system.

In order to validate the feasibility of this roadmap, the AM process was selected as the target manufacturing system, which was one of the most representative high-value manufacturing systems. By reviewing the current research of AM processes, energy consumption analysis was focused on the main research issue. There was currently a need for research about how to model, predict, and manage energy consumption on AM systems precisely. Due to the complexity of AM systems, energy consumption is impacted by many features during the entire manufacturing phases, pre-process, building process, and post-process. This research focused on the building process

because of its uncertainty. However, the other two manufacturing phases also consume energy, which can be analysed as one future work.

Energy consumption impact features were considered based on the data generation process of AM, which includes four primary datasets, process operation dataset, working environment dataset, design-relevant dataset, and material condition dataset. These four primary datasets can cover all the data collected during the AM processing. To collect more data, an IoT-based data sensing and collection system were designed and developed, comparing to the original monitoring system in the case study, the IoT system collected over 50% of the entire data. Based on the collected data, two energy consumption modelling approach were built with a better result compared with benchmarks. However, the methodology was only validated on one AM system, which was SLS due to the budget of this research. This research could validate the method on another AM system to prove the generality on AM, which can be considered as another future work.

In order to manage energy consumption, this research proposed a design-relevant data based energy consumption modelling and prediction based on multi-source data analytics, especially the design-relevant data. Then, a deep learning based PSO was generated to optimise the design-relevant features. Part designers and process operators decided these features. Twelve features were extracted in the case study relying on the CAD models. This approach can be developed as software or an add-on package to help people to make their decisions, which can be one of the possible industrial applications from this research. However, the optimisation results are validated by the proposed model, which needs to be tested by real experiments.

The proposed method is a data-driven approach which is highly dependent on historical data. Although different AM technologies may have different working mechanisms and principles, the approach in exploiting such data to facilitate process modelling and analytics remain similar. In addition, the data required in this research can be generally collected from other AM processes based on the method proposed in this study, or the collected data can be converted to the same data characteristic to match the input requirement. In practice, this research has been collecting the data

from one AM system for more than two years, including processing data, material condition information, and CAD model information. It will not only raise the cost of the research but also extend the research time to build the model based on another AM system. However, benefitting from the increasingly completed monitoring system and Internet of Thing (IoT) technologies, the AM system is collecting more and more data from the process and related objects. In the future, this method will be validated on other AM technologies to prove its generality.

7.3 Conclusions

In conclusion, the common theme throughout this research was to improve the AM system that promote the intelligentisation level of the AM system, in terms of analysing energy consumption. A framework was designed to provide a general guide of how to analyse energy consumption by using advanced data analytics technologies. In order to solve the problem of multi-source data integration and modelling, this research proposed an approach for integrating AM multi-source data by using the technologies of clustering and deep learning. Then, the design-relevant data was focused, and the AM energy consumption was predicted. Furthermore, to reducing the AM energy consumption, a deep-learning driven PSO algorithm was proposed. In comparison with conventional PSO, the proposed PSO can obtain lower energy consumption with a short convergence process. This thesis has demonstrated the entire process of AM energy consumption modelling, prediction, and management. In the future, the AM will be increasingly employed in many industry fields. The research of AM energy will become increasingly important.

References

- ALEKSANDER, I. & MORTON, H. 1990. *An introduction to neural computing*, Chapman and Hall London.
- ALTMAN, N. S. 1992. An introduction to kernel and nearest-neighbor nonparametric regression. *The American Statistician*, 46, 175-185.
- ASADOLLAHI-YAZDI, E., GARDAN, J. & LAFON, P. 2018. Multi-Objective Optimization of Additive Manufacturing Process. *IFAC-PapersOnLine*, 51, 152-157.
- ATZORI, L., IERA, A. & MORABITO, G. 2010. The internet of things: A survey. *Computer networks*, 54, 2787-2805.
- BABIC, B., NESIC, N. & MILJKOVIC, Z. 2008. A review of automated feature recognition with rule-based pattern recognition. *Computers in Industry*, 59, 321-337.
- BAI, Q. 2010. Analysis of particle swarm optimization algorithm. *Computer and information science*, 3, 180.
- BAUMERS, M., TUCK, C., BOURELL, D. L., SREENIVASAN, R. & HAGUE, R. 2011. Sustainability of additive manufacturing: measuring the energy consumption of the laser sintering process. *Proceedings of the Institution of Mechanical Engineers, Part B: Journal of Engineering Manufacture*, 225, pp.2228-2239.
- BAUMERS, M., TUCK, C., WILDMAN, R., ASHCROFT, I. & HAGUE, R. 2012. Energy inputs to additive manufacturing: does capacity utilization matter? *EOS*, 1000, 30-40.
- BECKER, R. & GRZESIAK, A. 2009. Rapid manufacturing in automation applications. *Innovative Developments in Design and Manufacturing*. CRC Press.
- BENSINGH, R. J., MACHAVARAM, R., BOOPATHY, S. R. & JEBARAJ, C. 2019. Injection molding process optimization of a bi-aspheric lens using hybrid artificial neural networks (ANNs) and particle swarm optimization (PSO). *Measurement*, 134, 359-374.

- BOSE, R. 2009. Advanced analytics: opportunities and challenges. *Industrial Management & Data Systems*, 109, 155-172.
- BOYES, H., HALLAQ, B., CUNNINGHAM, J. & WATSON, T. 2018. The industrial internet of things (IIoT): An analysis framework. *Computers in Industry*, 101, 1-12.
- BROOK WU, Y. F., LI, Q., BOT, R. S. & CHEN, X. 2006. Finding nuggets in documents: A machine learning approach. *Journal of the American Society for Information Science and Technology*, 57, 740-752.
- CALIGNANO, F., MANFREDI, D., AMBROSIO, E. P., BIAMINO, S., PAVESE, M. & FINO, P. 2014. Direct Fabrication of Joints based on Direct Metal Laser Sintering in Aluminum and Titanium Alloys. *Procedia CIRP*, 21, 129-132.
- CAVALHEIRO, J. & CARREIRA, P. 2016. A multidimensional data model design for building energy management. *Advanced Engineering Informatics*, 30, 619-632.
- CHAN, S. L., LU, Y. & WANG, Y. 2018. Data-driven cost estimation for additive manufacturing in cybermanufacturing. *Journal of Manufacturing Systems*, 46, 115-126.
- CHEN, A.-N., WU, J.-M., LIU, K., CHEN, J.-Y., XIAO, H., CHEN, P., LI, C.-H. & SHI, Y.-S. 2018. High-performance ceramic parts with complex shape prepared by selective laser sintering: a review. *Advances in Applied Ceramics*, 117, 100-117.
- CHEN, S.-M. & HUANG, Z.-C. 2017. Multiattribute decision making based on interval-valued intuitionistic fuzzy values and particle swarm optimization techniques. *Information Sciences*, 397-398, 206-218.
- CHERGUI, A., HADJ-HAMOU, K. & VIGNAT, F. 2018. Production scheduling and nesting in additive manufacturing. *Computers & Industrial Engineering*, 126, 292-301.
- CHONG, C.-Y. & KUMAR, S. P. 2003. Sensor networks: evolution, opportunities, and challenges. *Proceedings of the IEEE*, 91, 1247-1256.
- CHOUDHARY, A. K., HARDING, J. A. & TIWARI, M. K. 2008. Data mining in manufacturing: a review based on the kind of knowledge. *Journal of Intelligent Manufacturing*, 20, 501.
- COMMISSION, E. 2015. The Factories of the Future.
- DANIELSSON, P.-E. 1980. Euclidean distance mapping. *Computer Graphics and image processing*, 14, 227-248.
- DAS, P., CHANDRAN, R., SAMANT, R. & ANAND, S. 2015. Optimum part build orientation in additive manufacturing for minimizing part errors and support structures. *Procedia Manufacturing*, 1, 343-354.
- DEB, K., PRATAP, A., AGARWAL, S. & MEYARIVAN, T. 2002. A fast and elitist multiobjective genetic algorithm: NSGA-II. *IEEE Transactions on Evolutionary Computation*, 6, 182-197.

- DEHOFF, R. 2015. In-Situ Process. Monitoring and Big. Data Analysis for Additive. Manufacturing of Ti-6Al-4V. *Workshop Presentation*, 1-21.
- DIEGEL, O., SINGAMNENI, S., REAY, S. & WITHELL, A. 2010. Tools for sustainable product design: additive manufacturing.
- DIETMAIR, A. & VERL, A. 2009. A generic energy consumption model for decision making and energy efficiency optimisation in manufacturing. *International Journal of Sustainable Engineering*, 2, 123-133.
- FAYYAD, U., PIATETSKY-SHAPIRO, G. & SMYTH, P. 1996. From data mining to knowledge discovery in databases. *AI magazine*, 17, 37-37.
- FORD, S. & DESPEISSE, M. 2016. Additive manufacturing and sustainability: an exploratory study of the advantages and challenges. *Journal of Cleaner Production*, 137, 1573-1587.
- FRANK, A. G., DALENOGARE, L. S. & AYALA, N. F. 2019. Industry 4.0 technologies: Implementation patterns in manufacturing companies. *International Journal of Production Economics*, 210, 15-26.
- GAJSKI, D. D., VAHID, F., NARAYAN, S. & GONG, J. 1994. *Specification and design of embedded systems*, Prentice Hall Englewood Cliffs.
- GARDAN, J. 2016. Additive manufacturing technologies: state of the art and trends. *International Journal of Production Research*, 54, 3118-3132.
- GARDAN, N. & SCHNEIDER, A. 2015. Topological optimization of internal patterns and support in additive manufacturing. *Journal of Manufacturing Systems*, 37, 417-425.
- GEBISA, A. W. & LEMU, H. G. 2017. Design for manufacturing to design for Additive Manufacturing: Analysis of implications for design optimality and product sustainability. *Procedia Manufacturing*, 13, 724-731.
- GIBSON, I. & ROSEN, D. 2015. *Stucker B (2010) additive manufacturing technologies: 3D printing, rapid prototyping, and direct digital manufacturing*. Springer Science+ Business Media, New York.
- GIBSON, I., ROSEN, D. W. & STUCKER, B. 2010. Design for additive manufacturing. *Additive Manufacturing Technologies*. Springer.
- GROSS, B. C., ERKAL, J. L., LOCKWOOD, S. Y., CHEN, C. & SPENCE, D. M. 2014. Evaluation of 3D printing and its potential impact on biotechnology and the chemical sciences. ACS Publications.
- GUBBI, J., BUYYA, R., MARUSIC, S. & PALANISWAMI, M. 2013. Internet of Things (IoT): A vision, architectural elements, and future directions. *Future Generation Computer Systems*, 29, 1645-1660.
- HÄLLGREN, S., PEJRYD, L. & EKENGREN, J. 2016. 3D data export for Additive Manufacturing-improving geometric accuracy. *Procedia CIRP*, 50, 518-523.
- HAMAMOTO, S. 1999. Development and validation of genetic algorithm-based facility layout a case study in the pharmaceutical industry. *International Journal of Production Research*, 37, 749-768.

- HAN, J., KAMBER, M. & PEI, J. 2011. *Data mining: concepts and techniques*, Elsevier.
- HAN, J., PRATT, M. & REGLI, W. C. 2000. Manufacturing feature recognition from solid models: a status report. *IEEE Transactions on Robotics and Automation*, 16, 782-796.
- HAN, Q., SETCHI, R. & KARIHALOO, B. 2015. Challenges and Opportunities in the Additive Layer Manufacturing of Al-Al₂O₃ Nanocomposites.
- HECHT-NIELSEN, R. 1992. III.3 - Theory of the Backpropagation Neural Network**Based on “nonindent” by Robert Hecht-Nielsen, which appeared in Proceedings of the International Joint Conference on Neural Networks 1, 593–611, June 1989. © 1989 IEEE. In: WECHSLER, H. (ed.) *Neural Networks for Perception*. Academic Press.
- HU, L., LIU, Y., PENG, C., TANG, W., TANG, R. & TIWARI, A. 2018. Minimising the energy consumption of tool change and tool path of machining by sequencing the features. *Energy*, 147, 390-402.
- HUANG, R., RIDDLE, M., GRAZIANO, D., WARREN, J., DAS, S., NIMBALKAR, S., CRESKO, J. & MASANET, E. 2016. Energy and emissions saving potential of additive manufacturing: the case of lightweight aircraft components. *Journal of Cleaner Production*, 135, 1559-1570.
- HUSSEIN, A., HAO, L., YAN, C., EVERSON, R. & YOUNG, P. 2013. Advanced lattice support structures for metal additive manufacturing. *Journal of Materials Processing Technology*, 213, 1019-1026.
- ISO/ASTM 2015. Additive Manufacturing-General Principles-Terminology. 52900. Switzerland: Contract No.: ISO/ASTM 52900:2015(E).
- JANAHIRAMAN, T. V., AHMAD, N. & NORDIN, F. H. Extreme Learning Machine and Particle Swarm Optimization in optimizing CNC turning operation. IOP Conference Series: Materials Science and Engineering, 2018. IOP Publishing, 012086.
- KAGERMANN, H., HELBIG, J., HELLINGER, A. & WAHLSTER, W. 2013. *Recommendations for Implementing the Strategic Initiative INDUSTRIE 4.0: Securing the Future of German Manufacturing Industry; Final Report of the Industrie 4.0 Working Group*, Forschungsunion.
- KELLENS, K., YASA, E., DEWULF, W. & DUFLOU, J. 2010. Environmental assessment of selective laser melting and selective laser sintering. *Going Green—Care Innovation: From Legal Compliance to Energy-efficient Products and Services, Paper*, 5.
- KELLENS, K., YASA, E., RENALDI, R., DEWULF, W., KRUTH, J.-P. & DUFLOU, J. Energy and Resource Efficiency of SLS/SLM Processes (Keynote Paper). SFF Symposium 2011, 2011. 1-16.
- KENNEDY, J. 2011. Particle swarm optimization. *Encyclopedia of machine learning*. Springer.

-
- KIM, B.-I. & SON, S.-J. 2012. A probability matrix based particle swarm optimization for the capacitated vehicle routing problem. *Journal of Intelligent Manufacturing*, 23, 1119-1126.
- KIM, S. G., THEERA-AMPORN PUNT, N., FANG, C.-H., HARWANI, M., GRAMA, A. & CHATERJI, S. 2016. Opening up the blackbox: an interpretable deep neural network-based classifier for cell-type specific enhancer predictions. *BMC systems biology*, 10, 54.
- KOHA VI, R. A study of cross-validation and bootstrap for accuracy estimation and model selection. *Ijcai*, 1995. Montreal, Canada, 1137-1145.
- KUO, R. J. & LIN, L. M. 2010. Application of a hybrid of genetic algorithm and particle swarm optimization algorithm for order clustering. *Decision Support Systems*, 49, 451-462.
- LECUN, Y., BENGIO, Y. & HINTON, G. 2015a. Deep learning. *nature*, 521, 436.
- LECUN, Y., BENGIO, Y. & HINTON, G. 2015b. Deep learning. *Nature*, 521, 436-444.
- LEE, J., BAGHERI, B. & KAO, H.-A. 2015a. A cyber-physical systems architecture for industry 4.0-based manufacturing systems. *Manufacturing letters*, 3, 18-23.
- LEE, M. H. 1993. The knowledge-based factory. *Artificial Intelligence in Engineering*, 8, 109-125.
- LEE, M. P., COOPER, G. J., HINKLEY, T., GIBSON, G. M., PADGETT, M. J. & CRONIN, L. 2015b. Development of a 3D printer using scanning projection stereolithography. *Scientific reports*, 5, 9875.
- LI, L., LIU, J., MA, Y., AHMAD, R. & QURESHI, A. 2019. Multi-view feature modeling for design-for-additive manufacturing. *Advanced Engineering Informatics*, 39, 144-156.
- MA, J., HARSTVEDT, J. D., DUNAWAY, D., BIAN, L. & JARADAT, R. 2018. An exploratory investigation of Additively Manufactured Product life cycle sustainability assessment. *Journal of Cleaner Production*, 192, 55-70.
- MEREDIG, B. 2017. Industrial materials informatics: Analyzing large-scale data to solve applied problems in R&D, manufacturing, and supply chain. *Current Opinion in Solid State and Materials Science*, 21, 159-166.
- MIN, Z., WENFENG, L., ZHONGYUN, W., BIN, L. & XIA, R. A RFID-based material tracking information system. *Automation and Logistics, 2007 IEEE International Conference on*, 2007. IEEE, 2922-2926.
- MONTGOMERY, D. C., PECK, E. A. & VINING, G. G. 2012. *Introduction to linear regression analysis*, John Wiley & Sons.
- MORADI, M. H. & ABEDINI, M. 2012. A combination of genetic algorithm and particle swarm optimization for optimal DG location and sizing in distribution systems. *International Journal of Electrical Power & Energy Systems*, 34, 66-74.

- MORITZ, T. & MALEKSAEEDI, S. 2018. 4 - Additive manufacturing of ceramic components. *In: ZHANG, J. & JUNG, Y.-G. (eds.) Additive Manufacturing*. Butterworth-Heinemann.
- MUJA, M. & LOWE, D. G. 2009. Fast approximate nearest neighbors with automatic algorithm configuration. *VISAPP (1)*, 2, 2.
- NOROUZI, M., FLEET, D. J. & SALAKHUTDINOV, R. R. Hamming distance metric learning. *Advances in neural information processing systems*, 2012. 1061-1069.
- O'REGAN, P., PRICKETT, P., SETCHI, R., HANKINS, G. & JONES, N. 2016. Metal based additive layer manufacturing: variations, correlations and process control. *Procedia Computer Science*, 96, 216-224.
- PANDA, B. N., GARG, A. & SHANKHWAR, K. 2016. Empirical investigation of environmental characteristic of 3-D additive manufacturing process based on slice thickness and part orientation. *Measurement*, 86, 293-300.
- PARK, C.-W., KWON, K.-S., KIM, W.-B., MIN, B.-K., PARK, S.-J., SUNG, I.-H., YOON, Y. S., LEE, K.-S., LEE, J.-H. & SEOK, J. 2009. Energy consumption reduction technology in manufacturing—A selective review of policies, standards, and research. *International Journal of Precision Engineering and Manufacturing*, 10, 151-173.
- PAUL, R. & ANAND, S. 2012. Process energy analysis and optimization in selective laser sintering. *Journal of Manufacturing Systems*, 31, 429-437.
- PEDREGOSA, F., VAROQUAUX, G., GRAMFORT, A., MICHEL, V., THIRION, B., GRISEL, O., BLONDEL, M., PRETTENHOFER, P., WEISS, R. & DUBOURG, V. 2011. Scikit-learn: Machine learning in Python. *Journal of Machine Learning Research*, 12, 2825-2830.
- PENG, T., KELLENS, K., TANG, R., CHEN, C. & CHEN, G. 2018. Sustainability of additive manufacturing: An overview on its energy demand and environmental impact. *Additive Manufacturing*, 21, 694-704.
- PEREIRA, R. I., DUPONT, I. M., CARVALHO, P. C. & JUCÁ, S. C. 2018. IoT embedded linux system based on Raspberry Pi applied to real-time cloud monitoring of a decentralized photovoltaic plant. *Measurement*, 114, 286-297.
- PERHINSCHI, M. & PERHINSCHI, M. A modified genetic algorithm for the design of autonomous helicopter control system. *Guidance, Navigation, and Control Conference*, 1997. 3630.
- PIATESKI, G. & FRAWLEY, W. 1991. *Knowledge discovery in databases*, MIT press.
- PONCHE, R., HASCOËT, J.-Y., KERBRAT, O. & MOGNOL, P. 2017. A new global approach to design for additive manufacturing. *Additive Manufacturing Handbook*. CRC Press.
- QIN, J., LIU, Y. & GROSVENOR, R. 2016. A Categorical Framework of Manufacturing for Industry 4.0 and Beyond. *Procedia CIRP*, 52, 173-178.

- QIN, J., LIU, Y. & GROSVENOR, R. 2017. A Framework of Energy Consumption Modelling for Additive Manufacturing Using Internet of Things. *Procedia CIRP*, 63, 307-312.
- QIN, J., LIU, Y. & GROSVENOR, R. 2018. Multi-source data analytics for AM energy consumption prediction. *Advanced Engineering Informatics*, 38, 840-850.
- QIN, J., LIU, YING AND GROSVENOR, ROGER 2017. Data analytics for energy consumption of digital manufacturing systems using Internet of Things method. *IEEE International Conference on Automation Science and Engineering*. Xi'an, China,.
- QUINLAN, J. R. 2014. *C4. 5: programs for machine learning*, Elsevier.
- RAJESWARAN, J. & BLACKSTONE, E. H. 2018. multilevel data analysis: What? Why? How? *The Journal of thoracic and cardiovascular surgery*, 155, 210-211.
- RAJU, M., GUPTA, M. K., BHANOT, N. & SHARMA, V. S. 2018. A hybrid PSO-BFO evolutionary algorithm for optimization of fused deposition modelling process parameters. *Journal of Intelligent Manufacturing*, 1-16.
- RISTESKA STOJKOSKA, B. L. & TRIVODALIEV, K. V. 2017. A review of Internet of Things for smart home: Challenges and solutions. *Journal of Cleaner Production*, 140, 1454-1464.
- RÖHLER, A. B. & CHEN, S. An analysis of sub-swarms in multi-swarm systems. *Australasian Joint Conference on Artificial Intelligence*, 2011. Springer, 271-280.
- ROSEN, D. W. 2007. Computer-aided design for additive manufacturing of cellular structures. *Computer-Aided Design and Applications*, 4, 585-594.
- RUMELHART, D. E., MCCLELLAND, J. L. & GROUP, P. R. 1988. *Parallel distributed processing*, IEEE.
- SALONITIS, K. 2014. 10.03 - Stereolithography. In: HASHMI, S., BATALHA, G. F., VAN TYNE, C. J. & YILBAS, B. (eds.) *Comprehensive Materials Processing*. Oxford: Elsevier.
- SEALY, W. 2011. Additive manufacturing as a disruptive technology: how to avoid the pitfall. *American Journal of Engineering and Technology Research Vol*, 11.
- SHEVCHIK, S. A., KENEL, C., LEINENBACH, C. & WASMER, K. 2018. Acoustic emission for in situ quality monitoring in additive manufacturing using spectral convolutional neural networks. *Additive Manufacturing*, 21, 598-604.
- SHI, Y. Particle swarm optimization: developments, applications and resources. *evolutionary computation*, 2001. Proceedings of the 2001 Congress on, 2001. IEEE, 81-86.
- SHROUF, F., ORDIERES, J. & MIRAGLIOTTA, G. Smart factories in Industry 4.0: A review of the concept and of energy management approached in production

- based on the Internet of Things paradigm. *Industrial Engineering and Engineering Management (IEEM)*, 2014 IEEE International Conference on, 2014. IEEE, 697-701.
- SING, S. L., WIRIA, F. E. & YEONG, W. Y. 2018. Selective laser melting of lattice structures: A statistical approach to manufacturability and mechanical behavior. *Robotics and Computer-Integrated Manufacturing*, 49, 170-180.
- SING, S. L., YEONG, W. Y., WIRIA, F. E., TAY, B. Y., ZHAO, Z., ZHAO, L., TIAN, Z. & YANG, S. 2017. Direct selective laser sintering and melting of ceramics: a review. *Rapid Prototyping Journal*, 23, 611-623.
- SKOWYRA, J., PIETRZAK, K. & ALHNAN, M. A. 2015. Fabrication of extended-release patient-tailored prednisolone tablets via fused deposition modelling (FDM) 3D printing. *European Journal of Pharmaceutical Sciences*, 68, 11-17.
- SOE, S. P. 2012. Quantitative analysis on SLS part curling using EOS P700 machine. *Journal of Materials Processing Technology*, 212, 2433-2442.
- SREENIVASAN, R. & BOURELL, D. 2010. Sustainability Study in Selective Laser Sintering- An Energy Perspective. Minerals, Metals and Materials Society/AIME, 420 Commonwealth Dr., P. O. Box 430 Warrendale PA 15086 USA.
- STEED, C. A., HALSEY, W., DEHOFF, R., YODER, S. L., PAQUIT, V. & POWERS, S. 2017. Falcon: Visual analysis of large, irregularly sampled, and multivariate time series data in additive manufacturing. *Computers & Graphics*, 63, 50-64.
- STOCK, T. & SELIGER, G. 2016. Opportunities of Sustainable Manufacturing in Industry 4.0. *Procedia CIRP*, 40, 536-541.
- STURM, L. D., WILLIAMS, C. B., CAMELIO, J. A., WHITE, J. & PARKER, R. 2017. Cyber-physical vulnerabilities in additive manufacturing systems: A case study attack on the .STL file with human subjects. *Journal of Manufacturing Systems*, 44, 154-164.
- TANG, D., DAI, M., SALIDO, M. A. & GIRET, A. 2016a. Energy-efficient dynamic scheduling for a flexible flow shop using an improved particle swarm optimization. *Computers in Industry*, 81, 82-95.
- TANG, Y., MAK, K. & ZHAO, Y. F. 2016b. A framework to reduce product environmental impact through design optimization for additive manufacturing. *Journal of Cleaner Production*, 137, 1560-1572.
- TANG, Y. & ZHAO, Y. F. 2016. A survey of the design methods for additive manufacturing to improve functional performance. *Rapid Prototyping Journal*, 22, 569-590.
- TANIKELLA, N. G., WITTBRODT, B. & PEARCE, J. M. 2017. Tensile strength of commercial polymer materials for fused filament fabrication 3D printing. *Additive Manufacturing*, 15, 40-47.

- TELENKO, C. & SEEPERSAD, C. C. Assessing energy requirements and material flows of selective laser sintering of Nylon parts. Proceedings of the Solid Freeform Fabrication Symposium 2010, 2010. 8-10.08.
- THOMPSON, M. K., MORONI, G., VANEKER, T., FADEL, G., CAMPBELL, R. I., GIBSON, I., BERNARD, A., SCHULZ, J., GRAF, P. & AHUJA, B. 2016. Design for Additive Manufacturing: Trends, opportunities, considerations, and constraints. *CIRP annals*, 65, 737-760.
- TOMSOFTWARE. 2015. *EOS-Formats* [Online]. Available: <https://github.com/tomsoftware/EOS-Formats/blob/master/README.md> [Accessed].
- UHLMANN, E., PONTES, R. P., LAGHMOUCHI, A. & BERGMANN, A. 2017. Intelligent Pattern Recognition of a SLM Machine Process and Sensor Data. *Procedia CIRP*, 62, 464-469.
- VAHABLI, E. & RAHMATI, S. 2017. Hybrid estimation of surface roughness distribution in FDM parts using analytical modeling and empirical investigation. *The International Journal of Advanced Manufacturing Technology*, 88, 2287-2303.
- WAHLSTER, W. From Industry 1.0 to Industry 4.0: Towards the 4th Industrial Revolution. Forum Business meets Research, 2012.
- WANG, C.-H. & HSU, L.-C. 2008. Using genetic algorithms grey theory to forecast high technology industrial output. *Applied Mathematics and Computation*, 195, 256-263.
- WANG, L. & ALEXANDER, C. A. 2016. Additive Manufacturing and Big Data. *International Journal of Mathematical, Engineering and Management Sciences*, 1, 107-121.
- WANG, Z., ABDULLA, R., PARKER, B., SAMANIPOUR, R., GHOSH, S. & KIM, K. 2015. A simple and high-resolution stereolithography-based 3D bioprinting system using visible light crosslinkable bioinks. *Biofabrication*, 7, 045009.
- WATSON, J. & TAMINGER, K. 2015. A decision-support model for selecting additive manufacturing versus subtractive manufacturing based on energy consumption. *Journal of Cleaner Production*.
- WATSON, J. & TAMINGER, K. 2018. A decision-support model for selecting additive manufacturing versus subtractive manufacturing based on energy consumption. *Journal of Cleaner Production*, 176, 1316-1322.
- WĘGŁOWSKI, M. S., BŁACHA, S. & PHILLIPS, A. 2016. Electron beam welding – Techniques and trends – Review. *Vacuum*, 130, 72-92.
- WOHLERS, T. 2016. *Wohlers report 2016*, Wohlers Associates, Inc.
- WOHLERS, T. & GORNET, T. 2014. History of additive manufacturing. *Wohlers report*, 24, 118.
- WONG, T.-T. 2015. Performance evaluation of classification algorithms by k-fold and leave-one-out cross validation. *Pattern Recognition*, 48, 2839-2846.

- XIONG, J., ZHANG, G., HU, J. & LI, Y. 2013. Forecasting process parameters for GMAW-based rapid manufacturing using closed-loop iteration based on neural network. *The International Journal of Advanced Manufacturing Technology*, 69, 743-751.
- XU, F., DHOKIA, V., COLEGROVE, P., MCANDREW, A., WILLIAMS, S., HENSTRIDGE, A. & NEWMAN, S. T. 2018. Realisation of a multi-sensor framework for process monitoring of the wire arc additive manufacturing in producing Ti-6Al-4V parts. *International Journal of Computer Integrated Manufacturing*, 31, 785-798.
- YAGER, R. R. 2004. A framework for multi-source data fusion. *Information Sciences*, 163, 175-200.
- YASHIRO, T., KOBAYASHI, S., KOSHIZUKA, N. & SAKAMURA, K. An Internet of Things (IoT) architecture for embedded appliances. Humanitarian Technology Conference (R10-HTC), 2013 IEEE Region 10, 2013. IEEE, 314-319.
- YE, Z., ZHU, J., LI, Q., MO, B., LEI, B., LI, Y., WANG, C. & HUANG, C. 2018. A novel method of reliability-centered process optimization for additive manufacturing. *Microelectronics Reliability*, 88-90, 1151-1156.
- YILDIZ, A. R. 2013. A new hybrid differential evolution algorithm for the selection of optimal machining parameters in milling operations. *Applied Soft Computing*, 13, 1561-1566.
- YIN, S. & KAYNAK, O. 2015. Big data for modern industry: challenges and trends [point of view]. *Proceedings of the IEEE*, 103, 143-146.
- YOSOFI, M., KERBRAT, O. & MOGNOL, P. 2019. Additive manufacturing processes from an environmental point of view: a new methodology for combining technical, economic, and environmental predictive models. *The International Journal of Advanced Manufacturing Technology*, 102, 4073-4085.
- YUSUP, N., ZAIN, A. M. & HASHIM, S. Z. M. 2012. Overview of PSO for optimizing process parameters of machining. *Procedia Engineering*, 29, 914-923.
- ZHANG, H., NAGEL, J. K., AL-QAS, A., GIBBONS, E. & LEE, J. J.-Y. 2018a. Additive Manufacturing with Bioinspired Sustainable Product Design: A Conceptual Model. *Procedia Manufacturing*, 26, 880-891.
- ZHANG, H., XIE, J., GE, J., LU, W. & ZONG, B. 2018b. An Entropy-based PSO for DAR task scheduling problem. *Applied Soft Computing*, 73, 862-873.
- ZHANG, Y., BERNARD, A., GUPTA, R. K. & HARIK, R. 2014. Evaluating the Design for Additive Manufacturing: A Process Planning Perspective. *Procedia CIRP*, 21, 144-150.
- ZHAO, X. & ROSEN, D. W. 2017. A data mining approach in real-time measurement for polymer additive manufacturing process with exposure controlled projection lithography. *Journal of Manufacturing Systems*, 43, 271-286.

- ZHOU, W., PIRAMUTHU, S., CHU, F. & CHU, C. 2017. RFID-enabled flexible warehousing. *Decision Support Systems*, 98, 99-112.
- ZOU, J., CHANG, Q., OU, X., ARINEZ, J. & XIAO, G. 2019. Resilient adaptive control based on renewal particle swarm optimization to improve production system energy efficiency. *Journal of Manufacturing Systems*, 50, 135-145.

Appendix A Advanced Data Analytics Technologies

In order to solve the industrial problems, advanced data analytics technologies must be well understood. Data mining, machine learning and deep learning are three of the most popular and useful advanced data analytics technologies, which are reviewed in this section.

A.1 Data mining

Data mining is one of the most popular technologies of the advanced data analytics. Data mining is also known as ‘knowledge discovery in databases (KDD) (Piateski and Frawley, 1991). In manufacturing, data is the most important communication carrier. The volume of data may increase at what can be deemed an abnormal rate. However, data application is usually limited in scope. Vast amounts of raw data is hardly used for manufacturing activities. It is described as ‘rich data but poor information’. From the 1990s, manufacturing began to introduce the data mining technologies for receiving valuable information (Lee, 1993). Since then, the application of data mining has always drawn manufacturing researcher’s attention. It became an indispensable technology for many areas of manufacturing, such as machining, assembly, production processing.

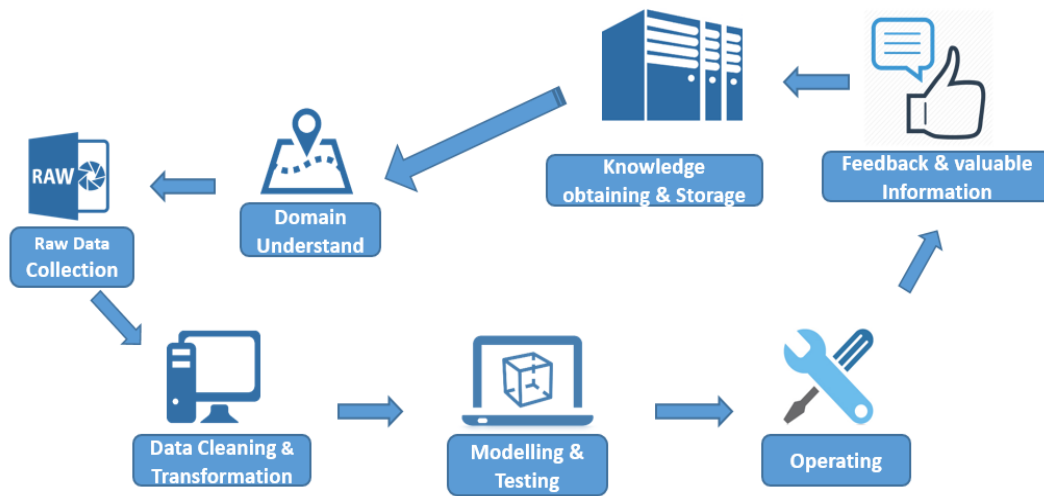


Figure A.1 Data Mining Processing in Manufacturing

Typically, the process of data mining follows five stage process, which are Selection, Pre-processing, Transformation, Data Mining and Interpretation/Evaluation. By applying this process, the relevant knowledge is discovered from raw data (Fayyad et al., 1996). In the perspective of manufacturing field, the processing of data mining was defined differently. Several extra steps were included, which is shown in the Figure 2.8 with seven steps. This process starts at the Domain understanding, which the current existing knowledge is employed to determine and clear the input and target features. Once the target has been confirmed, the raw data needs to be collected following the specific purposes. Then, in the step of Data cleaning and transformation, the collected data is cleaned without strange data, such as noise data, missing data and outlier. The cleaned data is also transferred into the required data format which is suitable for data integration and modelling. After the modelling, the results will be used for operating the controlling system. The feedback and the valuable information are also displayed and stored after the implementation. This information and knowledge will update the domain knowledge for future research (Choudhary et al., 2008).

A.2 Conventional machine learning algorithms

Machine learning refer to a set of methods which can detect required patterns in data and the patterns are used to predict future trend, which can associate people to make the decision. Generally, machine learning is divided into two types of learning

approaches, the supervised learning approach and the unsupervised learning approach. The supervised learning is the most widely used machine learning approach in practice, including classification and regression. On the other hand, one of the best applications of unsupervised learning is the clustering. In this subsection, three supervised learning machine learning algorithms will be introduced which are Linear Regression (LR), Decision Tree (DT), and k -Nearest Neighbors (k -NN).

1. **Linear Regression (LR)** is a linear approach to modelling the relationship between input and output values. The inputs can be single or multiple variables. There are usually two aims of LR, prediction and variation explanation. For the prediction, LR is applied to fit the predictive model to the response dataset and explanatory variables. When the model is developed, the predictive values are obtained by put the variables into the model. Another functional goal of LR is to explain the strength of relationship between the explanatory variables the response (target value), especially for determining the linear relationship. This function can also identify the redundant information of the response (Montgomery et al., 2012). A typical LR is described as following equations:

$$\hat{y}_{LR}(w_{LR}, x_{LR}) = w_{LR0} + w_{LR1}x_{LR1} + \dots + w_{LRp}x_{LRp} \quad (\text{A.1}),$$

where \hat{y}_{LR} is the predicted attribute and $w_{LR} = (w_0, w_1, \dots, w_p)$ is the weight for each input in the combination. Therefore, discovering the best set of w is the most fundamental job in this method. Three different algorithms can be used to search for the best set of weights: Ordinary Least Squares Regression, Ridge Regression and Bayesian Regression. To build the LR predictive model, several assumptions are made about input variables, target values and the relationship. The major assumptions are like, weak exogeneity, linearity, constant variance, independence, and lack of perfect multicollinearity.

2. **Decision Tree (DT)** is one of the fundamental classifiers, which is structured like a flowchart. Every internal node, branch and a leaf node of a decision tree represents an attribute, a result, and a class label, and the topmost node is called

the root. Depending on the attribute values, the unknown tuple is classified within each individual leaf node storing the class information, which are the classification rules of a decision tree (Han et al., 2011).

ID3 (Iterative Dichotomiser), C4.5 and CART are three decision tree algorithms, which approach the non-backtracking structure to ‘divide-and-conquer’ from top to bottom. This type of algorithm selects the ‘best’ attribute from all attributes by using an attribute selection measure, like information gain or Gini index. Therefore, the attribute selection measure is one of the features distinguishing the algorithms, which is also known as ‘splitting rules’. (The other feature is the attribute selection rule in the tree building.) There are three frequently used attribute selection measures; information gain, gain ratio and Gini index. As the measure of ID3, the information gain requires the minimum information to classify the tuples, which means this measure finds a simple tree from the minimum number of tests (Quinlan, 2014).

3. ***k*-Nearest Neighbors (*k*-NN)** is a very simple supervised learning algorithm for both classification and regression, which requires zero parameter setting. This algorithm searches the nearest test sample for specified training samples based on the distance metric, which Euclidean distance is a common distance here (Danielsson, 1980):

$$d_{knn}(x_i, x_l) = \sqrt{(x_{i1} - x_{l1})^2 + (x_{i2} - x_{l2})^2 + \dots + (x_{ip} - x_{lp})^2} \quad (\text{A.2})$$

For the discrete variable, like text classification, the overlap metric or hamming distance is used for determining the distances (Norouzi et al., 2012). The hamming distance tracks the number of positions at the corresponding symbols is different between two strings. For example, the hamming distance between ‘Cardiff**2019**’ and ‘Swansea**2020**’ is 2, where only the bold bytes are counted. Due to its simplicity, this algorithm is used to solve many different problems, such as metric learning, feature extraction, dimension reduction, decision boundary and data reduction (Muja and Lowe, 2009).

A.3 Deep learning

Different to conventional machine learning, Neural Networks are inspired by networks of living neurons, which are shown as the systems of ‘neurons’. These ‘neurons’ exchange the information between each other associating numeric connection weights. The weights are able to be updated by using the data, which represents the learning processing (Aleksander and Morton, 1990). A basic ‘neuron’ model consisted of three elements that are ‘several connecting links’, ‘a linear combiner’ and ‘an activation function’, which is shown in Figure 2.9.

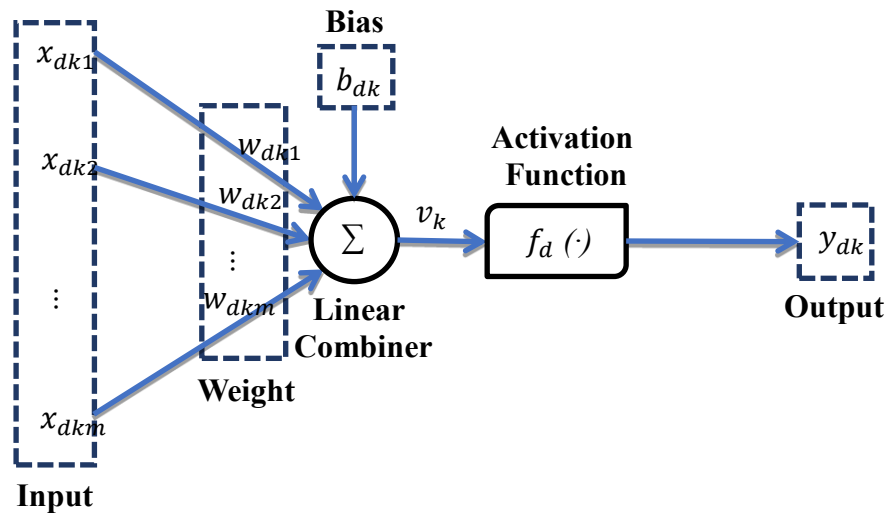


Figure A.2 The ‘K’ nonlinear neuron model

Every connecting link is characterized by the weight w_{dki} , where k represents neurons of the K layer, and i represents this connecting link. The linear combiner is used to add all of the weighted input signals. The activation function is able to define the output which is limited within an allowed amplitude range which is normally as $[0, 1]$ or $[-1, 1]$. As shown in Figure 2.9, the model includes a bias (b_{dk}). This bias is used for changing the input of the activation function basic on the requirement of the function.

In addition, neurons of ‘K’ layer are also described as a set of equations:

$$u_{dk} = \sum_{i=1}^m w_{dki} x_i \quad (\text{A.3})$$

$$y_{dk} = f_d(u_{dk} + b_{dk}) \quad (\text{A.4})$$

Then the net input $v_{dk} = u_{dk} + b_{dk}$, so:

$$y_{dk} = f_d(v_{dk}) \quad (\text{A.5}),$$

which the $f_d(\cdot)$ is activation function, such as Threshold Function and Sigmoid Function. Generally, the neural network is constituted by neurons within the layers. There are three basic layered neural network classifications, single-layer feedforward networks, multilayer feedforward networks' and recurrent networks.

In order to build the neural networks model, the learning algorithm is necessary to be known as one of the most important components. The backpropagation is a popular learning algorithm of multilayers neural networks which includes one or many hidden layers to revise the weights. The learning process is two steps. At first the output values are received by the neural networks which is with initial weights from input values. Then, an error signal is obtained by comparing between the actual and desired outputs (Hecht-Nielsen, 1992).

The neuron shown in Figure 2.9 is also seen as the neuron in hidden or output layer (the 'k' layer) of a multilayer neural network. The inputs x_{dk} are also the outputs of the previous layer (the 'j' layer), so they can be marked as y_{dj} . So the net inputs:

$$v_{dk} = \sum_j w_{djk} y_{dj} + b_{dk} \quad (\text{A.6}),$$

and outputs of the 'k' layer, y_{dk} :

$$y_{dki} = f_d(v_{dk}) \quad (\text{A.7}),$$

where $f(\cdot)$ is activation function. Generally, the activation function is non-linear and differentiable, therefore, the logistic function or sigmoid function is applied, which is:

$$f_{sig}(z) = \frac{1}{1 + e^{-z}} \quad (\text{A.8}),$$

which can be differentiated by z ,

$$\frac{\partial f}{\partial z}(z) = f(z)(1 - f(z)) \quad (\text{A.9})$$

From the equation (1), actual outputs of 'k' layer is calculated. Comparing with the desired output, the error is obtained by using the squared error function:

$$E_{dk} = \frac{1}{2}(O_{dk} - y_k)^2 \quad (\text{A.10}),$$

where the E_{dk} is the squared error, the O_{dk} is the desired outputs of 'k' layer. The reason of the factor $\frac{1}{2}$ is to remove the exponent.

The target of the backpropagation is received the corrected weight using a correcting value (Δw_{djk}). The Δw_{djk} can be calculated from the gradient descent:

$$\Delta w_{djk} = -\eta \frac{\partial E_d}{\partial w_{djk}} \quad (\text{A.11}),$$

where η is called learning rate. As the chain rule:

$$\frac{\partial E_d}{\partial w_{djk}} = \frac{\partial E_d}{\partial y_{dk}} \frac{\partial y_{dk}}{\partial v_{dk}} \frac{\partial v_{dk}}{\partial w_{djk}} \quad (\text{A.12}),$$

and

$$\frac{\partial v_{dk}}{\partial w_{djk}} = \frac{\partial}{\partial w_{djk}} \left(\sum_{j=1}^m w_{dki} x_i + b_{dk} \right) = y_{dj} \quad (\text{A.13})$$

According to the equation (2),

$$\frac{\partial y_{dk}}{\partial v_{dk}} = \frac{\partial}{\partial v_{dk}} f_d(v_{dk}) = f_d(v_{dk})(1 - f_d(v_{dk})) \quad (\text{A.14}),$$

and according to the equation (3),

$$\frac{\partial E_{dk}}{\partial y_{dk}} = \frac{\partial}{\partial y_{dk}} \frac{1}{2} (O_{dk} - y_{dk})^2 = y_{dk} - O_{dk} \quad (\text{A.15})$$

The learning algorithm of backpropagation uses this error to adjust weights of all layers from the output to the input (Rumelhart et al., 1988). With the algorithm, the model can upgrade the weight of each neuron, which is considered as the learning capability.

Appendix B Additional Results and Datasets

B.1 More Results of Different Clustering Quantity

Table B.1 Conventional ML results using layer-levelled dataset in 1 to 20 clusters.

Clusters	LR		DT		<i>k</i> -NN	
	MCC	RMSE (kWh/kg)	MCC	RMSE (kWh/kg)	MCC	RMSE (kWh/kg)
1	0.5799	64.2580	0.6661	62.7905	0.5296	43.1550
2	0.5720	100.3767	0.5254	143.3810	0.3944	49.1802
3	0.2994	248.1262	0.0328	105.0982	0.5193	45.0737
4	0.2888	794.9748	0.3055	129.5172	0.3145	51.8955
5	0.2595	1436.7553	0.5466	103.3907	0.2605	48.3878
6	0.0985	667.0310	0.0729	149.1981	0.2435	43.2525
7	0.4247	210.7593	0.4254	104.5026	0.3127	46.7922
8	0.0696	361.1748	0.5673	87.1092	0.1913	53.7604
9	0.4892	394.7965	0.3872	100.5944	0.3658	45.8448
10	0.4978	205.6747	0.3162	99.5842	0.5058	45.4644
15	0.4070	124.8918	0.1816	133.5043	0.4756	48.0096
20	0.3444	149.4259	0.3271	131.0927	0.4716	46.7576

Table B.2 Convectional ML results using merged dataset in 1 to 20 clusters.

Clusters	LR		DT		<i>k</i> -NN	
	MCC	RMSE (kWh/kg)	MCC	RMSE (kWh/kg)	MCC	RMSE (kWh/kg)
1	0.6069	115.0557	0.6903	59.5850	0.5403	54.2386
2	0.4732	127.7264	0.1819	110.8348	0.4124	49.9239
3	0.0741	372.3821	0.4412	97.7057	0.4203	44.1683
4	0.3605	838.7617	0.2797	121.4489	0.3197	48.9306
5	0.4024	1161.7069	0.6116	93.7099	0.3011	52.2378
6	0.3753	407.5528	0.1867	103.3263	0.2351	45.8685
7	0.4451	201.6085	0.4821	93.6605	0.4212	44.8881
8	0.1365	257.9760	0.3262	98.5770	0.1723	52.3058
9	0.5216	394.3280	0.4754	96.5295	0.2978	46.7471
10	0.4331	142.1725	0.3000	90.4353	0.4005	47.0695
15	0.4442	123.0823	0.1673	136.5256	0.3970	45.8066
20	0.3878	148.8892	0.3353	139.3908	0.5093	45.1356

B.2 Design-relevant Dataset

Table B.3 The entire design-relevant dataset

Part filling degree	PartRate wl	PartRate hl	PartRate wh	Part height	Part Bottom area	Total filling degree	TotalRate wl	TotalRate hl	TotalRate wh	Bottom area	Heigh	NumPart
8.996	0.100	0.079	1.267	48.395	1286.173	8.280	0.541	0.450	1.202	2585.639	311	45
20.317	1.294	0.673	1.923	59.242	468.536	17.022	0.553	0.264	2.096	2480.893	176.7	59
25.118	1.211	0.366	3.310	35.281	548.913	15.891	0.538	0.428	1.258	2581.136	296.4183	115
9.129	1.211	0.436	2.779	82.302	1012.383	6.892	0.528	0.528	1.000	2508.800	363.7444	41
10.079	0.835	0.279	2.989	29.148	315.591	10.541	0.536	0.113	4.753	2477.000	76.6857	27
9.344	0.681	0.355	1.920	93.241	2712.602	10.613	0.492	0.339	1.450	2018.679	217.2668	5
24.622	0.330	0.547	0.603	89.987	864.191	10.765	0.544	0.570	0.954	2434.704	381.4096	34
21.650	0.926	0.557	1.662	83.079	1199.230	4.868	0.520	0.691	0.752	2238.271	453.5429	13
14.106	0.974	0.475	2.051	29.331	200.809	2.342	0.564	0.257	2.193	2518.024	171.9048	38
9.183	0.473	0.392	1.206	51.016	229.531	2.143	0.488	0.175	2.782	1821.576	107.1787	12
17.745	0.947	0.317	2.985	27.331	725.750	6.602	0.627	0.064	9.801	1953.420	35.7136	4
11.252	2.949	1.658	1.778	90.741	437.839	9.125	0.515	0.187	2.748	2294.050	125.099	20
7.814	1.036	0.222	4.676	46.106	859.766	7.477	0.536	0.106	5.066	2553.330	73.0429	10
13.598	0.901	0.032	28.193	16.550	1876.734	7.335	0.472	0.073	6.486	2023.008	47.6253	4
6.032	1.408	0.179	7.859	36.426	1771.598	4.678	0.543	0.212	2.556	2476.450	143.4911	11
9.768	0.969	1.511	0.641	73.530	239.702	3.724	0.534	0.225	2.371	1748.363	128.8164	26
7.118	1.948	0.722	2.699	68.395	803.790	4.722	0.537	0.458	1.173	2566.860	316.4426	32
31.040	1.009	0.386	2.612	54.211	1279.488	21.154	0.543	0.227	2.397	2485.550	153.3029	15
5.746	0.607	0.197	3.087	30.375	403.181	5.344	0.541	0.443	1.220	2577.383	305.9876	90

Continue to next page

(Continued)

23.177	1.108	0.147	7.549	26.208	1154.746	22.731	0.541	0.094	5.776	2498.567	63.6453	9
30.754	0.434	0.083	5.216	40.082	1819.161	10.414	0.538	0.241	2.234	2544.425	165.581	5
18.261	0.954	0.786	1.213	89.551	389.515	13.822	0.530	0.208	2.554	2512.897	142.9217	38
5.176	5.483	0.919	5.964	45.653	333.555	4.301	0.542	0.106	5.110	2547.612	72.7074	28
18.086	0.378	0.057	6.690	40.955	766.644	2.356	0.518	0.179	2.899	2369.075	120.8879	7
27.745	0.762	0.595	1.281	41.925	169.351	12.206	0.534	0.124	4.326	2428.042	83.2623	43
23.317	0.573	0.268	2.141	58.791	225.593	4.177	0.514	0.164	3.138	2200.487	107.2002	19
11.772	0.803	0.196	4.092	32.609	806.868	11.196	0.540	0.081	6.685	2557.011	55.5837	13
10.538	1.084	0.062	17.510	19.210	1950.530	6.553	0.483	0.046	10.455	1976.620	29.5429	2
13.663	1.070	0.407	2.630	45.537	469.855	12.720	0.524	0.072	7.249	2473.824	49.6762	21
16.026	0.791	0.425	1.862	72.216	512.652	11.349	0.550	0.254	2.163	2602.279	174.9661	33
22.227	0.742	0.405	1.830	26.186	130.024	6.265	0.528	0.140	3.766	2532.076	97.1462	73
9.824	0.786	0.248	3.162	76.304	1241.760	5.617	0.537	0.369	1.453	2549.203	254.5667	16
26.159	2.295	0.783	2.930	56.990	514.920	14.096	0.545	0.122	4.448	2069.423	75.4667	11
8.385	1.125	0.530	2.124	40.652	405.370	8.427	0.534	0.374	1.426	2576.257	259.9667	82
34.795	0.829	0.257	3.225	24.324	674.949	8.280	0.532	0.166	3.198	2417.187	112.1035	23
8.862	0.379	0.352	1.075	128.041	1985.207	6.999	0.542	0.426	1.270	2622.473	296.6568	16
16.123	1.009	0.384	2.631	22.042	117.991	7.929	0.510	0.056	9.032	1968.721	35.0667	25
13.800	0.839	0.988	0.849	192.074	1827.364	5.041	0.530	0.649	0.817	2562.885	451.2	17
6.059	1.985	0.820	2.420	81.477	745.884	3.870	0.544	0.458	1.187	2533.781	312.7593	27
11.751	3.001	0.467	6.421	52.093	1181.899	7.428	0.543	0.320	1.695	2655.043	224.0333	28

Continue to next page

(Continued)

4.708	0.495	0.201	2.464	68.249	803.899	2.824	0.575	0.326	1.761	2384.846	210.1867	12
23.028	0.424	0.593	0.715	51.030	316.801	10.175	0.551	0.164	3.358	1547.433	86.9333	16
30.653	1.165	0.754	1.544	42.746	328.560	8.883	0.501	0.178	2.821	2146.171	116.2667	24
21.372	1.180	0.415	2.840	42.666	387.249	13.951	0.539	0.182	2.966	2590.797	125.9643	32
17.662	1.831	0.852	2.149	58.131	373.505	11.510	0.553	0.237	2.338	2413.347	156.2667	43
10.035	0.690	1.936	0.357	321.096	1377.624	14.442	0.544	0.788	0.691	2612.598	545.8734	20
8.050	0.460	0.560	0.822	220.490	2536.552	13.563	0.518	0.486	1.064	2501.766	338.1047	12
10.184	1.828	0.931	1.964	76.592	611.148	7.236	0.540	0.156	3.462	2603.404	108.2667	18
23.773	0.838	0.601	1.394	72.623	501.900	8.526	0.524	0.343	1.528	2461.853	235.0667	51
14.673	0.981	0.644	1.524	42.967	340.892	7.565	0.543	0.240	2.259	2587.914	165.8333	55
6.987	1.116	0.244	4.580	34.718	508.560	7.706	0.543	0.339	1.604	2593.979	234.0333	51
12.034	1.057	0.610	1.734	106.513	2390.635	11.172	0.550	0.541	1.016	2585.512	371.02	24
17.588	1.315	1.684	0.781	188.497	1110.563	9.346	0.532	0.825	0.645	2546.881	570.6848	54
11.313	0.877	0.271	3.236	40.084	699.673	10.435	0.540	0.377	1.434	2582.768	260.5134	47
20.027	0.895	0.512	1.750	80.049	758.624	4.545	0.502	0.318	1.576	2279.717	214.6667	12
23.104	1.234	0.441	2.796	40.828	595.113	4.693	0.492	0.171	2.871	1917.705	107.0004	10
5.572	4.003	0.330	12.132	28.436	595.757	4.908	0.554	0.171	3.234	2530.330	115.7513	28
8.833	1.019	0.508	2.005	90.382	1489.528	4.994	0.549	0.690	0.796	2620.010	476.5526	35
7.633	2.773	0.312	8.897	42.339	1795.021	7.732	0.534	0.181	2.957	2595.734	125.9132	15
9.830	1.867	0.462	4.044	27.080	413.194	5.758	0.623	0.061	10.172	2241.628	36.7505	9
37.750	1.234	1.045	1.181	76.988	610.567	18.498	0.531	0.248	2.144	2434.868	167.7095	41
30.645	0.496	0.212	2.337	54.480	755.898	20.965	0.546	0.341	1.600	2433.545	227.8639	31
4.840	0.770	0.301	2.558	125.028	5055.569	3.820	0.471	0.276	1.706	2219.167	189.5	2

Continue to next page

(Continued)

9.317	0.940	0.532	1.765	81.886	1001.940	2.741	0.490	0.265	1.847	1705.939	156.5587	5
11.877	0.703	0.334	2.103	38.109	706.549	13.949	0.560	0.217	2.582	2571.963	146.9601	22
31.685	0.425	0.283	1.500	50.227	570.190	13.918	0.556	0.225	2.470	2582.399	153.3333	21
31.869	0.395	0.326	1.213	55.269	289.325	6.025	0.478	0.242	1.975	1919.449	153.3333	11
16.748	0.919	0.616	1.492	49.947	673.953	3.776	0.653	0.109	5.984	2195.976	63.2806	5
7.147	0.453	0.335	1.350	106.278	1078.863	10.923	0.525	0.299	1.755	2435.601	203.8359	12
4.232	0.604	0.473	1.276	150.794	1697.661	3.037	0.541	0.419	1.292	2644.929	292.9461	11
41.401	0.938	0.266	3.524	21.115	246.114	5.226	0.527	0.119	4.428	2476.983	81.6	26
10.135	0.997	0.438	2.275	49.123	525.833	3.538	0.596	0.131	4.552	1630.554	68.5052	6
24.692	2.709	1.056	2.566	28.954	81.426	3.657	0.574	0.166	3.465	1228.415	76.6667	20
4.303	1.107	0.315	3.511	70.744	1056.296	6.468	0.541	0.223	2.432	2632.619	155.1881	16
6.220	0.554	0.253	2.188	82.425	1602.543	5.786	0.536	0.151	3.542	2442.111	102.1333	5
10.378	0.366	0.150	2.437	47.562	1075.177	6.882	0.466	0.222	2.097	1603.289	130.4	9
13.217	0.071	0.236	0.302	105.840	1552.359	12.974	0.560	0.460	1.216	2304.188	295.4197	44
17.135	0.688	0.151	4.560	31.109	531.164	6.628	0.542	0.218	2.488	2466.396	146.9372	30
20.108	1.924	1.210	1.590	66.160	601.926	11.101	0.588	0.323	1.822	2185.567	196.6667	20
5.797	7.809	0.756	10.324	35.916	437.531	4.989	0.536	0.174	3.085	2567.034	120.202	42
13.422	1.517	0.813	1.867	63.136	769.802	4.659	0.510	0.220	2.320	2038.235	139.0464	12
13.207	1.104	0.493	2.237	43.060	799.276	4.211	0.524	0.148	3.548	2491.805	101.8667	10
14.717	0.965	0.109	8.891	27.880	1034.999	12.748	0.494	0.118	4.189	2355.213	81.3938	14
17.374	0.544	0.102	5.323	27.938	1100.316	4.852	0.604	0.305	1.983	2361.819	190.5333	13
4.576	1.216	0.401	3.034	136.646	3153.981	3.942	0.547	0.312	1.751	2350.640	204.8	3

Continue to next page

(Continued)

19.163	2.929	1.253	2.338	107.565	1573.665	16.239	0.525	0.218	2.407	2260.758	143.0371	11
25.288	1.224	0.948	1.292	76.483	478.774	12.691	0.536	0.312	1.720	2558.357	215.2757	27
10.872	0.799	0.524	1.523	91.184	990.052	5.118	0.541	0.362	1.495	2622.536	251.9429	19
11.523	0.949	0.293	3.244	61.684	1077.097	9.214	0.519	0.145	3.579	2356.059	97.6571	9
19.438	0.332	0.251	1.322	47.645	609.267	5.034	0.609	0.164	3.713	1427.107	79.3829	7
13.798	1.900	0.291	6.528	20.796	238.395	9.437	0.546	0.106	5.173	2559.432	72.291	50
23.254	0.654	0.163	4.009	38.505	467.869	13.181	0.540	0.306	1.766	2362.726	202.2354	39
7.056	0.383	0.270	1.416	106.029	1490.951	6.422	0.545	0.329	1.656	2634.065	228.861	11
2.124	1.583	0.914	1.732	171.712	3201.548	1.490	0.547	0.293	1.863	2194.927	185.9428	3
26.043	2.212	8.390	0.264	197.676	623.303	11.413	0.506	0.324	1.563	2332.575	219.7646	114
24.305	0.361	0.378	0.956	43.829	432.394	9.464	0.537	0.219	2.446	2579.023	152.0788	34
5.452	0.389	0.185	2.103	26.738	176.188	16.888	0.536	0.049	10.888	2586.627	34.2081	38
37.607	0.322	0.504	0.638	52.552	360.427	8.368	0.528	0.296	1.783	2512.167	204.2029	81
36.458	1.312	0.099	13.298	15.496	612.257	15.658	0.482	0.193	2.495	2110.806	127.8089	38
28.504	1.161	0.318	3.651	27.250	335.289	15.157	0.517	0.153	3.386	2316.880	102.2667	46
28.567	1.211	0.511	2.372	27.992	165.777	13.368	0.530	0.118	4.490	2102.161	74.3667	67
5.458	0.981	0.176	5.571	44.035	2088.241	4.914	0.540	0.639	0.845	2613.217	444.475	33
11.235	0.334	0.157	2.127	63.719	1329.322	5.059	0.540	0.466	1.159	2587.446	322.4	16
6.059	1.985	0.820	2.420	81.477	745.884	3.870	0.544	0.458	1.187	2533.781	312.7593	27

B.3 Design-relevant Feature Optimisation Process

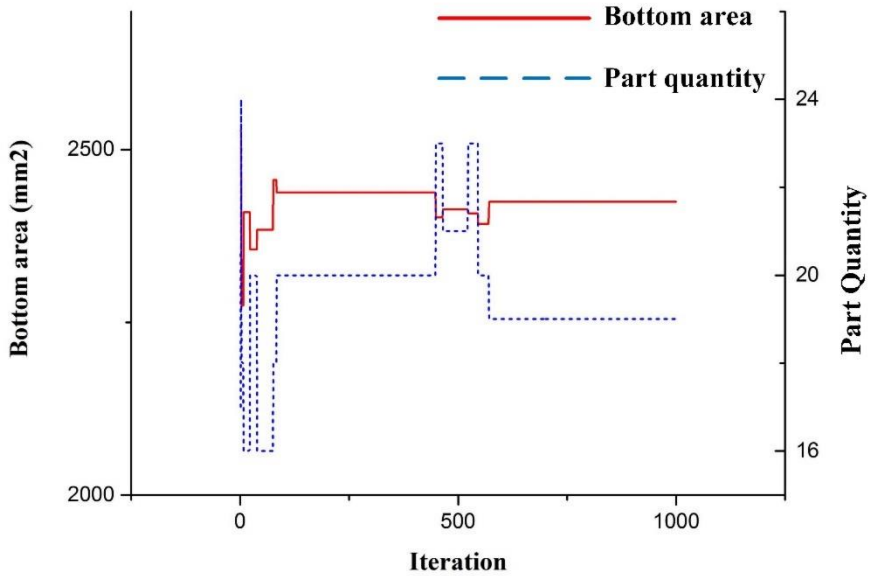


Figure B. 1 Bottom area and part quantity optimisation (designer-and-operator-oriented) process for Build No.1

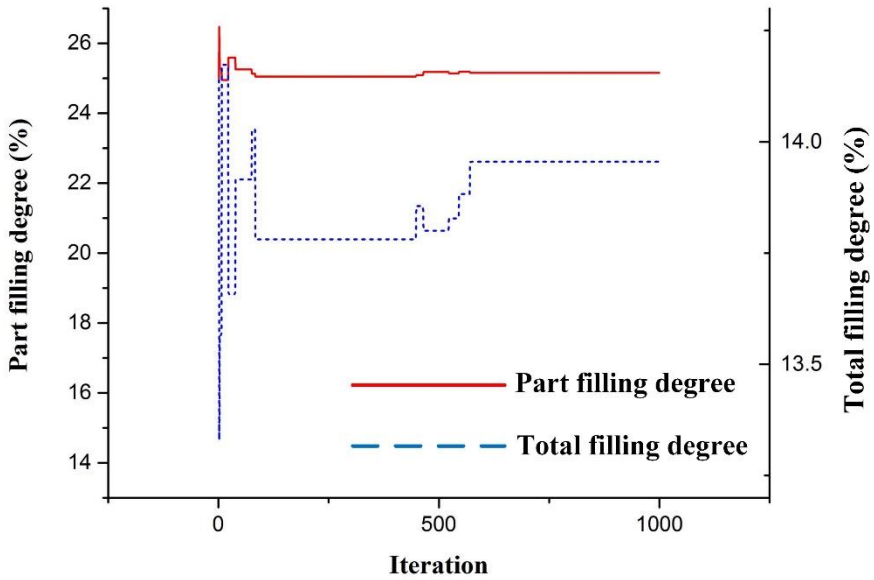


Figure B. 2 Filling degree of part and total optimisation (designer-and-operator-oriented) process for Build No.1

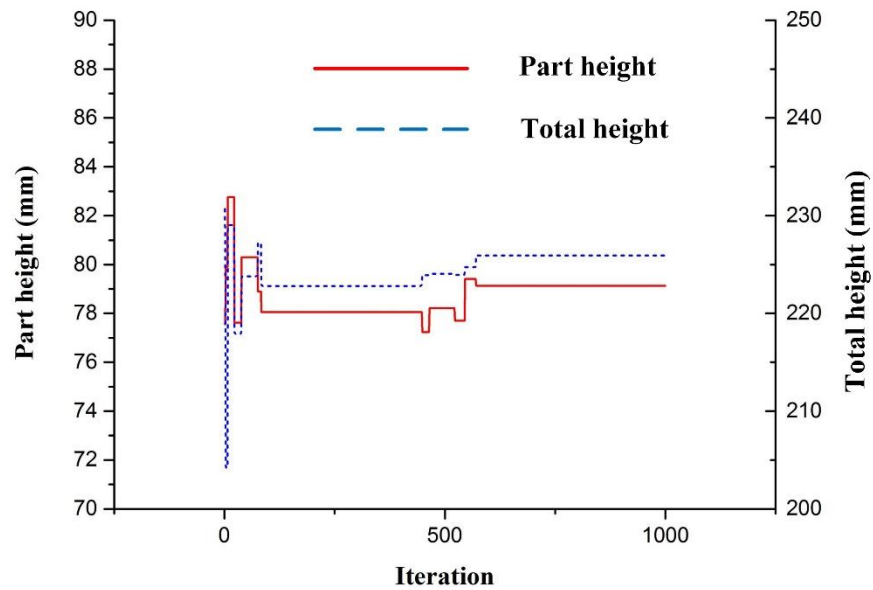


Figure B.3 Height of part and total optimisation (designer-and-operator-oriented) process for Build No.1

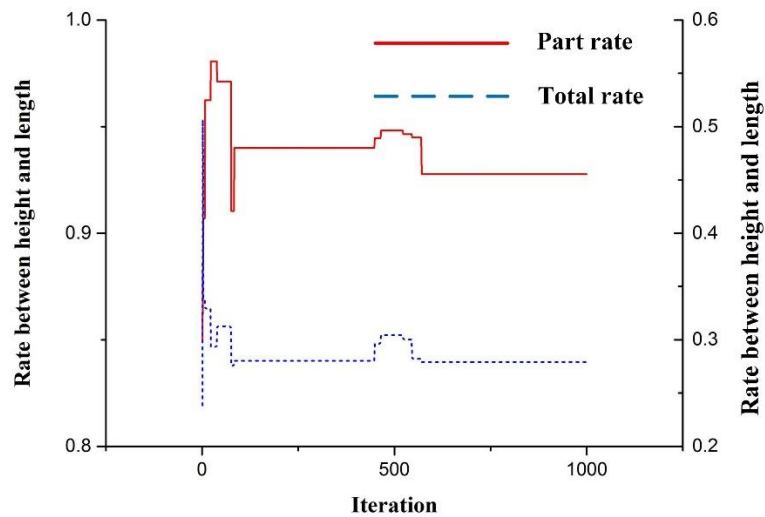


Figure B. 4 Rate between height and length of part and total build optimisation (designer-and-operator-oriented) process for Build No.1

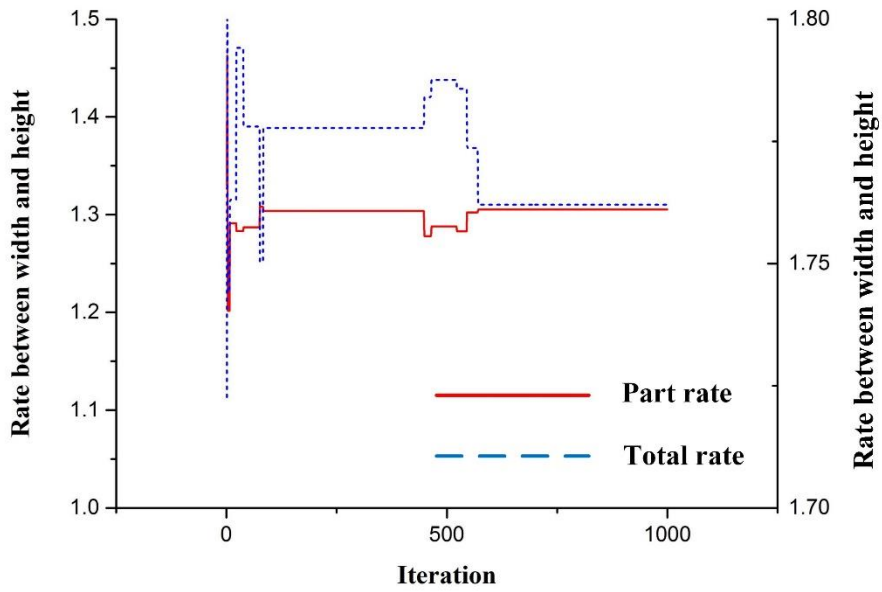


Figure B. 5 Rate between width and height of part and total build optimisation (designer-and-operator-oriented) process for Build No.1

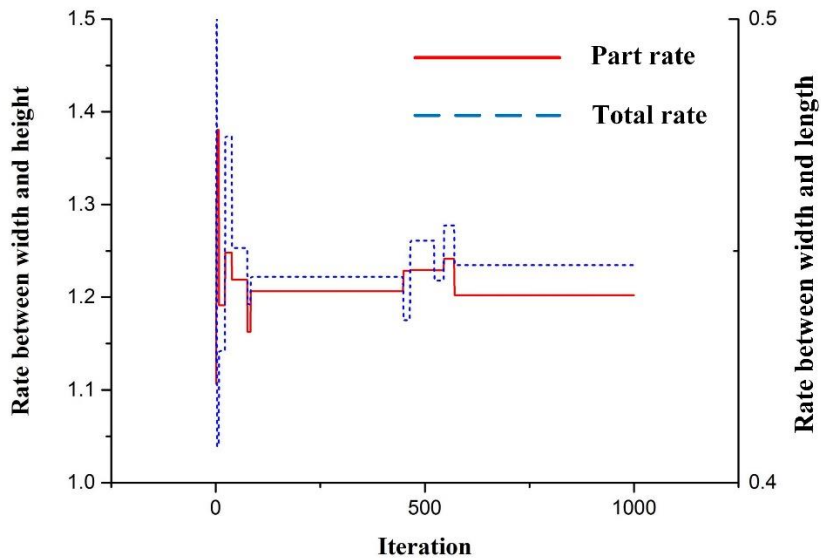


Figure B. 6 Rate between width and length of part and total build optimisation (designer-and-operator-oriented) process for Build No.1

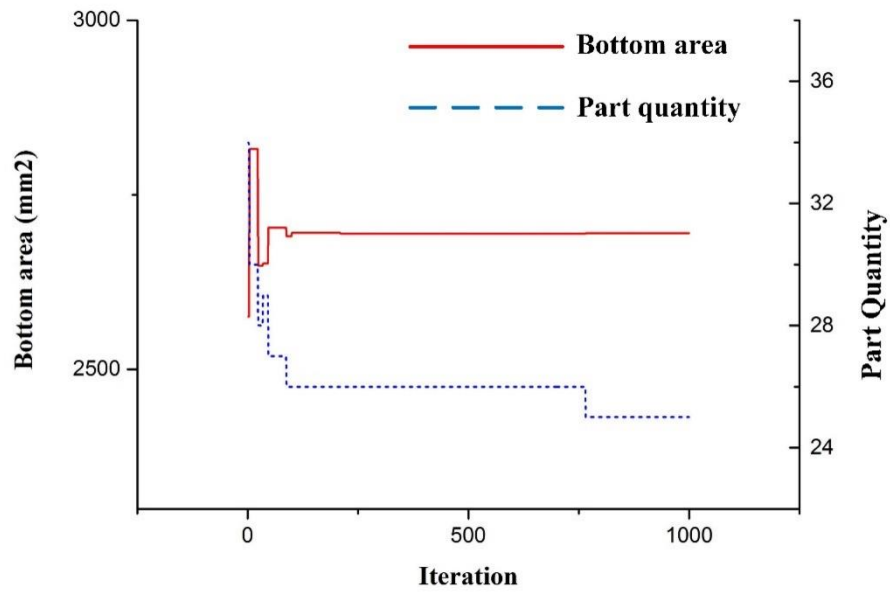


Figure B. 7 Bottom area and part quantity optimisation (designer-and-operator-oriented) process for Build No.2

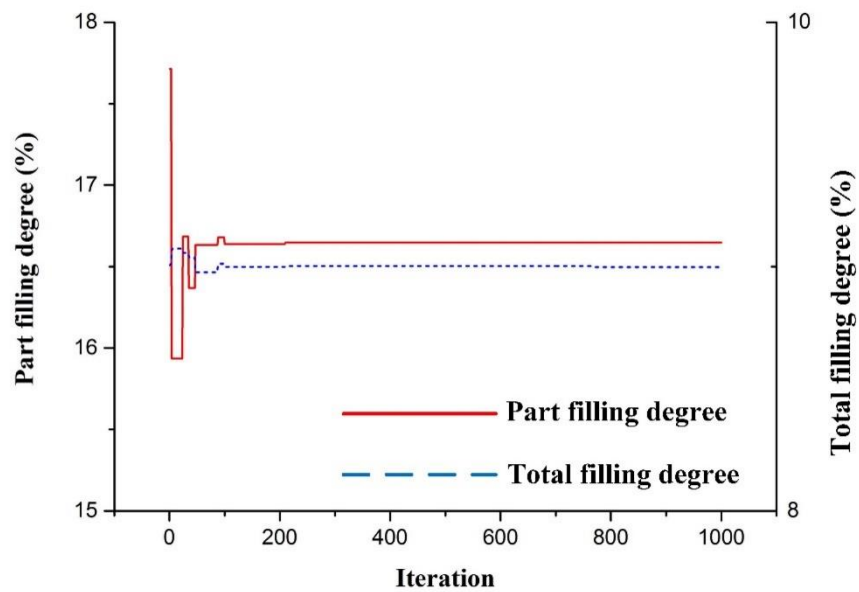


Figure B. 8 Filling degree of part and total optimisation (designer-and-operator-oriented) process for Build No.2

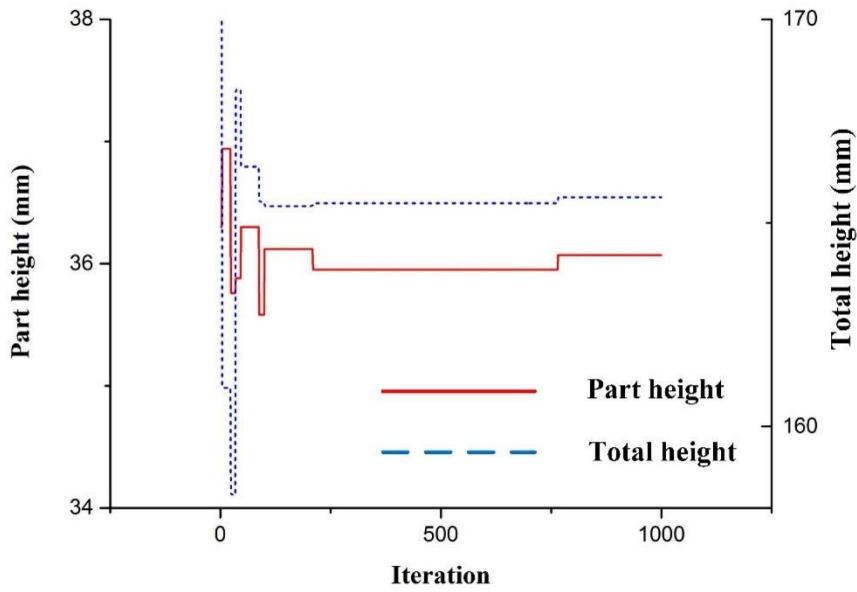


Figure B. 9 Height of part and total optimisation (designer-and-operator-oriented) process for Build No.2

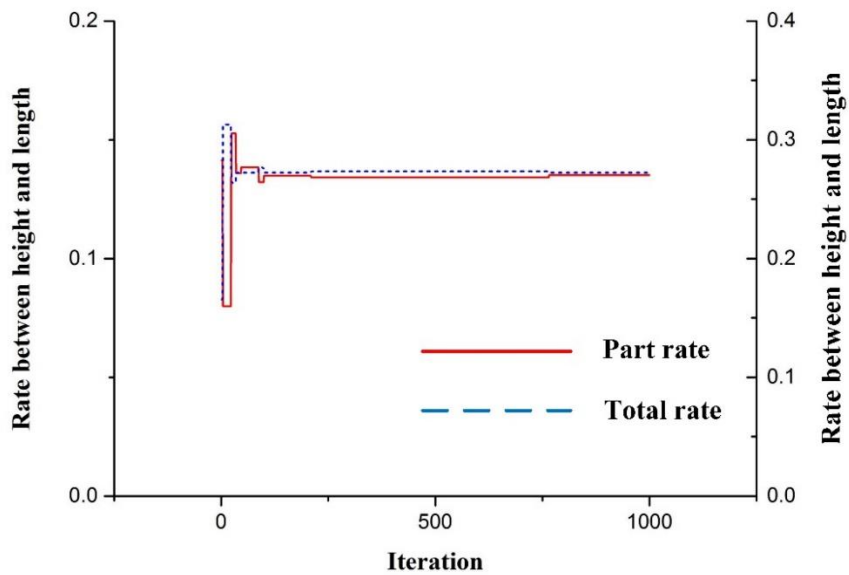


Figure B. 10 Rate between height and length of part and total build optimisation (designer-and-operator-oriented) process for Build No.2

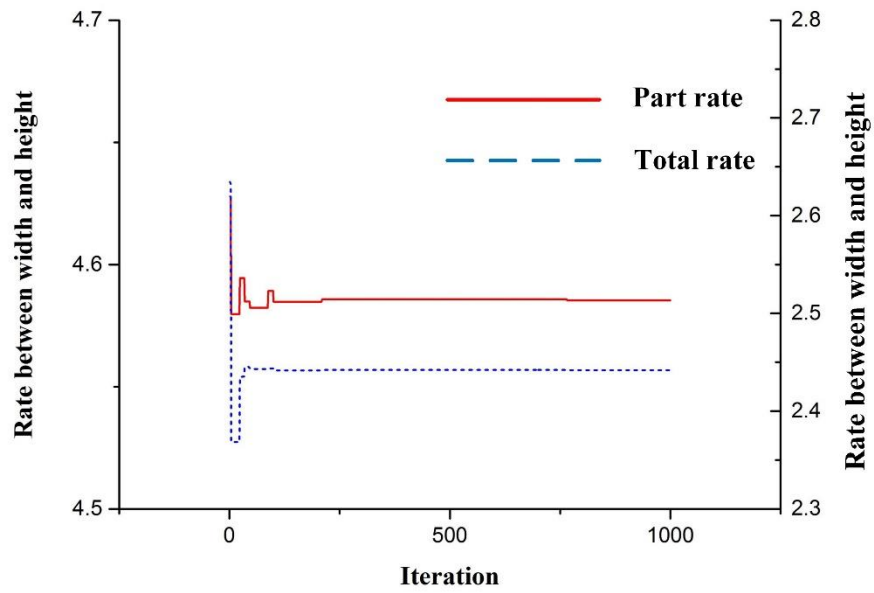


Figure B. 11 Rate between width and height of part and total build optimisation (designer-and-operator-oriented) process for Build No.2

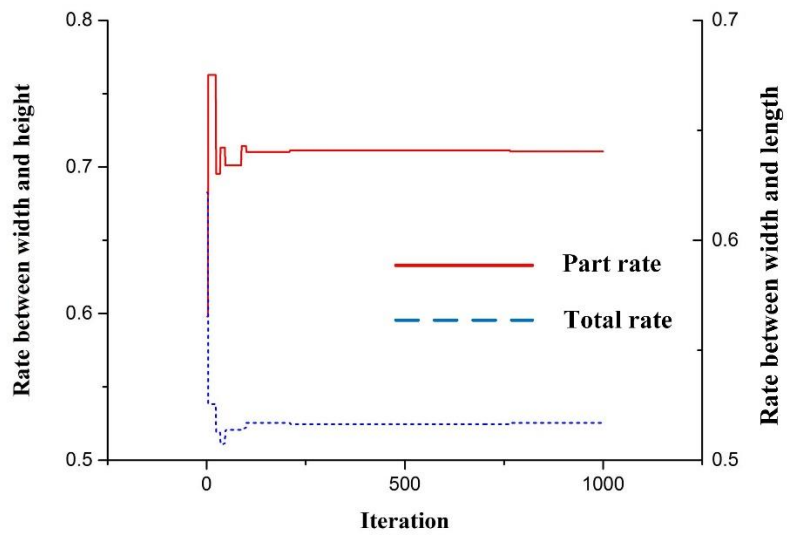


Figure B. 12 Rate between width and length of part and total build optimisation (designer-and-operator-oriented) process for Build No.2

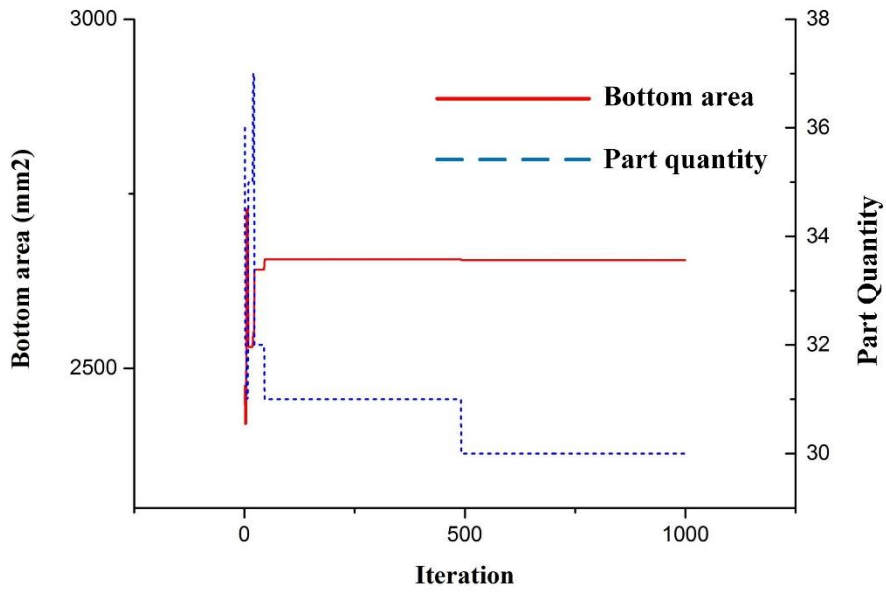


Figure B. 13 Bottom area and part quantity optimisation (designer-and-operator-oriented) process for Build No.3

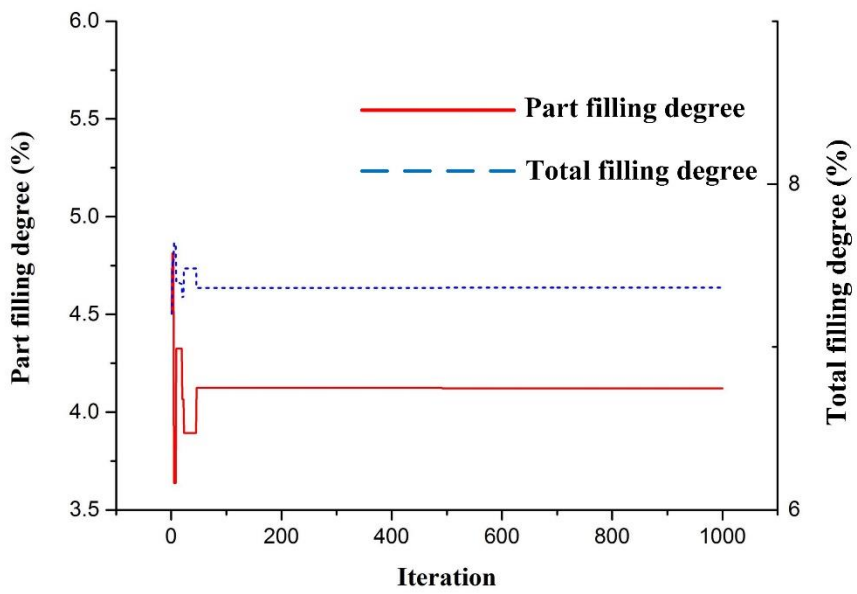


Figure B. 14 Filling degree of part and total optimisation (designer-and-operator-oriented) process for Build No.3

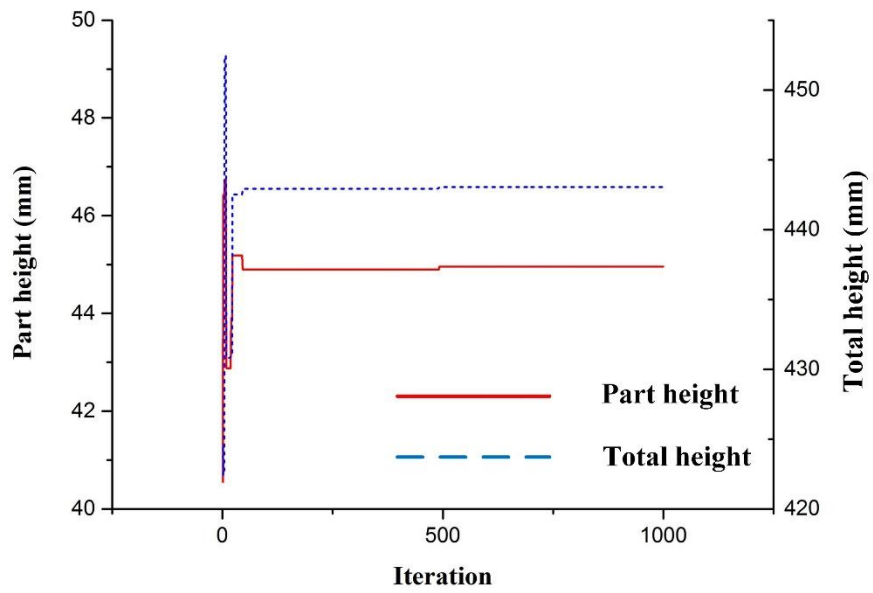


Figure B. 15 Height of part and total optimisation (designer-and-operator-oriented) process for Build No.3

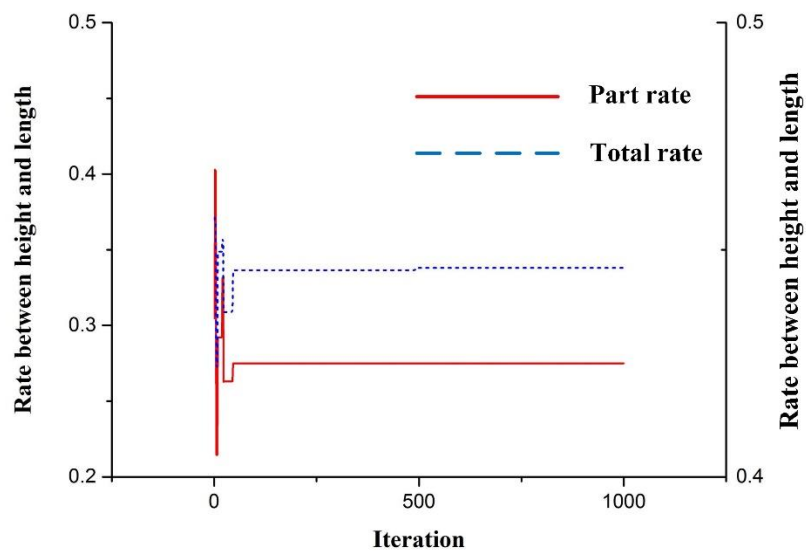


Figure B. 16 Rate between height and length of part and total build optimisation (designer-and-operator-oriented) process for Build No.3

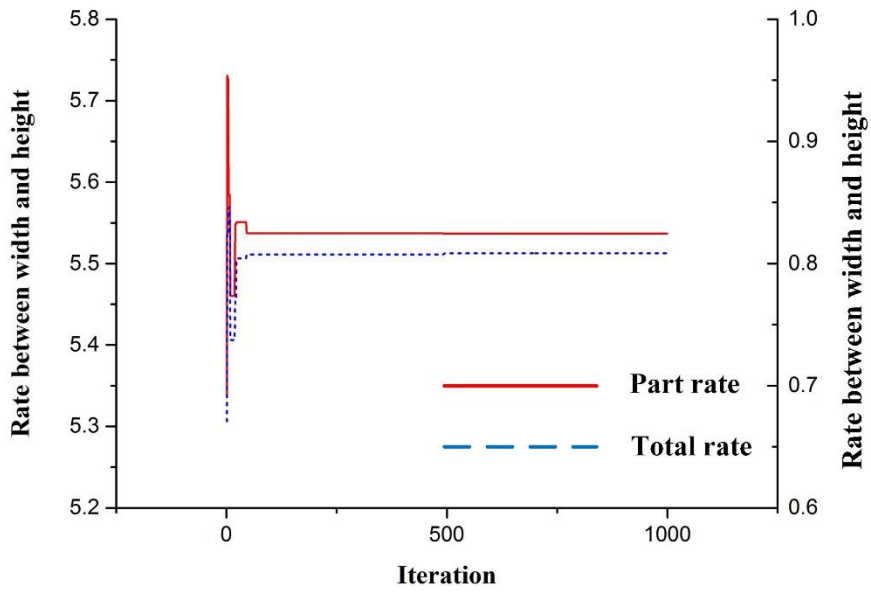


Figure B. 17 Rate between width and height of part and total build optimisation (designer-and-operator-oriented) process for Build No.3

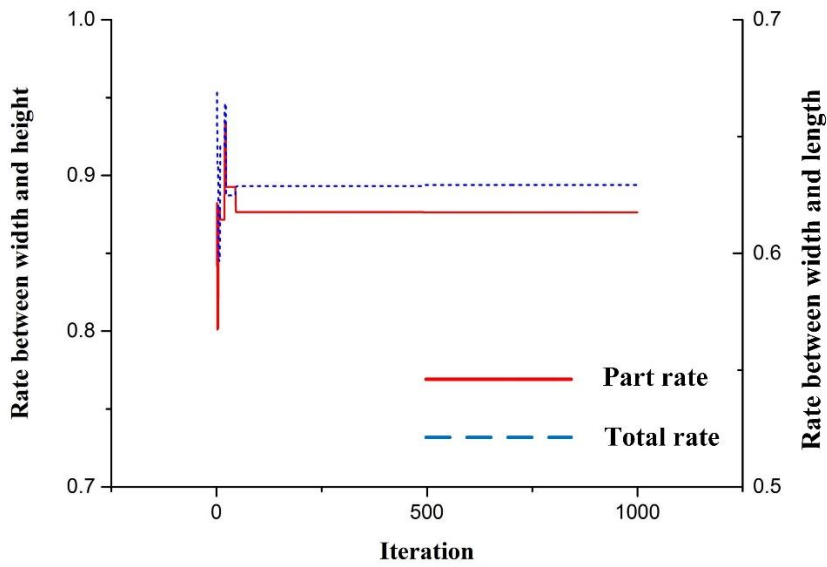


Figure B. 18 Rate between width and length of part and total build optimisation (designer-and-operator-oriented) process for Build No.3

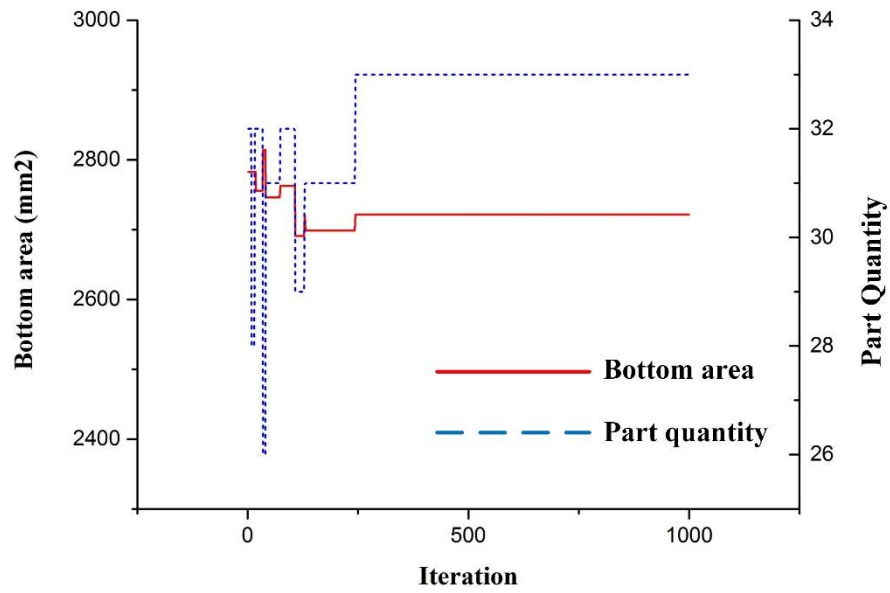


Figure B. 19 Bottom area and part quantity optimisation (designer-and-operator-oriented) process for Build No.4

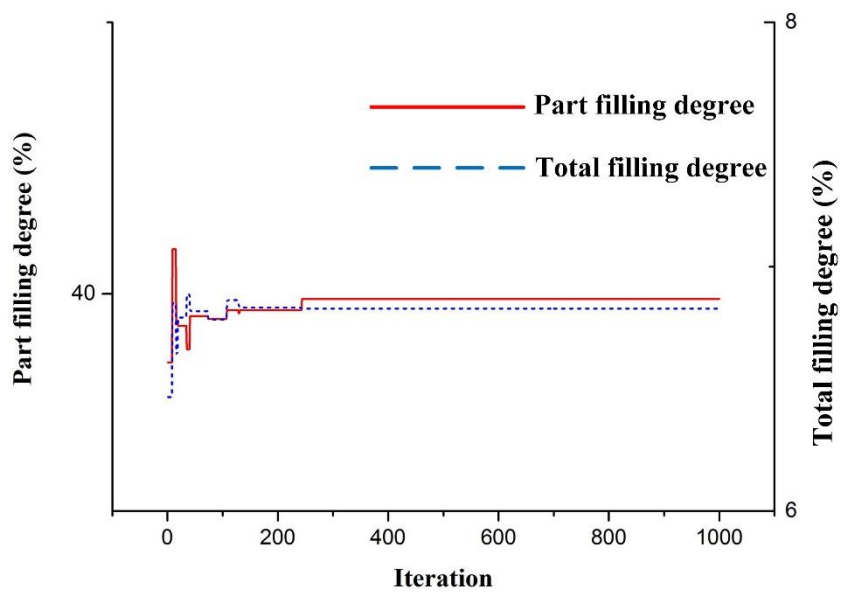


Figure B. 20 Filling degree of part and total optimisation (designer-and-operator-oriented) process for Build No.4

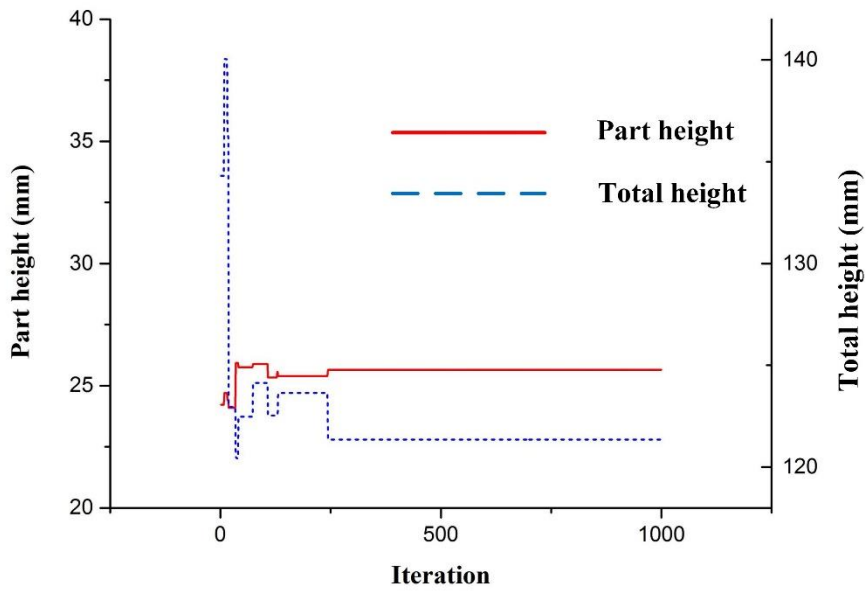


Figure B. 21 Height of part and total optimisation (designer-and-operator-oriented) process for Build No.4

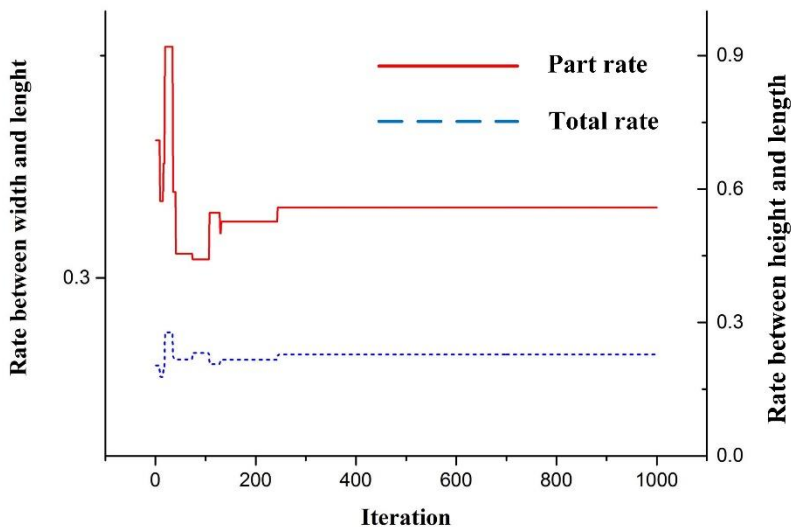


Figure B. 22 Rate between height and length of part and total build optimisation (designer-and-operator-oriented) process for Build No.4

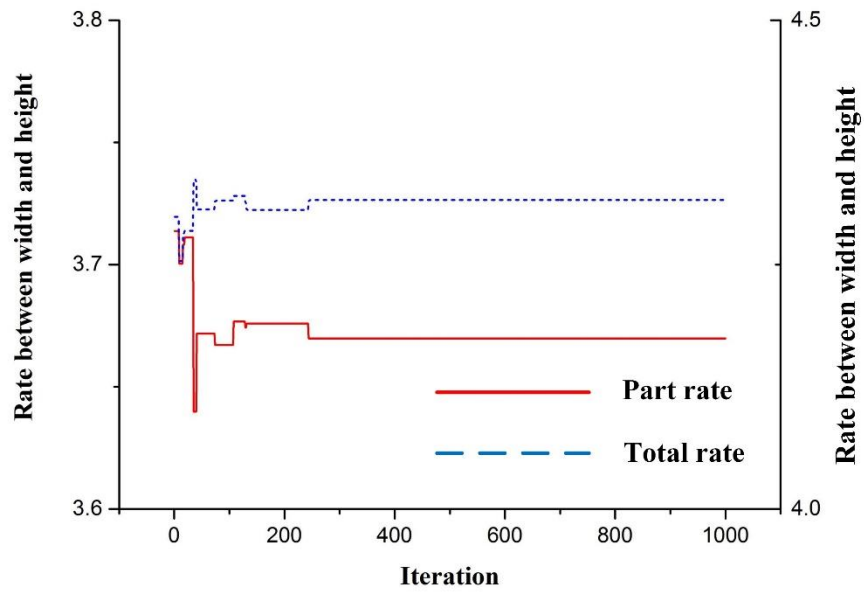


Figure B. 23 Rate between width and height of part and total build optimisation (designer-and-operator-oriented) process for Build No.4

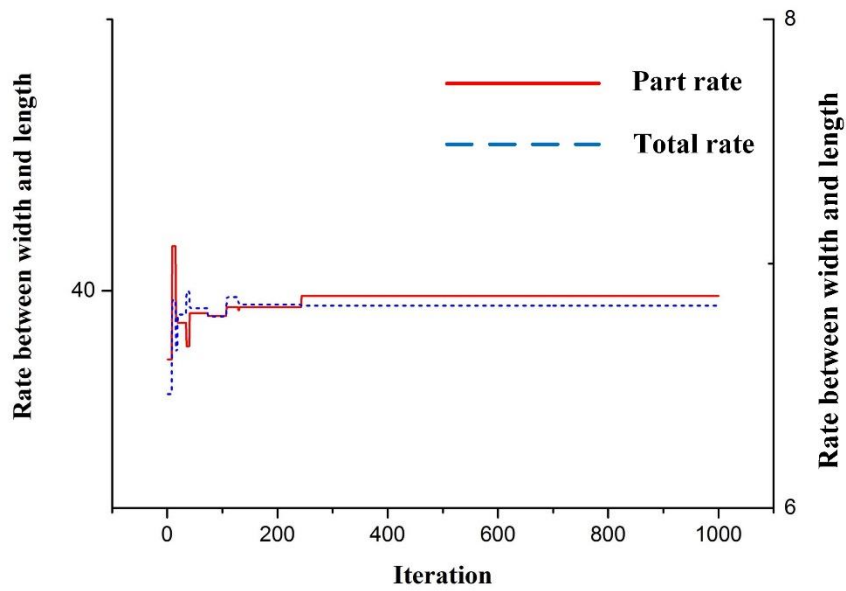


Figure B. 24 Rate between width and length of part and total build optimisation (designer-and-operator-oriented) process for Build No.4

Appendix C Core Programming Coding

C.1 IoT Platform Data Sensing and Collecting

```
1. sense1GPIO=4
2. GPIO2=24
3. HOST= "10.2.1.10"
4. PORT= 8889
5. #Basic parameter setting
6. s=socket.socket(socket.AF_INET, socket.SOCK_STREAM)
7. s.connect((HOST, PORT))
8. SensorData=()
9. #server connection
10. #Temperature and humidity data collection
11. def Get_Temp_Humid_Data(a):
12.     import Adafruit_DHT #package Adafruit_DHT is used
13.     sensor=Adafruit_DHT.DHT11
14.     gpio=a
15.     humidity, temperature=Adafruit_DHT.read_retry(sensor,gpio)
16.     if humidity is None and temperature is None:
17.         print ('Failed to Get Reading. Please retry')
18.     else:
19.         return temperature, humidity
20. #Keep collecting data and send it to server
21. while 1:
22.     data=s.recv(1024)
23.     print data
24.     if data=='Get':
25.         SensorData=Get_Temp_Humid_Data(sense1GPIO)
26.         Sense2=Get_Temp_Humid_Data(GPIO2)
27.         print 'Data Assigned: ', SensorData, ' and ', Sense2
28.         if SensorData is None and Sense2 is None:
29.             time.sleep(5)
30.         string1=(SensorData, Sense2)
31. s.close
```

C.2 Ad-hoc Wireless Network Data Receiving

```

1. GPIO1=21
2. GPIO2=20
3. HOST = "10.2.1.10"      # Symbolic name meaning all available interfaces
4. PORT1=8888
5. PORT2 = 8889          # Arbitrary non-privileged port
6. s.listen(10)          #function to deal with handling connections
7. d.listen(10)
8. #Parameter setting
9. def createfile():
10.     f=open(file, 'w')
11.     writer=csv.writer(f, quotechar=" ")
12.     writer.writerow(['Pi Number, Date and Time, Temperature 1 (*C), Humidity 1, Temperature 2 (*C),
Humidity 2'])
13. def writefile(pi, t1, h1, t2, h2):
14.     f=open(file, 'a')
15.     writer=csv.writer(f, quotechar=" ")
16.     now=datetime.datetime.now()
17.     writer.writerow([pi, now, t1, h1, t2, h2])
18. def write_local_sensors():
19.     temp1, humid1=Get_Temp_Humid_Data(GPIO1)
20.     if temp1 is None: #and temp2 is None:
21.         time.sleep(2)
22.     temp2, humid2 = (0,0)
23.     writefile(1, temp1, humid1, temp2, humid2)
24. def clientthread(conn, pi):
25.     import time          #Send message to clients
26.     conn.send('Get')     #loop so function does not terminate
27.     print 'Getting'     #receive from client
28.     time.sleep(1)
29.     data=conn.recv(1024)
30.     if data is None:
31.         time.sleep(2)
32.         print 'were waiting'
33.     print data
34.     for char in '\0':
35.         data=data.replace(char, "")
36.     temp1, humid1, temp2, humid2 = tuple(filter(None, data.split(',')))
37.     return (data)
38. #Receiving data from client RPIS
39. while 1:#keep talking to client
40.     createfile()
41.     #wait for connection
42.     conn1, addr1 = s.accept()
43.     print 'Connected to ' +addr1[0]
44.     conn2, addr2 = d.accept()
45.     print 'Connected to ' +addr2[0]
46.     while True:
47.         write_local_sensors()
48.         time.sleep(5)
49.         data2=start_new_thread(clientthread, (conn2, 2))
50.         time.sleep(5)
51.         data1=start_new_thread(clientthread , (conn1, 3))
52.         time.sleep(80)
53.         print data2
54. s.close()
55. d.close()

```


C.3 Benchmark Algorithms

```

1. #import packages (only important ones are shown here)
2. from sklearn import preprocessing, cross_validation, svm
3. from sklearn.preprocessing import MinMaxScaler
4. from sklearn.linear_model import LinearRegression, RidgeCV, LogisticRegression
5. #import datasets
6. Build_info=pd.read_csv('~\Build-level_dataset.csv')
7. target=pd.read_csv('~\Label_Real1.csv')
8. target=target.drop(['Unnamed: 0'], axis=1)
9. Layer_info1=pd.read_csv('~\Layer-level_dataset.csv')
10. merge_dataset=pd.merge(Build_info, Layer_info1, left_index=True, right_index=True)
11. for j in range(0,5): # Five-fold cross validation
12.     x_train, x_test, y_train, y_test = cross_validation.train_test_split(input_data,target,test_size=0.2,rand
om_state=j)
13.     scaler = MinMaxScaler(copy=True, feature_range=(0, 1))
14.     x_train=scaler.fit_transform(x_train)
15.     x_test=scaler.fit_transform(x_test)
16. #Linear Regression
17.     LR = linear_model.LinearRegression()
18.     LR.fit(x_train,y_train)
19.     predictions_LR = LR.predict(x_test)
20.     a_LR = np.reshape(predictions_LR,len(predictions_LR))
21.     b_LR = np.reshape(y_test.values.astype('float'),len(predictions_LR))
22.     co_LR = np.corrcoef(a_LR,b_LR)[1,0]
23.     rms_LR = sqrt(mean_squared_error(predictions_LR, y_test))
24.     mae_lr=mean_absolute_error(y_test, predictions_LR)
25. #Desion Tree
26.     DT = tree.DecisionTreeRegressor()
27.     DT.fit(x_train,y_train)
28.     predictions_DT=DT.predict(x_test)
29.     accuracy_DT=DT.score(x_test,y_test)
30.     a_DT = np.reshape(predictions_DT,len(predictions_DT))
31.     b_DT = np.reshape(y_test.values.astype('float'),len(predictions_DT))
32.     co_DT = np.corrcoef(a_DT,b_DT)[1,0]
33.     rms_DT = sqrt(mean_squared_error(predictions_DT, y_test))
34.     mae_dt=mean_absolute_error(y_test, predictions_DT)
35. #k-nearest neighbours
36.     knn = neighbors.KNeighborsRegressor(10, 'distance')
37.     knn.fit(x_train,y_train)
38.     predictions_knn = knn.predict(x_test)
39.     a_knn = np.reshape(predictions_knn,len(predictions_knn))
40.     b_knn = np.reshape(y_test.values.astype('float'),len(predictions_knn))
41.     co_knn = np.corrcoef(a_knn,b_knn)[1,0]
42.     rms_knn = sqrt(mean_squared_error(predictions_knn, y_test))
43.     mae_knn=mean_absolute_error(y_test, predictions_knn)

```

C.4 Merged Neural Network

```

1. #import keras as the main package for building neural network
2. import keras.layers
3. from keras.models import Sequential
4. from keras.layers import Dense, Dropout, noise, Embedding, LSTM, Merge
5. from keras import optimizers
6. from keras.optimizers import RMSprop, TFOptimizer, adam\
7. #import datasets
8. Build_info=pd.read_csv('~/.Build-level_dataset.csv')
9. target=pd.read_csv('~/.Label_Real1.csv')
10. target=target.drop(['Unnamed: 0'], axis=1)
11. Layer_info1=pd.read_csv('~/.Layer-level_dataset.csv')
12. Mcc_dnn=[]
13. for j in range (5): # Five-fold cross validation
14.     x_train1, x_test1, y_train, y_test = cross_validation.train_test_split(Build_info,target,test_size=0.2,ra
        ndom_state=j)
15.     x_train2, x_test2, y_train, y_test = cross_validation.train_test_split(Layer_info,target,test_size=0.2,ra
        ndom_state=j)
16.     x_test2=np.load('E:/Blake/PhD/EOSP700Experiment/Data/Dataset/Dataset_designfeature(SecP)/x_te
        st2.npy')
17.     scaler = MinMaxScaler(copy=True, feature_range=(0, 1))
18.     x_train1=scaler.fit_transform(x_train1)
19.     x_test1=scaler.fit_transform(x_test1)
20.     x_train2=scaler.fit_transform(x_train2)
21.     x_test2=scaler.fit_transform(x_test2)
22.     model1 = Sequential() #Neural network for build-level dataset
23.     model1.add(Dense(50, input_dim=x_train1.shape[1], activation = 'relu'))
24.     model1.add(Dense(50, activation='relu'))
25.     model1.add(Dense(50, activation='relu'))
26.     model1.add(Dropout(0.2))
27.     model1.add(Dense(50, activation='relu'))
28.     model1.add(Dense(50, activation='relu'))
29.     model2 = Sequential() #Neural network for layer-level dataset
30.     model2.add(Dense(200, input_dim=x_train2.shape[1], activation = 'relu'))
31.     model2.add(Dense(200, activation='relu'))
32.     model2.add(Dropout(0.2))
33.     model2.add(Dense(200, activation='relu'))
34.     #model2.add(Dense(100, activation='relu'))
35.     model = Sequential() #Neural network for combination
36.     model.add(Merge([model1, model2], mode='concat'))
37.     model.add(Dense(1, activation='linear'))
38.     model.summary()
39.     adam(lr=0.005, beta_1=0.9, beta_2=0.999, epsilon=1e-08, decay=0.0) #train the model
40.     model.compile(loss='mean_absolute_error',
41.                 optimizer='Adam',
42.                 metrics=['accuracy'])
43.     history = model.fit([x_train1, x_train2], y_train.values.astype('float'),
44.                       validation_split=0.2,
45.                       batch_size=2,
46.                       epochs=200,
47.                       verbose=1,
48.                       validation_data=(x_test1, x_test2), y_test.values.astype('float'))
49.     predictions = model.predict([x_test1, x_test2]) #Test the model

```

C.5 Design-relevant Dataset Generation

```

1. #define a few function for the caculation
2. def filling_degree(dataset):
3.     dataset['BoxVolume (cm³)']=dataset['Length (mm)']*dataset['Width (mm)']*dataset['Height (mm)']/1000
4.     dataset['Filling degree_parts(%)']=dataset['Volume (cm³)']/dataset['BoxVolume (cm³)']*100
5.     dataset['BoxVolume (cm³)'][len(dataset)]=dataset['Length (mm)'][len(dataset)-1]*dataset['Width (mm)'][len(dataset)-1]*dataset['Height (mm)'][len(dataset)-1]/1000
6.     a=dataset['Filling degree_parts(%)'].drop(len(dataset)-1)
7.     dataset['Filling degree_parts(%)'][len(dataset)-1]=geometric_mean(a)
8.     filling_degree_average=dataset['Filling degree_parts(%)'][len(dataset)-1]
9.     filling_degree_total=dataset['Volume (cm³)'][len(dataset)-1]/dataset['BoxVolume (cm³)'][len(dataset)-1]*100
10.    return dataset, filling_degree_average,filling_degree_total
11.    def dimension_rate(dataset):
12.        dataset['Width/Length']=dataset['Width (mm)']/dataset['Length (mm)']
13.        dataset['Height/Length']=dataset['Height (mm)']/dataset['Length (mm)']
14.        dataset['Width/Height']=dataset['Width (mm)']/dataset['Height (mm)']
15.        b=dataset['Width/Length'].drop(len(dataset)-1)
16.        c=dataset['Height/Length'].drop(len(dataset)-1)
17.        d=dataset['Width/Height'].drop(len(dataset)-1)
18.        dataset['Width/Length'][len(dataset)-1]=geometric_mean(b)
19.        dataset['Height/Length'][len(dataset)-1]=geometric_mean(c)
20.        dataset['Width/Height'][len(dataset)-1]=geometric_mean(d)
21.        wl_Arate=dataset['Width/Length'][len(dataset)-1]
22.        hl_Arate=dataset['Height/Length'][len(dataset)-1]
23.        wh_Arate=dataset['Width/Height'][len(dataset)-1]
24.        wl_Trate=dataset['Width (mm)'][len(dataset)-1]/dataset['Length (mm)'][len(dataset)-1]
25.        hl_Trate=dataset['Height (mm)'][len(dataset)-1]/dataset['Length (mm)'][len(dataset)-1]
26.        wh_Trate=dataset['Width (mm)'][len(dataset)-1]/dataset['Height (mm)'][len(dataset)-1]
27.        dimension_rate=(wl_Arate,hl_Arate,wh_Arate,wl_Trate,hl_Trate,wh_Trate)
28.    return dataset, dimension_rate
29.    #caculat design-relevant data
30.    def Design_data(dataset):
31.        Part_fillingDeg=filling_degree(dataset)[1]
32.        Total_fillingDeg=filling_degree(dataset)[2]
33.        #dimension_rate=dimension_rate(dataset)[1]
34.        PartRate_wl,PartRate_hl,PartRate_wh,TotalRate_wl,TotalRate_hl,TotalRate_wh=dimension_rate(dataset)[1]
35.        Bottom_area=dataset['Width (mm)'][len(dataset)-1]*dataset['Length (mm)'][len(dataset)-1]/1000
36.        Heigh=dataset['Height (mm)'][len(dataset)-1]
37.        NumPart=int(len(dataset))-1
38.        De_data_tem=(file[0:-4],Part_fillingDeg,Total_fillingDeg,
39.                    PartRate_wl,PartRate_hl,PartRate_wh,TotalRate_wl,TotalRate_hl,TotalRate_wh,Bottom_area,Heigh,NumPart)
40.    return De_data_tem
41.    path2='~/STLInfor'
42.    data_dir_list = os.listdir(path2)
43.    for file in data_dir_list:
44.        designpath = path2 + '/' + file
45.        dataset2=read_data(designpath)
46.        dataset2=filling_degree(dataset2)[0]
47.        dataset2=dimension_rate(dataset2)[0]
48.        design=(Design_data(dataset2))
49.        DesignData.append(design)
50.    De_data=pd.DataFrame(DesignData,columns=['Build Date','Part filling degree','Total filling degree',
51.        'PartRate_wl','PartRate_hl','PartRate_wh','TotalRate_wl','TotalRate_hl','TotalRate_wh','Bottom_area','Heigh','NumPart'])
52.    De_data.to_csv('~/Design_dataset.csv')

```